MULTI-MODE STABILIZATION OF TORSIONAL OSCILLATIONS IN SINGLE AND MULTI-MACHINE SYSTEMS USING EXCITATION CONTROL

by

Andrew Yan

B.S.E.E., University of Texas at Arlington, 1977

M.A.Sc., University of British Columbia, 1979

A THESIS SUBMITTED IN PARTIAL FULFILLMENT OF
THE REQUIREMENTS FOR THE DEGREE OF
DOCTOR OF PHILOSOPHY

in

THE FACULTY OF GRADUATE STUDIES

(Department of Electrical Engineering)

We accept this thesis as conforming
to the required standard

THE UNIVERSITY OF BRITISH COLUMBIA

February , 1982

ABSTRACT

Subsynchronous Resonance (SSR) phenomena in a thermal-electric power system with series-capacitor-compensated transmission lines may cause damaging torsional oscillations in the shaft of the turbine-generator. This thesis deals with a wide-range multi-mode stabilization of single-machine and multi-machine SSR systems using output feedback excitation control. Chapter 1 summarizes the SSR countermeasures to date. Chapter 2 presents a unified electro-mechanical model for SSR studies, illustrates the torsional interaction between the electrical and mechanical systems, and demonstrates that multi-mass representation of the turbine-generator must be used for SSR studies. For the control design, a reduced order model is desirable. For the model reduction, modal analysis is applied to identify the excitable torsional modes, and a mass-spring equivalencing technique to retain only the unstable modes is developed in Chapter 3. Using the reduced order one-machine models, linear optimal excitation controls are designed in Chapter 4. The controls are further simplified by examining the eigenvalue sensitivity, and the results are tested on the linear and nonlinear full models. In Chapter 5, the stabilization technique is further extended and applied to a two-machine system and a three-machine system. The stabilizers still can be designed one machine at a time using a one-machine equivalent for each machine by retaining only the path with the strongest interacting current and the critical electrical resonance frequency as seen by the machine. To coordinate all controllers for the entire system, an iterative process is developed. The controllers thus designed are tested on linear and nonlinear full models. From both eigenvalue analysis and nonlinear dynamic performance tests of the one-machine, two-machine, and three-machine systems, a conclusion is drawn in Chapter 6 that the excitation controls thus designed by the

methods developed in this thesis can effectively stabilize single-machine and multi-machine SSR systems over a wide range of capacitor compensation.

TABLE OF CONTENTS

	Page
ABSTRACT	i
TABLE OF CONTENTS	iii
LIST OF TABLES	vi
LIST OF ILLUSTRATIONS	vii
ACKNOWLEDGEMENT	ix
NOMENCLATURE	x
1. INTRODUCTION	1
1.1 Subsynchronous Resonance	1
1.2 Countermeasures to SSR	3
1.3 Previous Works on Excitation Control of SSR	5
1.4 Scope of the Thesis	7
2. MODELLING POWER SYSTEMS FOR SSR STUDIES	8
2.1 Introduction	8
2.2 The Mechanical System	10
2.3 The Electrical System	13
2.4 Complete System Equations for Single and Multi-Machine Systems	16
2.5 The Torsional Interaction	19
3. MODEL REDUCTION OF A POWER SYSTEM FOR SSR STUDIES	22
3.1 Introduction	22
3.2 Torsional Resonance and the Unstable Modes	23
3.2.1 Natural Frequencies and Mode Shapes of the Mass-spring System	23 23
3.2.2 Damping and the Resonant Peak	26
3.2.3 Resonant Peaks of the Six Mass-spring System	27
3.2.4 Identification of the Unstable Torsional Modes	30

	Page
3.2.5 Modal Resonance Peaks and Unstable Modes	31
3.2.6 Other Uses of Modal Analysis in SSR Studies ...	31
3.3 Equivalent Mass-spring System	32
3.3.1 Mode Frequencies and the Adjustment of the Stiffness Constant	32
3.3.2 Mode Shapes of the Original and Equivalent Systems	35
3.3.3 Eigenvalues of the Original and Reduced Order Models	39
4. EXCITATION CONTROL DESIGN	43
4.1 Introduction	43
4.2 Linear Optimal Control	44
4.3 Eigenvalue Sensitivity	46
4.4 Reduced Order Controller via Eigenvalue Sensitivity Analysis	47
4.5 Examples of the Controller Design	48
4.6 The Output Feedback Control	51
4.7 Eigenvalue Analysis of the Simplified Controllers	53
4.8 Dynamic Performance Test Using Nonlinear Model	53
4.9 The Control Signal	65
5. MULTI-MACHINE SSR STUDIES	67
5.1 Introduction	67
5.2 A Two-machine and a Three-machine System	68
5.3 Prelimary Studies of the Two-machine System	72
5.4 Prelimary Studies of the Three-machine System	80
5.5 Controller Design Considerations of Multi-machine System	83
5.6 Controllers Design and Test of the Two-machine System..	85
5.6.1 Testing of Controllers Using Eigenvalue Analysis	88

Page

5.6.2 Dynamic Performance Test of the Two-machine System 90

5.7 Controllers Design and Test of the Three-machine System 99

5.7.1 Sensitivity Studies and Choice of Weighting Elements in [Q] 100

5.7.2 Dynamic Performance Test of the Three-machine System 107

5.8 Concluding Remarks of the Multi-machine SSR Studies ... 120

6. CONCLUSION 121

REFERENCE 123

APPENDIX I 126

APPENDIX II 127

APPENDIX III 129

LIST OF TABLES

Table		Page
3.1	Modal resonance peaks of the six mass-spring system	29
3.2	Magnitude of the resonant peaks of each mass using approximate modal analysis	29
3.3	Unstable modes of the SSR system	30
3.4-3.6	Eigenvalues of various SSR model at various system conditions	40-42
4.1	Typical value of the eigenvalue shift due to individual state feedback	49
4.2-4.4	Typical mechanical modes of the system with and without control at various operating conditions	54-56
5.1	Summary of the components and number of state in the two-machine system	69
5.2	Summary of the components and number of state in the three-machine system	71
5.3	Various machine operating conditions in the three-machine system	71
5.4	Unstable modes of the two-machine system	72
5.5	Typical mechanical modes of the two-machine system	74
5.6	Typical mechanical modes of the two-machine system using different models for the investigation of torsional interaction between machines	75
5.7	Unstable modes of the three-machine system	80
5.8	Typical mechanical modes of the three-machine system ...	81
5.9	Typical mechanical modes of the three-machine system using different models for the investigation of torsional interaction between machines	82
5.10	Testing sequence for the two-machine system	88
5.11	Typical mechanical modes of the two-machine system without and with control	89
5.12	Typical mechanical modes of the three-machine system with control	102

LIST OF ILLUSTRATIONS

Figure		Page
1.1	Photographs of the damaged generator, Mohave No. 1	2
2.1	Power system model for SSR studies	9
2.2	Modelling of the mass-spring system in the vicinity of the i-th rotational mass	11
2.3	The transmission system	13
2.4	Component of I in dq and DQ coordinates	17
2.5	Power variation of the one-machine infinite-bus system with the mass-spring system modelled in detail	20
2.6	Power variation of the one-machine infinite-bus system with the mass-spring system lumped into one mass	21
2.7	Power variation of the one-machine infinite-bus system with the mass-spring system lumped into one mass and a constant negative resistance inserted in the line	21
3.1	Mode shapes of the six mass-spring system	24
3.2	A torsional mass-spring system	26
3.3	A damped six mass-spring system with unity sinusoidal forcing torque	27
3.4	Variation of the least square error e_ω vs. the variation of K_{45} of the five mass equivalent...............	34
3.5	Variation of the least square error e_ω vs. the variation of K_{23} of the four mass equivalent	34
3.6	Mode shapes of the original and equivalent systems	38
4.1	Dynamic responses of ΔI_q and ΔI_{kq}	51
4.2	Dynamic responses of the power system without control ..	57-60
4.3	Dynamic responses of the power system with control	61-64
4.4	The control signal	66
4.5	The frequency sprectrum of the control signal	66
5.1	A two-machine power system	68
5.2	A three-machine power system	70

Figure | Page

Figure		Page
5.3-5.6	Variation of the real part of the unstable torsional modes of the two-machine system as capacitor compensation of the other line changes	76-79
5.7	Iterative scheme for adapting controller into the original system	84
5.8	Two subsystems resulting from the two-machine system ..	85
5.9	Mode shapes of the original and equivalent systems for machine 2 in the two-machine system	87
5.10	The two-machine system subjected to disturbance	90
5.11-5.12	Typical dynamic responses of the two-machine system without control	91-94
5.13-5.14	Typical dynamic responses of the two-machine system with control	95-98
5.15	Variation of mechanical damping as weighting elements of the damper winding currents change	103-104
5.16	Variation of mechanical damping as weighting elements of the stator currents change	105-106
5.17	The three-machine system subjected to disturbance	107
5.18-5.20	Typical responses of the three-machine system without control	108-113
5.21-5.23	Typical responses of the three-machine system with control	114-119

ACKNOWLEDGEMENT

I would like to express my grateful thanks and deepest gratitude to Dr. Yao-nan Yu and Dr. H. W. Dommel, supervisors of this project, for their continued interest, encouragement and guidance during the research work of this thesis.

Valuable advice from Dr. S. G. Hutton and Dr. M. D. Wvong during the course of this study is gratefully acknowledged.

I am grateful to the department of Electrical Engineering of the University of British Columbia for providing me with excellent typing facilities.

The financial support from the Natural Science and Engineering Research Council of Canada is gratefully acknowledged.

NOMENCLATURE

General

A	system matrix
B	control matrix
u	control vector
x	state vector of the system A
Q	symmetric positive semi-definite weighting matrix
R	symmetric positive definite weighting matrix
K	Riccati matrix
M	composite matrix as defined in (4.7)
Λ	eigenvalue matrix of M
A_c	system matrix of the controlled system
F	feedback matrix as defined in (4.21)
λ	eigenvalue of the system
X,V	eigenvector matrix of A_c and transpose of A_c respectively
$\dot{x}$	time derivative of x
∂	partial differential operator
s	Laplace tramsform operator
Δ	prefix denoting a linearized variable
o	subscript denoting initial condition
T	superscript denoting transpose
-1	superscript denoting inverse
j	complex operator $\sqrt{-1}$

Mass-spring system

M	inertia constant
K	shaft stiffness constant
D	damping coefficient
θ	rotor angular displacement in radian
ω	rotor speed in per unit
ω_o	synchronous speed which is one per unit
ω_b	base speed or 377 radian/second
q	modal angular displacement
Q_{mode}	eigenvector matrix of the mass-spring system

Synchronous Machine

I	instantaneous value of current
V	instantaneous value of voltage
Ψ	flux-linkage
R	resistance
X	reactance
δ	torque angle
T_e	electric torque
I_t	terminal current
V_t	terminal voltage
$P_e + jQ_e$	generator output power
d,q	subscript denoting direct- and quadrature-axis stator quantities
f	subscript denoting field circuit quantities
kd,kq	subscripts denoting direct- and quadrature-axis damper quantities
a	subscript denoting armature phase quantities
i (=1,2,3)	subscript denoting to which machine the quantity belongs

Transmission line

X_{ti}, R_{ti}	reactance and resistance of the i-th transformer
X_{Li}, R_{Li}	reactance and resistance of the i-th transmission line
X_{ci}	reactance of the capacitor in the i-th transmission line
c	subscript denoting quantities associate with capacitor

Exciter and Voltage Regulator

K_{Ai}	gain of the i-th regulator
T_{Ai}	time constant of the i-th regulator
T_{Ei}	time constant of the i-th exciter
V_{ref}	reference voltage

Governor and Steam Turbine System

K_g	actuator gain
T_1, T_2	actuator time constants
T_3	servomotor time constant
a	actuator signal
P_{GV}	power at gate outlet
T_{CH}	steam chest time constant
T_{RH}	reheater time constant
T_{CO}	cross-over time constant
F_{HP}	high pressure turbine power fraction
F_{IP}	medium pressure turbine power fraction
F_{LPA}	low pressure turbine A power fraction
F_{LPB}	low pressure turbine B power fraction
T_{HP}	high pressure turbine torque
T_{IP}	medium pressure torque
T_{LPA}, T_{LPB}	low pressure turbine torque

1. INTRODUCTION

1.1 Subsynchronous Resonance

The application of series capacitors to increase the power transfer capability of the transmission system is the best alternative to cope with the ever-increasing electric power damand, the unavaibility of generation sites to build thermal electric power plant at heavy load centers, and the difficulties in obtaining the right of way to build new transmission lines due to envirnomental and economical considerations. However, the series-capacitor-compensated transmission line will cause electrical resonance at certain frequencies which may excite the mechanical mode oscillations of the steam turbine and generator mass-spring system resulting in shaft damage and other detrimental effect to the power system. The term "Subsynchronous Resonance (SSR)" has been used to designate the oscillating phenomenon of the electrical and mechanical variables associated with turbine-generators connected to transmission systems with series capacitor compensation. Typical example of the damaging effect due to SSR is illustrated in Figure 1.1 ; there were two shaft failures at Mohave generating station in 1970 and 1971 [1].

Despite the hazards of SSR, utilities still favor the use of series capacitors to increase the power transfer capability. In order to overcome the problems caused by SSR, extensive effort has been made in analyzing the two shaft failures. Problems are identified as the induction generator effect, torsional interaction, and transient torques [2].

SSR phenomenon may occur in two different forms : the steady state SSR which is the result of induction generator effect and torsional

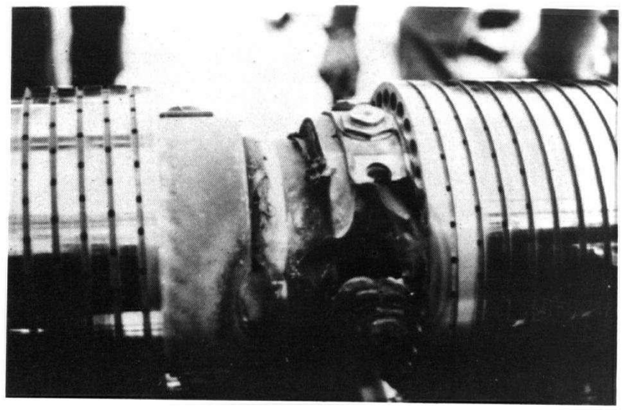

(a)

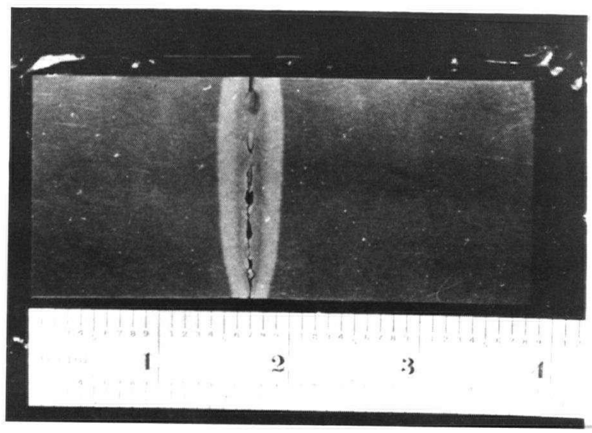

(b)

Figure 1.1 Photographs of

(a) Damaged collector, Mohave No. 1
(b) Cross section from damaged shaft.

* Pictures are taken from reference [3].

interaction, and the transient SSR which involves the transient torques on segments of the turbine-generator shaft caused by fault or switching operation in the electrical system.

1.2 Countermeasures to SSR

In the past decade, many countermeasures to SSR problems are proposed. Some significant ones are as follows:

1) Static blocking filter [2,4]

High quality factor blocking filters are inserted per-phase in between the high voltage winding of the step-up transformer and the neutral to block electrical resonance currents at the critical frequencies corresponding to the torsional modes of the turbine-generator mass-spring system. When perfectly tuned, the filters will block the currents at critical frequencies completely. But the filters may be detuned due to the change in system frequency after a disturbance or the change in ambient temperature which affects the filter's parametric values. A large space is required to install the filters and the basic insulation level of the step-up transformer must be increased; it is an expensive device.

2) Dynamic filter [5]

An active device which generates a voltage in series with the generator to nullify the subsynchronous voltage generated by any oscillating motion of the rotor, thereby preventing self excitation due to the torsional interaction. It is unaffected by the system frequency and the number of series capacitors in service. But it is quite costly because of the complex control system and the requirement of an isolated power source.

3) Dynamic stabilizer [6,7]

The device consists of thyristor controlled shunt reactors connected to the synchronous machine terminal. Control of SSR is achieved by modulating the thyristor switch firing angles to control the reactive power consumed by the reactors.

4) Bypassing the series capacitor

a) The series capacitor is bypassed with the aid of a dual gap which flashes at a lower current level to limit the transient torque build-up, and the gap is reset each time to a higher level allowing a current decay to the level for successful reinsertion of the capacitor. The dual gap flashing scheme can reduce the transient torque significantly [2].

b) In another scheme, called the NGH-SSR scheme [8,9], a thyristor pair in series with a resistor is inserted across the capacitor. By firing the thyristors by some control scheme, the capacitor's charges are dissipated through the resistor. However, this device cannot be used to stabilize the SSR system over a wide range of capacitor compensation [8].

5) Supplemental excitation control

By this method, signal obtained from a properly designed controller is used to modulate the output of the excitation in response to the torsional oscillations of the turbine-generator, and hence provides adequate damping to the SSR system.

Although the shaft failure incidents are ten years old, many ongoing researches are still focused on SSR , indicating that power engineers are still searching for more effective and less expensive means to overcome the problem. Of all the proposed countermeasures of SSR, the supplemental excitation control seems to be the least expensive means which needs further investigation.

1.3 Previous Works of Excitation Control of SSR

Excitation control of SSR involves the use of a control signal to modulate the output of the excitation system to enhance the damping of torsional modes of the generator mass-spring system. Many control schemes have been proposed [10-18], but it is very desirable to have a controller which can stabilize multi-mode SSR oscillations in a multi-machine power system over a wide range of capacitor compensation and operating conditions. The major approaches of the controller design are two:

1) Transfer function approach [10-16]

A linearized model is used for the controller design and it is mainly based upon the phase compensation concept; a transfer function representing the controller is assumed and the parameters of the controller are chosen such that it can stabilize the system. Since the generator mass-spring system representation plays a very important role in SSR studies, the control design based on a one lumped-mass generator model can only suppress the electrical resonance phenonmena [10-13], and cannot reduce the torsional interaction between the electrical and mechanical systems [12].

Unified electro-mechanical system model is also used in excitation control design [14-16], but the effectiveness of the controllers are verified on the linearized model [14], and neglecting the exciter voltage ceiling limits [15,16]. There is no evidence that those controllers can stabilize the SSR system over a wide range of operating conditions and capacitor compensation.

2) Linear Optimal Excitation Control

For the control design, a unified electrical and mechanical model is developed [17]. A linearized model is used for the control design, based upon modern control laws, and using a linear combination of feedback signals which collectively ensures proper damping to all torsional modes of the system [17,18].

Although application of linear optimal excitation control (LOEC) to power system dynamic stability control is well documented [19-21], it is relatively new in using LOEC for SSR stabilization. To apply LOEC to SSR problem, Yu,Wvong,and Tse had shown as the first step the feasibility of linear stabilization of SSR which is not optimal [17]. The work was continued by Yan,Wvong, and Yu [18] to develop LOEC of SSR. The control was tested on both linear and nonlinear full models. The results indicated that the LOEC can effectively stabilize the SSR system over a wide range of capacitor compensation and operating conditions.

But the design still requires improvement, especially in two aspects

1) The order of the model in [17,18] shall be further reduced for the controller design and the controller designed must be simplified to the extent that only a minimum number of measurable output feedback signals are required to implement the controller. Techniques of further reduction of the model and simplification of the final control must therefore be developed.
2) The excitation control of SSR must be applicable not only to the one-machine system but also to a multi-machine system. There is dynamic interaction between machines in a multi-machine SSR system, which may be divided into two categories:

a) The dynamic interaction of the low frequency oscillations between machines [22].

b) The interaction between the torsional modes of the mass-spring system of different machines [23].

1.4 Scope of the Thesis

This thesis deals with the output feedback linear optimal excitation control of one-machine and multi-machine SSR systems. Chapter two recapitulates all the basic equations of power system models for SSR studies. The torsional interaction effect between the electrical and mechanical systems is illustrated. In Chapter three, modal analysis is applied to the generator mass-spring system and a mass-spring equivalencing technique [24] for model reduction is developed. In Chapter four, procedures of linear optimal excitation control design are given, and the designed controller is implemented to the full model for both eigenvalue analysis and nonlinear dynamic performance tests. In Chapter five, the multi-machine SSR problem is examined, one machine equivalents of the multi-machine system are developed, and the excitation controls designed for a two-machine and a three-machine power system are implemented on the full models for eigenvalue analysis and nonlinear dynamic performance tests. Summary of all the important findings is given and a conclusion is drawn in Chapter six.

2. MODELLING POWER SYSTEMS FOR SSR STUDIES

2.1 Introduction

To accurately simulate the transient and dynamic behaviour of a power system, a proper and adequate model must be chosen. In conventional power system stability studies for which the low frequency oscillations (.5 - 2 Hz.) is of the main concern, the generator and turbine shaft stiffness, the amortisseur winding effect, and the armature and network transient may be neglected. However, for SSR studies, the emphasis in modelling system components is different. In order to account for the torsional oscillations of the mechanical mass-spring system and the torsional interaction between electrical and mechanical systems, those factors which are not important in conventional stability studies can no longer be neglected.

In the first part of this chapter, a summary of equations describing the power system for SSR studies is given. The complete model for a one machine system is shown in Figure 2.1, which consists of the turbine generator mass-spring system, the speed governor and the turbine torque [25], the generator and excitation [26], and the capacitor compensated transmission line. In the second part of this chapter, the complete system state equations are obtained. It is applicable to both single machine and multi-machine systems. Towards the end of this chapter, the effect of torsional interaction between mechanical and electrical systems is illustrated.

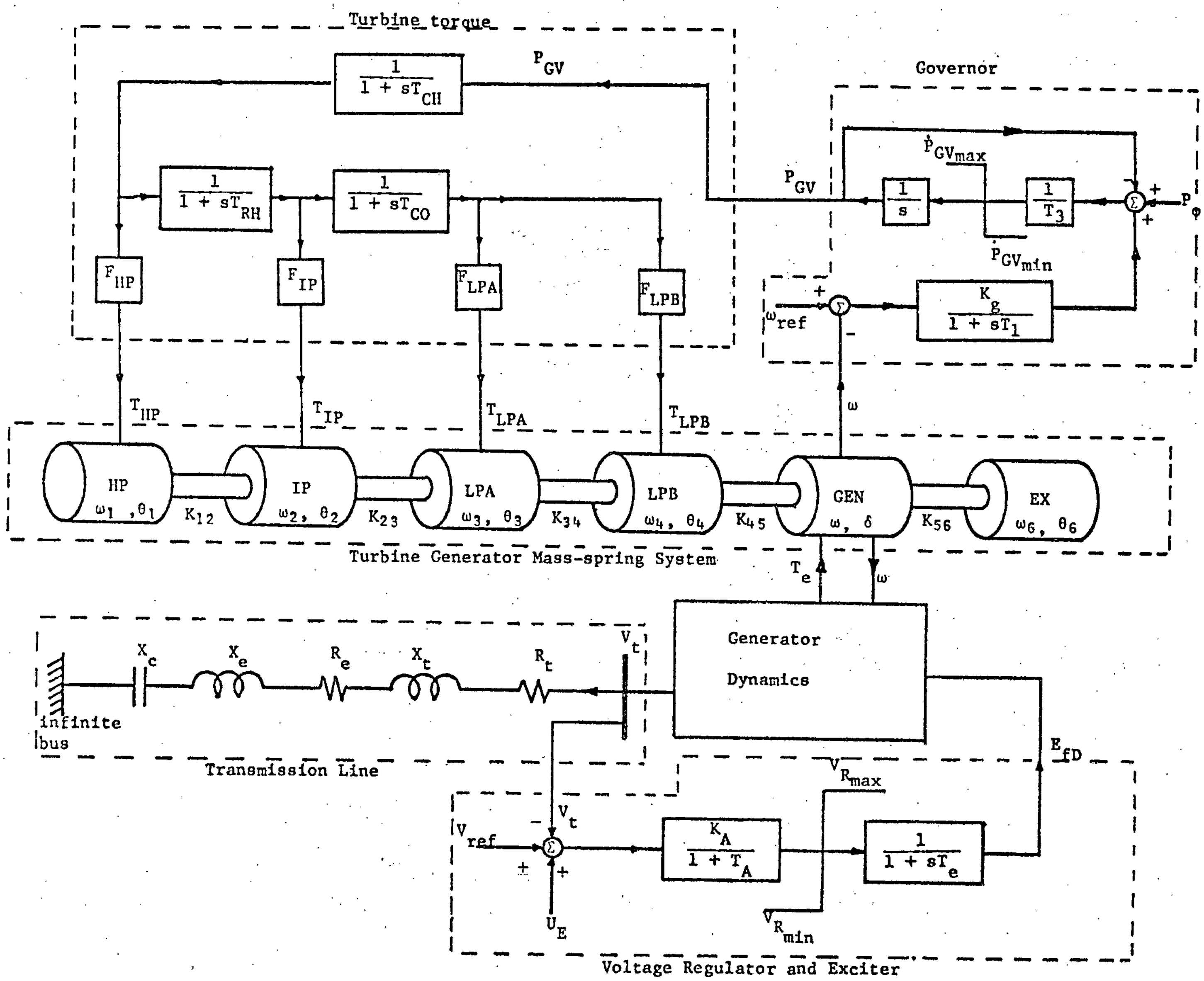

Figure 2.1 Power system model for SSR studies

2.2 The Mechanical System

Consider the torques of the steam turbines first, they may be written as

$$\dot{T}_{HP} = \frac{F_{HP}}{T_{CH}} P_{GV} - \frac{1}{T_{CH}} T_{HP} \tag{2.1}$$

$$\dot{T}_{IP} = \frac{F_{IP}}{F_{HP}\, T_{RH}} T_{HP} - \frac{1}{T_{RH}} T_{IP} \tag{2.2}$$

$$\dot{T}_{LPA} = \frac{F_{LPA}}{F_{IP}\, T_{CO}} T_{IP} - \frac{1}{T_{CO}} T_{LPA} \tag{2.3}$$

$$T_{LPB} = \frac{T_{LPB}}{T_{LPA}} T_{LPA} \tag{2.4}$$

where

P_{GV} : power at gate outlet

T_{CH} : steam chest time constant

T_{RH} : reheater time constant

T_{CO} : cross-over time constant

F_{HP} : high pressure turbine power fraction

F_{IP} : medium pressure turbine power fraction

F_{LPA} : low pressure turbine A power fraction

F_{LPB} : low pressure turbine B power fraction

T_{HP} : high pressure turbine torque

T_{IP} : medium pressure turbine torque

T_{LPA} : low pressure turbine A torque

T_{LPB} : low pressure turbine B torque

Consider the mass-spring system next. Assume that there is one high pressure turbine (HP), one medium pressure turbine (IP), two low pressure turbines (LPA,LPB), one generator (Gen), and one exciter (Ex),all on one shaft as shown in Figure 2.1. Although a more accurate mass-spring model is available by modelling shaft and masses in finite sections [34], a linear mass-spring model is recommended by an IEEE committee report for SSR analysis [35]. According to [35], it is assumed that

(a) There are six lumped masses, each with its inertia constant.

(b) The shaft between any two masses behaves like a linear torsional spring with negligible mass.

(c) There is mechanical damping to each rotating mass, although it is very difficult to determine [36].

Figure 2.2 illustrates the various torsional forces experienced by the i^{th} element on the mass-spring system. A positive torsional torque $K_{i,i+1}(\theta_{i+1} - \theta_i)$ on the right; a negative torque $-K_{i-1,i}(\theta_i - \theta_{i-1})$ on the left ; and an external torque T_i, a positive accelerating torque $M_i\dot{\omega}_i$, and a negative damping torque $-D_i\omega_i$ on the mass itself. A general equation of motion of the i^{th} rotor is as follows

$$M_i\dot{\omega}_i = T_i - D_i\omega_i + K_{i,i+1}(\theta_{i+1} - \theta_i) - K_{i-1,i}(\theta_i - \theta_{i-1}) \qquad (2.5)$$

where M_i : inertia constant of the i^{th} rotational mass

θ_i : angular displacement of the i^{th} rotational mass

$K_{i,i+i}$: torsional stiffness constant of the shaft between i^{th} and $i+1^{th}$ rotational mass

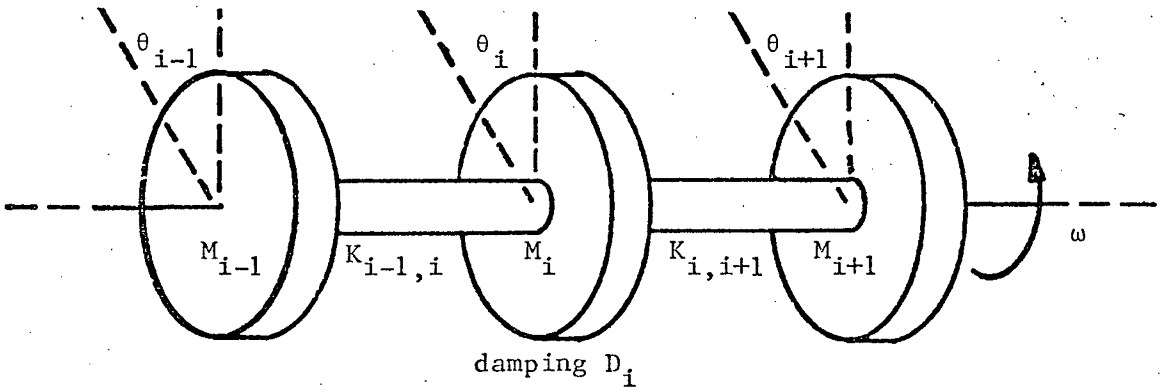

Figure 2.2 Modelling of the mass-spring system in the vicinity of the i^{th} rotational mass

Applying equation (2.5) to the six mass-spring system as shown in Figure 2.1, twelve differential equations are obtained :

High pressure turbine

$$\dot{\omega}_1 = \frac{K_{12}}{M_1}\theta_2 - \frac{K_{12}}{M_1}\theta_1 - \frac{D_1}{M_1}\omega_1 + \frac{T_{HP}}{M_1} \tag{2.6}$$

$$\dot{\theta}_1 = \omega_b(\omega_1 - \omega_o) \tag{2.7}$$

Medium pressure turbine

$$\dot{\omega}_2 = \frac{K_{12}}{M_2}\theta_1 - \left(\frac{K_{12}+K_{23}}{M_2}\right)\theta_2 + \frac{K_{23}}{M_2}\theta_3 - \frac{D_2}{M_2}\omega_2 + \frac{T_{IP}}{M_2} \tag{2.8}$$

$$\dot{\theta}_2 = \omega_b(\omega_2 - \omega_o) \tag{2.9}$$

Low pressure turbine A

$$\dot{\omega}_3 = \frac{K_{23}}{M_3}\theta_2 - \left(\frac{K_{23}+K_{34}}{M_3}\right)\theta_3 + \frac{K_{34}}{M_3}\theta_4 - \frac{D_3}{M_3}\omega_3 + \frac{T_{LPA}}{M_3} \tag{2.10}$$

$$\dot{\theta}_3 = \omega_b(\omega_3 - \omega_o) \tag{2.11}$$

Low pressure turbine B

$$\dot{\omega}_4 = \frac{K_{34}}{M_4}\theta_3 - \left(\frac{K_{34}+K_{45}}{M_4}\right)\theta_4 + \frac{K_{45}}{M_4}\theta_5 - \frac{D_4}{M_4}\omega_4 + \frac{T_{LPB}}{M_4} \tag{2.12}$$

$$\dot{\theta}_4 = \omega_b(\omega_4 - \omega_o) \tag{2.13}$$

Generator

$$\dot{\omega} = \frac{K_{45}}{M_5}\theta_4 - \left(\frac{K_{45}+K_{56}}{M_5}\right)\delta + \frac{K_{56}}{M_5}\theta_6 - \frac{D_5}{M_5}\omega - \frac{T_e}{M_5} \tag{2.14}$$

$$\dot{\delta} = \omega_b(\omega - \omega_o) \tag{2.15}$$

Exciter

$$\dot{\omega}_6 = \frac{K_{56}}{M_6}\delta - \frac{K_{56}}{M_6}\theta_6 - \frac{D_6}{M_6}\omega_6 \tag{2.16}$$

$$\dot{\theta}_6 = \omega_b(\omega_6 - \omega_o) \tag{2.17}$$

where δ : electrical angular displacement in electrical radian which is equal to the mechanical radian for a two-pole machine.

ω_i: speed of the i^{th} rotor in per unit.

ω_o: synchronous speed which is one per unit.

ω_b: base speed or 377 radian/second

θ : mechanical angular displacement in radian.

T_e: electric torque across the air gap in per unit.

Consider a speed governor next. The state equations may be written

$$\dot{a} = \frac{K_g}{T_1} (\omega_{ref} - \omega) - \frac{1}{T_1} a \tag{2.18}$$

$$\dot{P}_{GV} = \frac{1}{T_3} a - \frac{1}{T_3} (P_{GV} - P_o) \tag{2.19}$$

$$\dot{P}_{GV_{min}} \leq \dot{P}_{GV} \leq \dot{P}_{GV_{max}}$$

where

K_g : actuator gain

T_1 : actuator time constant

T_3 : servomotor time constant

a : actuator signal

ω : generator speed

ω_{ref}: reference speed

P_o : initial power reference

2.3 The Electrical System

A transmission system between any two buses is shown in Figure 2.3, where R_t is the transformer resistance, X_t is its reactance, R_L the transmission line resistance, X_L the line reactance, and X_c the capacitor reactance. For a one machine infinite system, V_t denotes the generator terminal voltage, V_o the infinte bus voltage, and V_c the voltage across the capacitor.

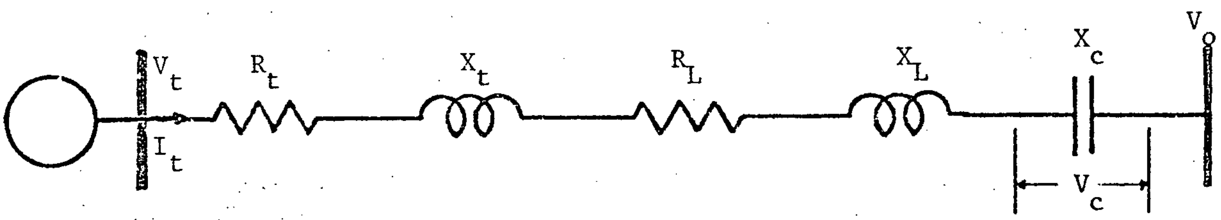

Figure 2.3 The transmission system

The general voltage equation becomes

$$[\ V_t\ ]_{phase} = [\ R\ ]\ [\ I_t\ ]_{phase} + [\ L\ ]\ \frac{d}{dt}\ [\ I_t\ ]_{phase} + [\ V_c\ ]_{phase} + [\ V_o\ ]_{phase} \qquad (2.20)$$

In Park's coordinates and for a balanced three-phase operation the d and q components of the generator terminal voltage become

$$V_d = \left(\frac{X_t + X_L}{\omega_b} \right) \dot{I}_d - (\ X_t + X_L\ )\ I_q + (\ R_t + R_L\ )\ I_d + V_{cd} + V_{od} \qquad (2.21)$$

$$V_q = \left(\frac{X_t + X_L}{\omega_b} \right) \dot{I}_q + (\ X_t + X_L\ )\ I_d + (\ R_t + R_L\ )\ I_q + V_{cq} + V_{oq} \qquad (2.22)$$

and the two infinite bus voltage components are

$$V_{od} = V_o \sin\delta_o$$
$$V_{oq} = V_o \cos\delta_o \qquad (2.23)$$

where V_o is the magnitude of the infinite bus voltage, and δ_o is the angle between machine terminal and the infinite bus. For a multi-machine system, V_o is not the infinite bus voltage anymore.

The capacitor voltages in the d-q coordinate become

$$\frac{\dot{V}_{cd}}{\omega_b} = V_{cq} + \omega\ X_c I_d \qquad (2.24)$$

$$\frac{\dot{V}_{cq}}{\omega_b} = -V_{cd} + \omega\ X_c I_q \qquad (2.25)$$

Equations for exciter and voltage regulator are

$$\dot{E}_{fD} = \frac{1}{T_E} V_R - \frac{1}{T_E} E_{fD} \tag{2.26}$$

$$\dot{V}_R = \frac{K_A}{T_A} (V_{ref} - V_t + U_E) \tag{2.27}$$

$$V_t = \sqrt{V_d^2 + V_q^2} \tag{2.28}$$

$$V_{R_{min}} \leq V_R \leq V_{R_{max}}$$

where

U_E is the supplementary control signal

K_A is the voltage regulator gain

T_A is the voltage regulator time constant

T_E is the exciter time constant

E_{fD} is the exciter output voltage

$V_{R_{min}}$ and $V_{R_{max}}$ are the regulator ceiling voltage

Previous work [18] found that five winding generator model with one damper winding on each of the d,q-axis is sufficient. The voltage equations of synchronous generator are [37,38]

$$V_d = \frac{\dot{\Psi}_d}{\omega_b} - \omega\Psi_q - R_a I_d \tag{2.29}$$

$$V_q = \frac{\dot{\Psi}_q}{\omega_b} + \omega\Psi_d - R_a I_q \tag{2.30}$$

$$V_f = \frac{\dot{\Psi}_f}{\omega_b} + R_f I_f \tag{2.31}$$

$$0 = \frac{\dot{\Psi}_{kd}}{\omega_b} + R_{kd} I_{kd} \tag{2.32}$$

$$0 = \frac{\dot{\Psi}_{kq}}{\omega_b} + R_{kq} I_{kq} \tag{2.33}$$

and the electric torque equation in per unit is

$$T_e = \Psi_d I_q - \Psi_q I_d \tag{2.34}$$

where the flux linkage

$$\begin{bmatrix} \Psi_d \\ \Psi_q \\ \Psi_f \\ \Psi_{kd} \\ \Psi_{kq} \end{bmatrix} = \begin{bmatrix} -X_d & & X_{md} & X_{md} & \\ & -X_q & & & X_{mq} \\ -X_{md} & & X_f & X_{md} & \\ -X_{md} & & X_{md} & X_{kd} & \\ & -X_{mq} & & & X_{kq} \end{bmatrix} \begin{bmatrix} I_d \\ I_q \\ I_f \\ I_{kd} \\ I_{kq} \end{bmatrix} \tag{2.35}$$

2.4 Complete System Equations for Single and Multi-machine Systems

The original nonlinear equations are used for time domain simulation , and the equations are linearized for eigenvalue analysis. The linearized electrical system equations may be written in the matrix form as follows

$$[\,B\,][\,\dot{X}_{II}\,] = [\,C\,][\,X_I\,] + [\,D\,][\,X_{II}\,] \tag{2.36}$$

Hence

$$[\,\dot{X}_{II}\,] = [\,A_{II,I}\,][\,X_I\,] + [\,A_{II,II}\,][\,X_{II}\,] \tag{2.37}$$

where

$$[\,A_{II,I}\,] = [\,B\,]^{-1}[\,C\,] \tag{2.38}$$

$$[\,A_{II,II}\,] = [\,B\,]^{-1}[\,D\,] \tag{2.39}$$

$[\,X_{I,II}\,]$ and $[\,X_{II,I}\,]$ represent the interaction between the mechanical system and the electrical system which can be combined with the linearized mechinical system equations to give

$$\begin{pmatrix} \dot{X}_I \\ \dot{X}_{II} \end{pmatrix} = \begin{pmatrix} A_{I,I} & A_{I,II} \\ A_{II,I} & A_{II,II} \end{pmatrix} \begin{pmatrix} X_I \\ X_{II} \end{pmatrix} \tag{2.40}$$

where

$$[\, X_I \,] = [\, \Delta\omega_1, \Delta\theta_1, \Delta\omega_2, \Delta\theta_2, \Delta\omega_3, \Delta\theta_3, \Delta\omega_4, \Delta\theta_4, \Delta\omega, \Delta\delta, \Delta\omega_6, \Delta\theta_6,$$

$$\Delta a, \Delta P_{GV}, \Delta T_{HP}, \Delta T_{IP}, \Delta T_{LPA} \,]^T \tag{2.41}$$

$$[\, X_{II}] = [\, \Delta I_d, \Delta I_q, \Delta I_f, \Delta I_{kd}, \Delta I_{kq}, \Delta V_{cd}, \Delta V_{cq}, \Delta V_R, \Delta E_{fd} \,]^T \tag{2.42}$$

Equation (2.40) may also be written compactly as

$$[\, \dot{X} \,] = [\, A \,][\, X \,] \tag{2.43}$$

For a multi-machine system where more than one machine is involved, the individual machine coordinate (d,q) may be referred to a common reference frame (D,Q) as follows:

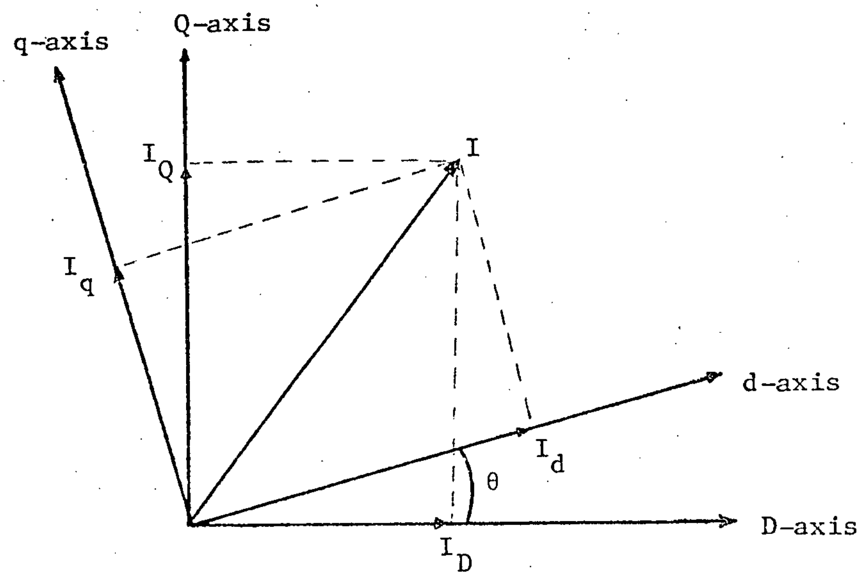

Figure 2.4 Component of I in dq and DQ coordinates

where

$$\begin{bmatrix} I_D \\ I_Q \end{bmatrix} = \begin{bmatrix} \cos\theta & -\sin\theta \\ \sin\theta & \cos\theta \end{bmatrix} \begin{bmatrix} I_d \\ I_q \end{bmatrix} \tag{2.44}$$

Linearized,

$$\begin{bmatrix} \Delta I_D \\ \Delta I_Q \end{bmatrix} = \begin{bmatrix} \cos\theta_0 & -\sin\theta_0 \\ \sin\theta_0 & \cos\theta_0 \end{bmatrix} \begin{bmatrix} \Delta I_d \\ \Delta I_q \end{bmatrix} + \begin{bmatrix} -(I_{do}\sin\theta_0 + I_{qo}\cos\theta_0) \\ (I_{do}\cos\theta_0 - I_{qo}\sin\theta_0) \end{bmatrix} \Delta\theta \tag{2.45}$$

Therefore

$$\begin{bmatrix} \Delta\dot{I}_D \\ \Delta\dot{I}_Q \end{bmatrix} = \begin{bmatrix} \cos\theta_0 & -\sin\theta_0 \\ \sin\theta_0 & \cos\theta_0 \end{bmatrix} \begin{bmatrix} \Delta\dot{I}_d \\ \Delta\dot{I}_q \end{bmatrix} + \begin{bmatrix} -(I_{do}\sin\theta_0 + I_{qo}\cos\theta_0) \\ (I_{do}\cos\theta_0 - I_{qo}\sin\theta_0) \end{bmatrix} \Delta\dot{\theta} \tag{2.46}$$

Inversely,

$$\begin{bmatrix} I_d \\ I_q \end{bmatrix} = \begin{bmatrix} \cos\theta & \sin\theta \\ -\sin\theta & \cos\theta \end{bmatrix} \begin{bmatrix} I_D \\ I_Q \end{bmatrix} \tag{2.47}$$

Linearized

$$\begin{bmatrix} \Delta I_d \\ \Delta I_q \end{bmatrix} = \begin{bmatrix} \cos\theta_0 & \sin\theta_0 \\ -\sin\theta_0 & \cos\theta_0 \end{bmatrix} \begin{bmatrix} \Delta I_D \\ \Delta I_Q \end{bmatrix} + \begin{bmatrix} (I_{Qo}\cos\theta_0 - I_{Do}\sin\theta_0) \\ -(I_{Do}\cos\theta_0 + I_{Qo}\sin\theta_0) \end{bmatrix} \Delta\theta \tag{2.48}$$

Therefore

$$\begin{bmatrix} \Delta\dot{I}_d \\ \Delta\dot{I}_q \end{bmatrix} = \begin{bmatrix} \cos\theta_0 & \sin\theta_0 \\ -\sin\theta_0 & \cos\theta_0 \end{bmatrix} \begin{bmatrix} \Delta\dot{I}_D \\ \Delta\dot{I}_Q \end{bmatrix} + \begin{bmatrix} (I_{Qo}\cos\theta_0 - I_{Do}\sin\theta_0) \\ -(I_{Do}\cos\theta_0 + I_{Qo}\sin\theta_0) \end{bmatrix} \Delta\dot{\theta} \tag{2.49}$$

For the multi-machine formulation, it is convenient to write

$$\begin{aligned} X_I &= [\, X_{I1}\,,\ X_{I2}\,,\ X_{I3}\,,\ \ldots\ldots\ldots\ldots,\ X_{Ii}\,]^T \\ X_{II} &= [\, X_{II1},\ X_{II2},\ X_{II3},\ldots\ldots\ldots\ldots,\ X_{IIi}\,]^T \end{aligned} \tag{2.50}$$

where X_{Ii} , X_{IIi} are the mechanical and electrical state variables of machine i, respectively.

2.5 The Torsional Interaction

When an electrical resonance occurs in the electrical system (including the generator stator and transmission line) at a subsynchronous frequency f_e, it will interact with the rotor and induce a pulsating torque at the frequency of ($60 - f_e$), which becomes a forcing torque to the mass-spring system. If the frequency of the oscillating torque equals to a torsional modal frequency f_m, the electrical resonance and the particular torsional mode will be mutually excited, and a voltage will be induced in stator winding at frequency $f_e = 60-f_m$. Thus the torsional interaction looks like a negative resistance to the electrical system and negative damping to the torsional system under these conditions.

To illustrate the effect of torsional interaction, the one machine infinite bus system as shown in Figure 2.1 is tuned so that SSR will occur.

The variation of electric power which is approximately equal to the electric torque in the per unit system, as shown in Figure 2.5, roughly consists of two components: a low frequency oscillation in the range of 1 - 2 Hz. , and a higher frequency oscillation . In this particular case, the subsynchronous torque increases with time.

The results of Figure 2.5 also can be synthesized as follows : First let the system be modified by lumping the six torsional masses into one. The power variations for the same system disturbance are shown as Figure 2.6. The responses as shown in Figure 2.5 and 2.6 are the same within 0.5 second but there is no subsynchronous torque component in

Figure 2.6 because of the modelling.

A constant negative resistance is then inserted in the transmission line of the above modified system. The system response for the same disturbance is shown in Figure 2.7. Although the mass-spring system model has been simplified, the subsynchronous torque component is substantial. The concept that the torsional system looks like a negative resistance to the electrical system is further verified. Of course, a static negative resistance representation of the torsional interaction is over-simplified in the SSR studies.

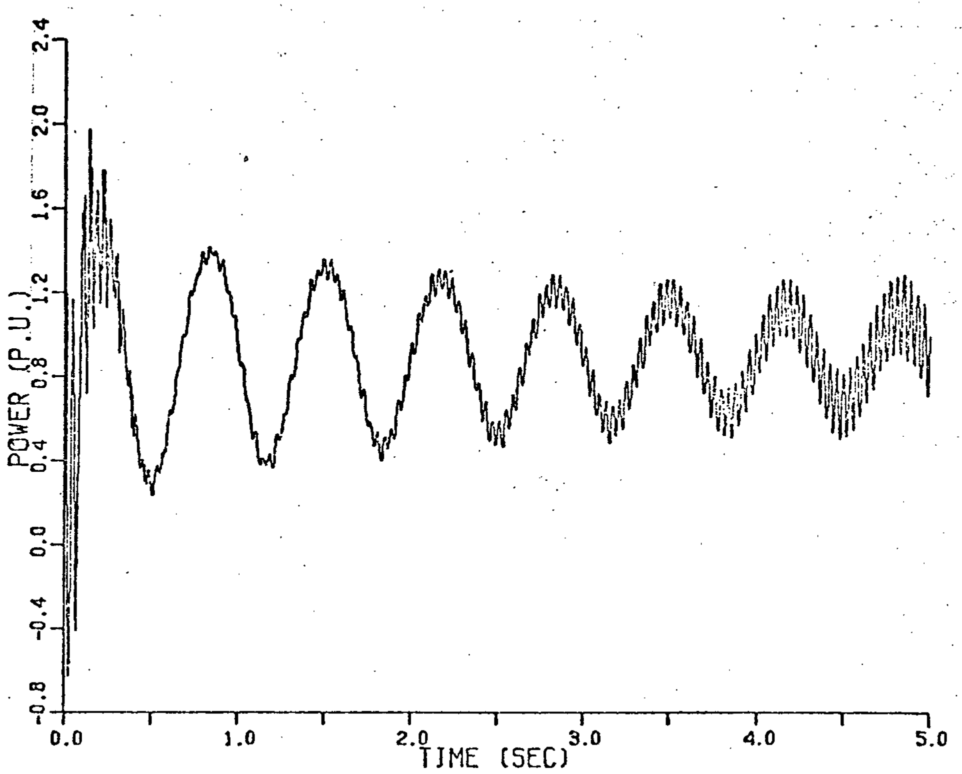

Figure 2.5 Power variation of the one-machine infinite bus system with the mass-spring system modelled in detail.

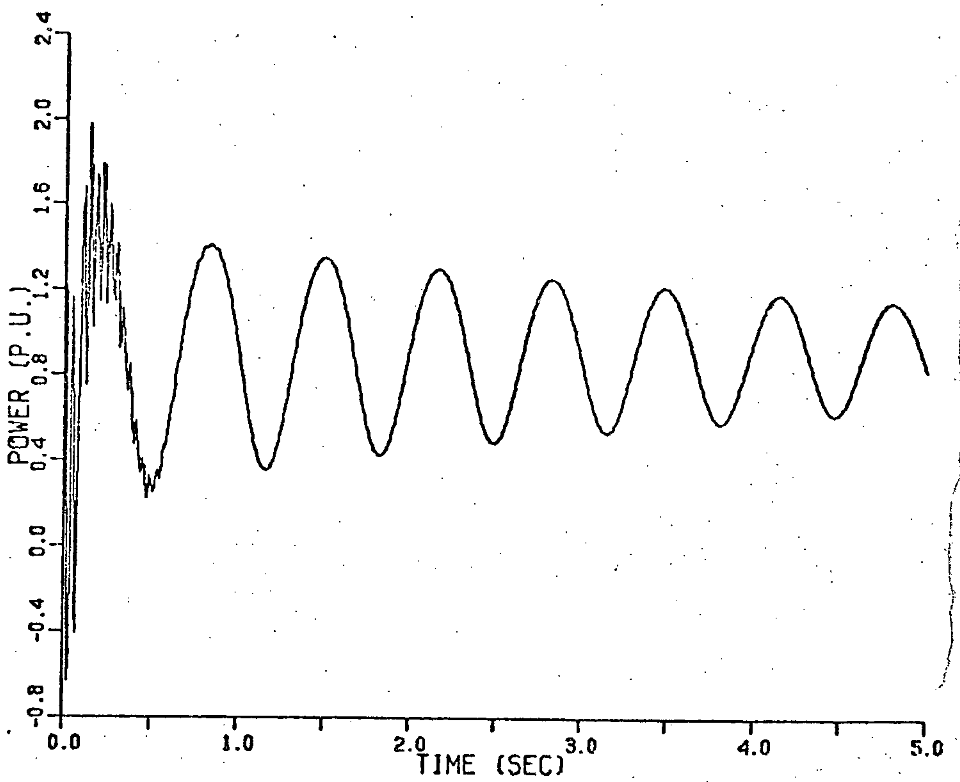

Figure 2.6 Power variation of the one-machine infinite bus system with the mass-spring system lumped into one mass.

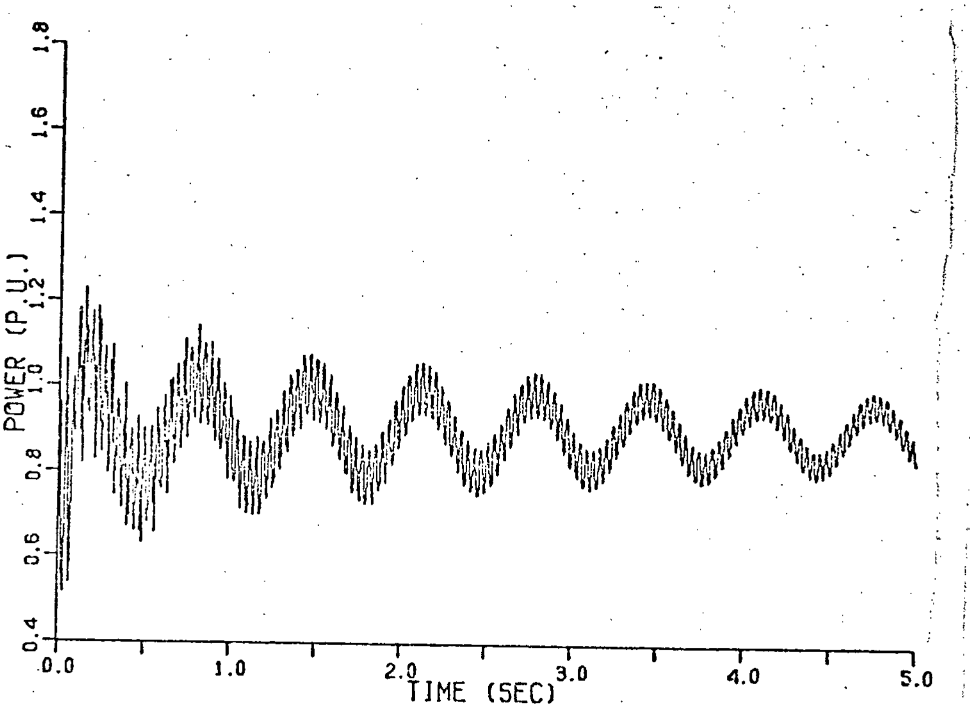

Figure 2.7 Power variation of the one-machine infinite bus system with the mass-spring system lumped into one mass and a constant negative resistance inserted in the transmission line.

3. MODEL REDUCTION OF A POWER SYSTEM FOR SSR STUDIES

3.1 Introduction

The requirement of including the torsional mass-spring system, the generator, and transmission system in one single unified model for SSR studies so that the torsional interaction of the electrical and mechanical systems will be automatically included inevitably results in a very high order system. For instance, the full model of a one-machine infinite-bus system for SSR studies developed in the last chapter is of 26th order. For some SSR studies, especially for the control design, a reduced order model is very desirable.

For an excitation control design, the steam turbine torque and governor equations together with a small time constant of the exciter can be neglected. The order of the model is reduced from 26th to 20th.

However, further order reduction is still necessary. A new technique of obtaining a reduced order equivalent mass-spring system is developed in this chapter by retaining the unstable torsional modes alone without changing their oscillating frequencies. The first step is to determine the relative instability among the unstable modes using modal analysis. The second step is to retain only the unstable torsional modes. Finally, the eigenvalues of the original model and the reduced order models are compared.

3.2 Torsional Resonance and the Unstable Modes

The prevailing techniques in SSR stability studies are either the frequency scanning method together with the torsional interaction equations [27] to determine the stability of the torsional modes one at a time, or apply either eigenvalue analysis or Nyguist criteria [28] to the unified electro-mechanical power system. Without the analysis, no one could confidently predict which mode is more vulnerable to torsional oscillations than others. In this section, a technique to identify the excitable torsional modes, or the mode which is vulnerable to torsional interaction, and to determine the relative instability of the unstable modes is presented. The technique requires no information about the electrical network, and is based on the modal analysis of the torsional mass-spring system alone.

3.2.1 Natural Frequencies and Mode Shapes of the Mass-spring System

The natural frequencies and the mode shapes of the turbine generator mass-spring system can be found as follows:

Consider an unforced and undamped mass-spring system as shown on top of Figure 3.1. The system can be described by a set of second order differential equations in matrix form as follows

$$\frac{1}{\omega_b}[\,M\,][\,\ddot{\theta}\,] + [\,K\,][\,\theta\,] = 0 \tag{3.1}$$

where

$$[\,M\,] = \text{diag}\ [\,M_1,\ M_2,\ M_3,\ M_4,\ M_5,\ M_6\,] \tag{3.2}$$

$$[\,\theta\,] = [\,\theta_1,\ \theta_2,\ \theta_3,\ \theta_4,\ \theta_5,\ \theta_6\,]^T \tag{3.3}$$

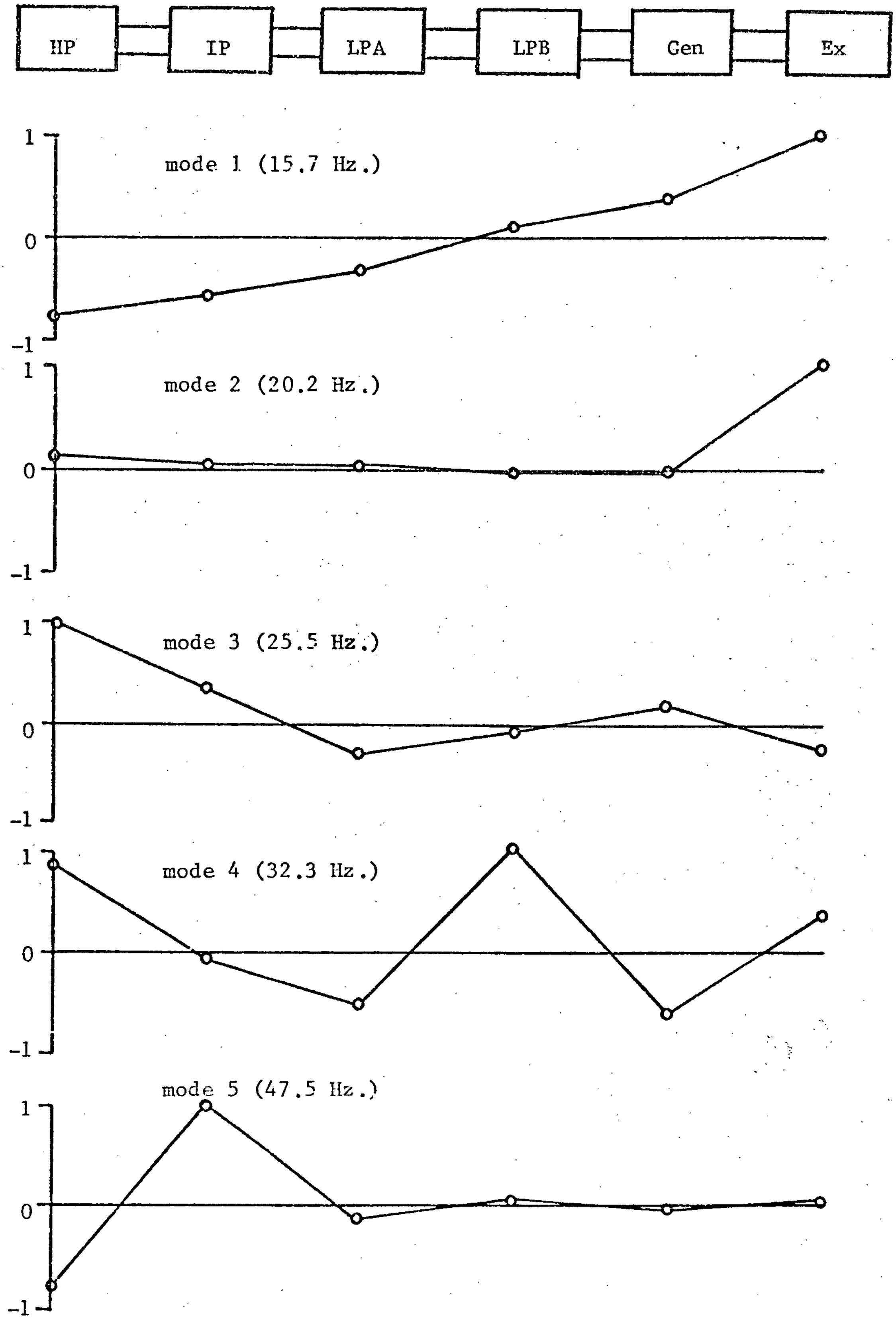

Figure 3.1 Mode Shapes of the six mass-spring system

$$[K] = \begin{bmatrix} K_{12} & -K_{12} & 0 & 0 & 0 & 0 \\ -K_{12} & (K_{12}+K_{23}) & -K_{23} & 0 & 0 & 0 \\ 0 & -K_{23} & (K_{23}+K_{34}) & -K_{34} & 0 & 0 \\ 0 & 0 & -K_{34} & (K_{34}+K_{45}) & -K_{45} & 0 \\ 0 & 0 & 0 & -K_{45} & (K_{45}+K_{56}) & -K_{56} \\ 0 & 0 & 0 & 0 & -K_{56} & K_{56} \end{bmatrix} \qquad (3.4)$$

where the subscripts 1,2,3,...,6 correspond to HP, IP, LPA, LPB, Gen, Ex respectively.

Assume that all masses oscillate at a resonant frequency ω_m, such that

$$\theta_i = X_i \sin(\omega_m t + \alpha) \qquad i = 1,2,.....,6 \qquad (3.5)$$

Substituting equation (3.5) into (3.1) gives

$$\left(\frac{\omega_m^2}{\omega_b}\right) [X] - [M]^{-1}[K][X] = 0 \qquad (3.6)$$

or

$$[M]^{-1}[K][X] = \lambda_m [X] \qquad (3.7)$$

where

$$\lambda_m = \omega_m^2 / \omega_b \qquad (3.8)$$

Therefore λ_m can be obtained by solving (3.7) and mode frequency ω_m can be calculated from

$$\omega_m = \sqrt{\lambda_m \omega_b} \qquad m = 0,1,...,5 \qquad (3.9)$$

There is an eigenvector X_m corresponding to each eigenvalue λ_m, which, when normalized with respect to the element with the largest magnitude gives the mode shape of that particular mode. The mode frequencies and the mode shapes of the mass-spring system are given in Figure 3.1. A mode shape gives the relative displacement of each spring-mass during normal mode vibration (when one particular mode is excited), but it gives no information about which mode is more unstable than the others. An alternative method will be introduced to overcome this difficulty in the subsequent sections.

3.2.2 Damping and the Resonant Peak

Figure 3.2 shows a torsional mass-spring system with an inertia constant M, a stiffness constant K, a damping coefficient D, and a forcing function $T_o \sin\omega t$

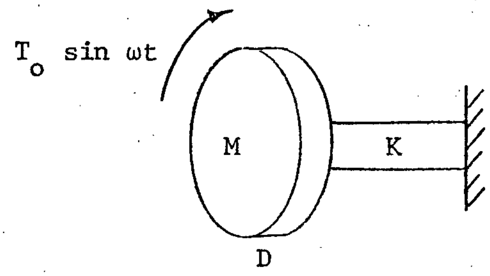

Figure 3.2 A torsional mass-spring system

The equation of motion of the system is

$$T = M\ddot{\theta} + D\dot{\theta} + K\theta \tag{3.10}$$

For a solution $\theta = X \sin(\omega t - \phi)$, we have

$$\frac{T_o \sin \omega t}{X} = (K - M\omega^2)\sin(\omega t - \phi) + D\omega\cos(\omega t - \phi) \tag{3.11}$$

In phasor notation

$$\frac{T_o}{X} = (K - M\omega^2) + jD\omega \tag{3.12}$$

Hence

$$X = \frac{T_o}{(K - M\omega^2) + j D\omega} \tag{3.13}$$

and the phase angle, ϕ is given by

$$\tan \phi = \frac{D\omega}{(K - M\omega^2)} \tag{3.14}$$

When the frequency of the forcing function equals the natural frequency of the system, the real part of the denominator of (3.13) vanishes and the equation becomes

$$X = \frac{T_o}{jD\omega} \tag{3.15}$$

During resonance, the amplitude X is directly proportional to the applied force and inversely proportional to the system damping. Therefore, a large applied force together with a small system damping will result in a large resonant peak.

3.2.3 Resonant Peaks of the Six Mass-spring System

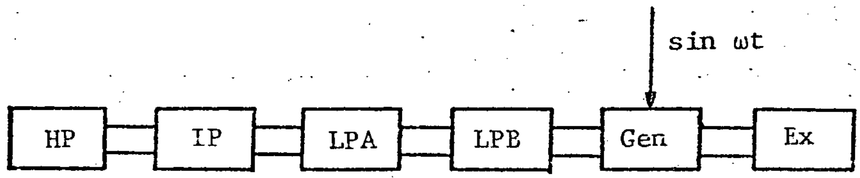

Figure 3.3 A damped six mass-spring system with unity sinusoidal forcing torque.

Consider a damped mass-spring system with unity sinusoidal forcing torque $\sin \omega t$ applied on the generator rotor as shown in Figure 3.3. The matrix equation in per unit describing the dynamical behaviour of the system becomes

$$\frac{1}{\omega_b} [M][\ddot{\theta}] + \frac{1}{\omega_b} [D][\dot{\theta}] + [K][\theta] = [T] \tag{3.16}$$

where $[M]$ and $[K]$ respectively are the inertia constant and stiffness coefficient matrices as shown in equations (3.2) and (3.4), and

$$[D] = \text{diag}\ [D_1, D_2, D_3, D_4, D_5, D_6]$$

$$[T] = [0 \quad 0 \quad 0 \quad 0 \quad \sin \omega t \quad 0]^T$$

Let the mechanical angular displacements $[\theta]$ be transformed into modal angular displacements $[q]$ by the eigenvector matrix $[Q_{mode}]$, from the eigenvalue analysis of the undamped system

$$[\theta] = [Q_{mode}][q] \tag{3.17}$$

Substituting (3.17) into (3.16) and premultiplying the whole equation by $[Q_{mode}]^T$, we have

$$\frac{1}{\omega_b}[M_{mode}][\ddot{q}] + \frac{1}{\omega_b}[D_{mode}][\dot{q}] + [K_{mode}][q]$$

$$= [T_{mode}] \tag{3.18}$$

where

$$\begin{aligned} [M_{mode}] &= [Q_{mode}]^T[M][Q_{mode}] \\ [K_{mode}] &= [Q_{mode}]^T[K][Q_{mode}] \\ [D_{mode}] &= [Q_{mode}]^T[D][Q_{mode}] \\ [T_{mode}] &= [Q_{mode}]^T[T] \end{aligned} \tag{3.19}$$

Note that $[T_{mode}]$ indicates the contribution of the applied force on each mode of vibration; both $[M_{mode}]$ and $[K_{mode}]$ are diagonal matrices because $[M]$ and $[K]$ are symmetrical.

Neglecting the off diagonal elements of $[D_{mode}]$, equation

(3.19) becomes six second order differential equations each of which corresponds to (3.10). Applying (3.15), the calculated magnitude of the resonant peaks for various modes for the unity forcing function $\sin \omega t$ of Figure 3.3 are shown in Table 3.1 . Multiplying the modal resonance peaks by its corresponding mode shapes as shown in Figure 3.1, gives the relative magnitude of the 'angular displacement' of each mass at the resonant frequencies. Results are shown in Table 3.2.

Table 3.1

Modal resonance peaks of the mass-spring system

mode 1	6.47
mode 2	1.00
mode 3	3.075
mode 4	4.56
mode 5	0.035

Table 3.2

Magnitude of the resonant peaks of each mass using approximate modal analysis

	HP	IP	LPA	LPB	Gen	Ex
mode 1	4.97	3.73	2.20	0.72	2.39	6.47
mode 2	0.125	0.07	0.017	0.05	0.04	1.00
mode 3	3.075	1.04	0.70	0.29	0.51	0.77
mode 4	3.94	0.20	2.29	4.56	2.83	1.72
mode 5	0.027	0.035	0.004	0.0007	0.0002	0.00003

3.2.4 Identification of the Unstable Torsional Modes

Neglecting the off diagonal elements of $[D_{mode}]$, equation (3.18) becomes six second order differential equations, each corresponds to one mode of vibration. Excluding mode 0, we shall have

$$\frac{1}{\omega_b} m_{mode_i} \ddot{q}_i + \frac{1}{\omega_b} d_{mode_i} \dot{q}_i + k_{mode_i} q_i = t_{mode_i} , \quad i=1,..,5 \qquad (3.20)$$

when the unity forcing torque sinωt is applied to the system, it is found that is this particular study

$$[T_{mode}] = [\ 0.373,\ 0.0374,\ 0.166,\ 0.6205,\ 0.0045\ ]$$

In the mean time

$$[D_{mode}] = [\ 0.22,\ 0.102,\ 0.127,\ 0.253,\ 0.163\ ]$$

When these results are compared with those from eigenvalue analysis as shown in Table 3.3

Table 3.3

Unstable modes of the SSR System

Mode	Frequency	Compensation	Eigenvalue
0	1 - 2 Hz	below 30%	
1	15.7 Hz	above 70%	$+1.7178 \pm j102.16$
4	32.3 Hz	at 50%,60%	$+0.7094 \pm j203.32$
3	25.5 Hz	at 40%,50%,60%,70%	$+0.5595 \pm j161.00$

there is an indication that if

$$(\ d_{mode} - t_{mode}\ ) < 0 \qquad (3.21)$$

the particular torsional mode is vulnerable to instability in this particular study.

3.2.5 Modal Resonance Peaks and Unstable Modes

The modal resonance peaks in Table 3.1 indicate the relative instability among the torsional modes. A large modal resonance peak means a large amplitude of vibration ,resulting in large negative damping due to the torsional interaction, and vice versa.

In additional to the six mass-spring system, several other systems are investigated using both eigenvalue analysis of the unified electro-mechanical model and modal resonance peak analysis of the mass-spring system. All results suggested that the modal resonance peaks can be used as an index to determine the relative instability among the unstable modes. In this particular case, mode 1 will be the most unstable one followed by mode 4 and mode 3 in that order.

3.2.6 Other uses of modal analysis in SSR Studies

Stability of a SSR system also depends upon the conditions of the electrical system. However, the modal analysis is a very useful first step to identify the excitable modes so that the range of frequency scanning can be narrowed, and the number of equations can be reduced. With the excitable modes identified, one can also construct equivalent mass-spring system by retaining only the unstable modes alone, which will be presented in the next section.

3.3 Equivalent Mass-spring system

As shown in Table 3.3, there are only three torsional modes in the study system. A low order equivalent mass-spring system may be obtained by retaining only the unstable modes as follow:

1) Mode 2 in Figure 3.6a is roughly equal to the exciter mass swings against the rest of the mass-spring system which can be eliminated according to the ongoing analysis. Combining the generator (Gen) and the exciter (Ex) masses together, eliminating mode 2, and keeping all other natural frequencies by adjusting the stiffness constant K_{45} between the low pressure turbine B (LPB) and the generator (Gen), result in an equivalent five mass-spring system.

2) The same procedure is applied to the high pressure turbine (HP) and the medium pressure turbine (IP). Combining the two masses and eliminating mode 5 by adjusting the stiffness constant K_{23} between the medium pressure turbine (IP) and the low pressure turbine A (LPA) result in an equivalent four mass-spring system.

3) Finally, the procedure is applied to the two low pressure turbines (LPA) and (LPB). Combining the two masses and elminating mode 1 by adjusting both stiffness constant K_{23} and K_{45} but one at a time, result in an equivalent three mass-spring system.

3.3.1 Mode Frequencies and the Adjustment of the Stiffness Constant

Mode frequencies of the mass-spring system depend upon the inertia constants and the stiffness constants. To retain other natural frequencies after combining the two neighbouring masses into one, the stiffness constants must be varied, which can be found as follows:

1) The initial eigenvalues are found from the characteristic equation of the six mass-spring system, each corresponds to a second order equation, and together they may be written in matrix form as

$$\left| \lambda [\, I \,] - [\, M \,]^{-1} [\, K \,] \right| = 0 \tag{3.22}$$

where

[M] is the inertia constant matrix of appropriate dimension

[K] is the spring coefficient matrix

[I] is the identity matrix

$\lambda = \omega^2/\omega_b$, $\omega_b = 377$ rad/sec.

2) To find a reduced order mass-spring system, one of the stiffness constant, say K_{ij} , is treated as an unknown. By substituting the known λ's already obtained from step (1) one at a time, an average K_{ij} is obtained.

3) The average K_{ij} value is substituted into equation (3.22) of the reduced order system, and eigenvalues are recalculated. The value is then adjusted according to the sensitivity coefficient, $\partial\omega_i/(\partial K_{ij})$, until the least square error of the natural frequencies of the equivalent reduced order system is the minimum. The least square error

$$e_\omega = \sum_{i=1}^{n} (\omega_{i_{desired}} - \omega_{i_{retained}})^2 \tag{3.23}$$

versus the variation of K_{45} of the equivalent five mass-spring system and K_{23} of the four mass-spring system are shown in Figure 3.4 and 3.5 respectively.

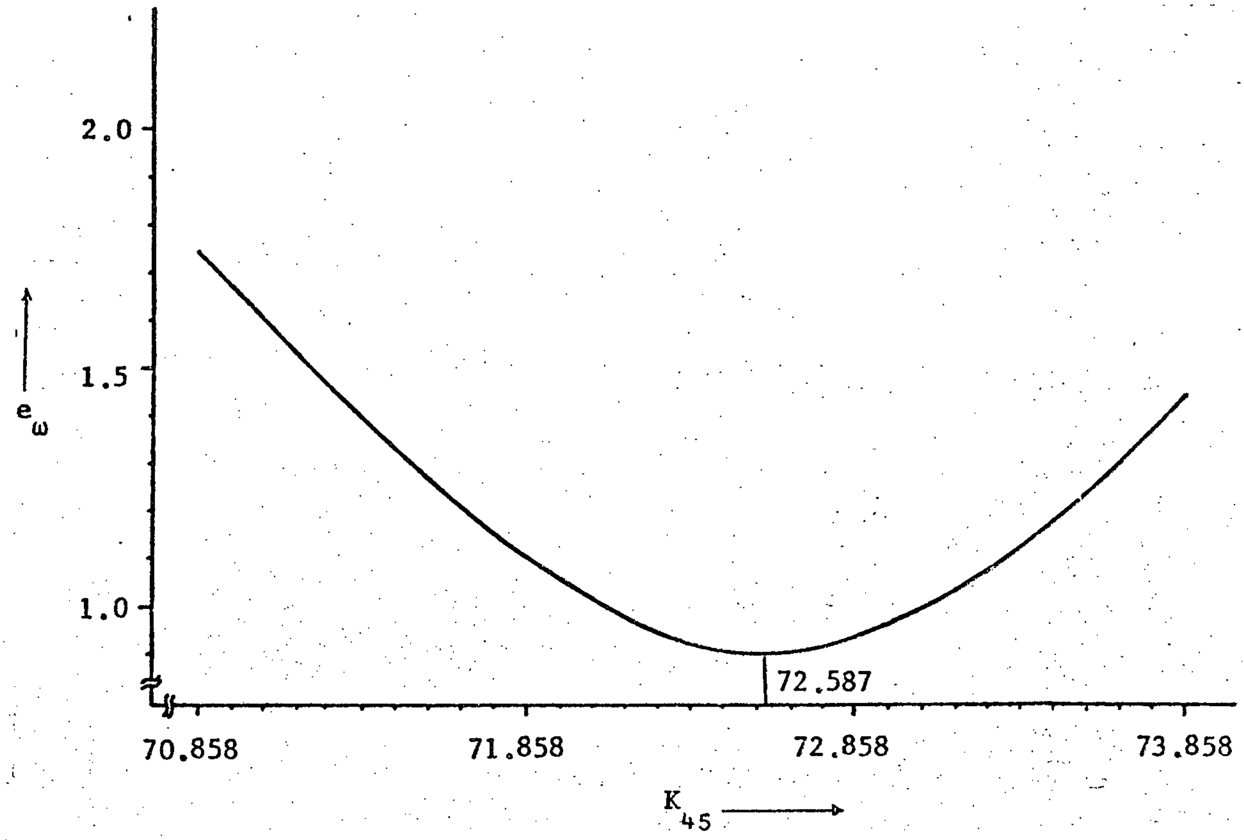

Figure 3.4 Variation of the least square error e_ω vs. the variation of K_{45} of the five mass equivalent.

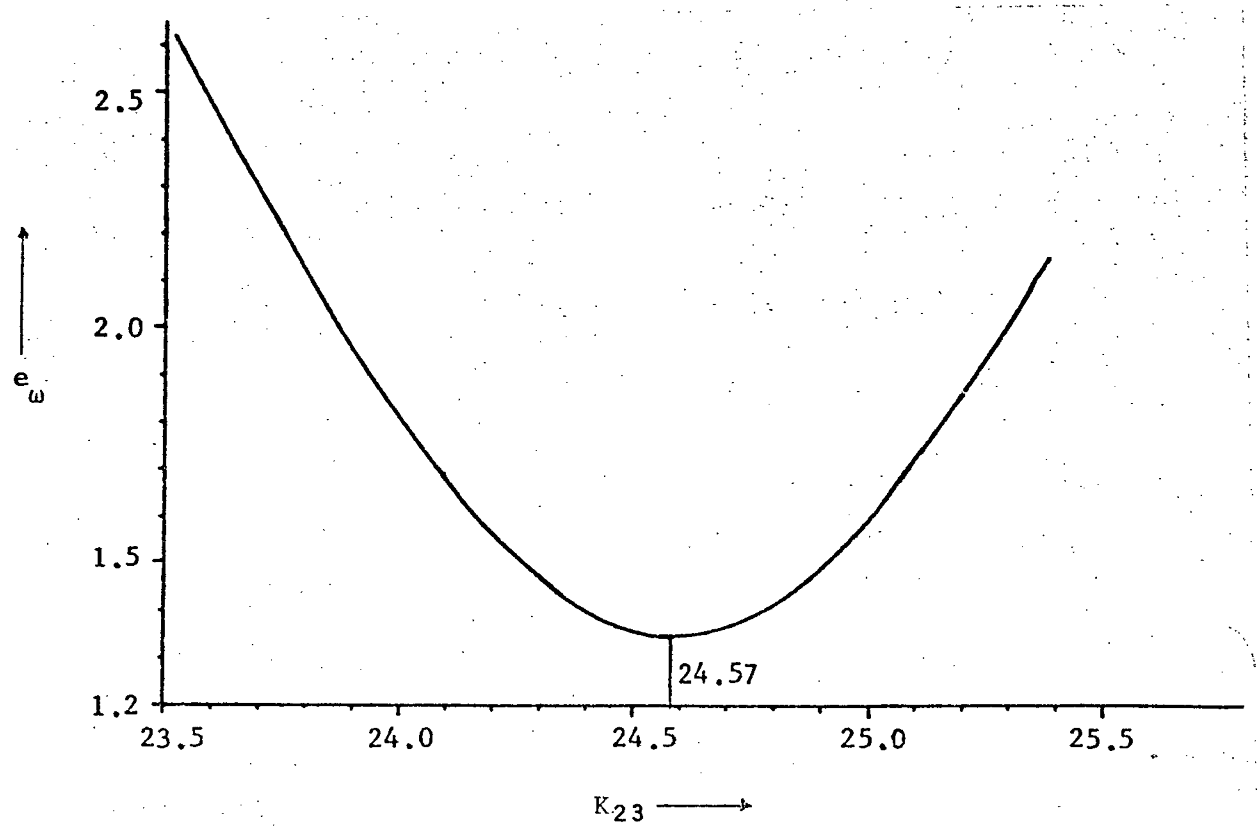

Figure 3.5 Variation of the least square error e_ω vs. the variation of K_{23} of the four mass equivalent.

3.3.2 Mode Shapes of the Original and Equivalent Systems

The eigenvalues of a system are unique, but the eigenvectors are not and can be normalized or multiplied by any non-zero scalar. Although an equivalent reduced order mass-spring system retains all the dominant eigenvalues of the original system, the validity remains to be proven: a reduced order model of the equivalent system shall have almost the same dominant eigenvector of the original system. In addition, the modal displacement of M_{Gen} shall be close to that of the original system so that the torsional interaction between the electrical and mechanical system can be accurately accounted for.

In this section, the normalized eigenvectors of the original and reduced order mass-spring systems are compared. Excluding mode 0, by which all the masses swing in unison, the eigenvectors of the original system before normalization are

$$\begin{bmatrix} -1.0428 & -1.5584 & -2.2820 & +0.5914 & -0.6161 \\ -0.7833 & -0.9168 & -0.4041 & -0.0299 & +0.7825 \\ -0.4595 & -0.2128 & +0.2713 & -0.3442 & -0.0886 \\ +0.1499 & +0.5601 & +0.1127 & +0.6847 & +0.0165 \\ +0.5007 & +0.5297 & -0.1960 & -0.4248 & -0.0350 \\ +1.3420 & -14.182 & +0.2982 & +0.2579 & +0.0007 \end{bmatrix} \qquad (3.24)$$

After normalization, they become

$$\begin{bmatrix} -0.7770 & +0.1099 & 1 & +0.864 & -0.7870 \\ -0.5840 & +0.0650 & +0.3420 & -0.0440 & 1 \\ -0.3420 & +0.0150 & -0.2290 & -0.5030 & -0.1130 \\ +0.1120 & -0.0400 & -0.0950 & 1 & +0.0210 \\ +0.3730 & -0.0370 & +0.1660 & -0.6210 & -0.0045 \\ 1 & 1 & -0.2530 & +0.3770 & +0.0009 \end{bmatrix} \qquad (3.25)$$

After eliminating mode 2, the eigenvectors of the reduced order five mass equivalent system by retaining mode frequencies 15.94 Hz., 25.46 Hz., 32.28 Hz., and 47.46 Hz., before normalization are

$$\begin{bmatrix} +1.0642 & +0.9543 & +0.6536 & +0.6161 \\ +0.7916 & +0.3310 & -0.0332 & -0.7825 \\ +0.4532 & -0.2135 & -0.3805 & +0.0887 \\ -0.1719 & -0.1009 & +0.7573 & -0.0166 \\ -0.5087 & +0.1467 & -0.4414 & +0.0034 \end{bmatrix} \tag{3.26}$$

Scaling the modal eigenvectors with respect to the original system before normalization (e.g., $\frac{-1.0428}{1.0642}$ x column 1, $\frac{-1.1810}{0.9543}$ x column 2, $\frac{0.5914}{0.6536}$ x column 3, 1 x column 4) gives

$$\begin{bmatrix} -1.0428 & -1.1810 & +0.5914 & +0.6161 \\ -0.7757 & -0.4096 & -0.0300 & -0.7825 \\ -0.4441 & +0.2642 & -0.3443 & +0.0887 \\ +0.1684 & +0.1249 & +0.6852 & -0.0166 \\ +0.4985 & -0.1816 & -0.3994 & +0.0034 \end{bmatrix} \tag{3.27}$$

Normalized with respect to the original system yields

$$\begin{bmatrix} -0.7770 & 1 & +0.8630 & -0.7870 \\ -0.5780 & +0.3470 & -0.0400 & 1 \\ -0.3310 & -0.2340 & -0.5020 & -0.1130 \\ +0.1250 & -0.1060 & 1 & +0.0210 \\ +0.3710 & +0.1540 & -0.5830 & -0.0045 \end{bmatrix} \tag{3.28}$$

After eliminating mode 5, by retaining the mode frequencies 15.82 Hz., 25.49 Hz., and 32.47 Hz., the eigenvectors of the four mass equivalent system before normalization are

$$\begin{pmatrix} -0.9534 & -0.8973 & +0.3436 \\ -0.4477 & +0.3383 & -0.4378 \\ +0.1785 & +0.1617 & +0.7580 \\ +0.5174 & -0.2231 & -0.4340 \end{pmatrix} \tag{3.29}$$

Scaling the eigenvectors with respect to the original system before normalization (e.g., $\frac{0.4595}{0.4477}$ x column 1, $\frac{0.2713}{0.3383}$ x column 2, $\frac{0.6847}{0.7580}$ x column 3) we have

$$\begin{pmatrix} -0.9785 & -0.7196 & +0.3103 \\ -0.4594 & +0.2713 & -0.3955 \\ +0.1832 & +0.1297 & +0.6847 \\ +0.5269 & -0.1869 & -0.3920 \end{pmatrix} \tag{3.30}$$

Normalization yields

$$\begin{pmatrix} -0.7290 & +0.6090 & +0.4530 \\ -0.3420 & -0.2300 & -0.5780 \\ +0.1360 & -0.1090 & 1 \\ +0.3930 & +0.1970 & -0.5730 \end{pmatrix} \tag{3.31}$$

Using the results in (3.25), (3.28), and (3.31), the mode shapes of the original, the five mass equivalent, and the four mass equivalent systems are shown in Figure 3.6a, 3.6b, and 3.6c respectively. Note that the mode shapes of the equivalent systems are close to those of the original system.

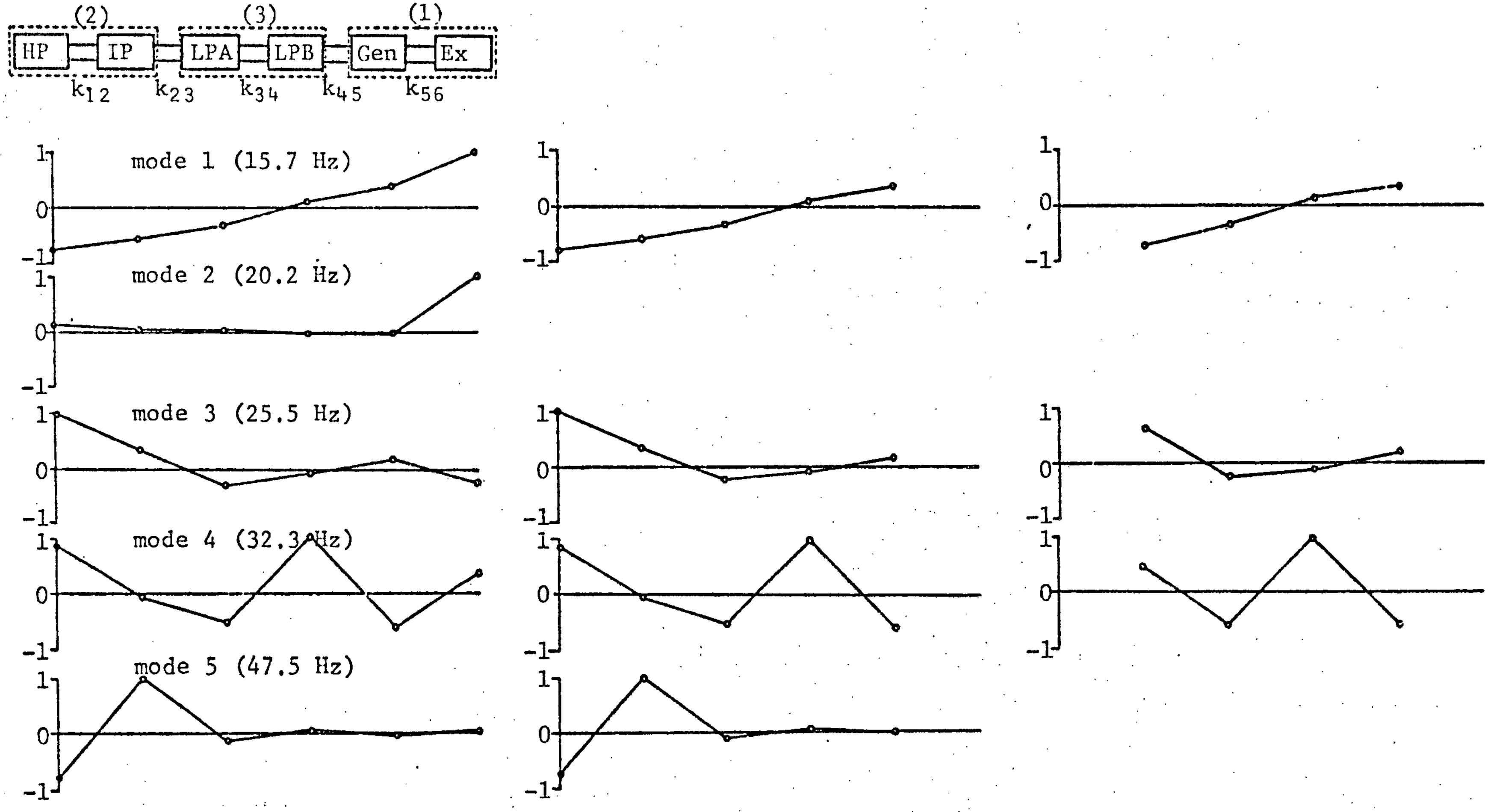

(a) Six mass-spring system (b) Five mass-spring system (c) Four mass-spring system

Figure 3.6 Mode Shapes of the original and Equivalent Systems

3.3.3 Eigenvalues of the original and reduced order models

After reducing the order of the original system model from 26th to 20 by neglecting turbine torque and governor equations, etc., the order is further reduced using mass-spring equivalencing technique developed in 3.3, resulting in a 16th or a 14th order model. The 14th order model, however, is valid up to 70% capacitor compensation because mode 1 is not considered in the model. Eigenvalues of the 26th, 16th, and 14th order models over a wide range of capacitor compensation are examined. Typical values are shown in Table 3.4 to 3.6. The 16th order model retains all the dominant eigenvalues over a wide capacitor range, and the 14th order model also retains most of the dominant properties except for very high compensation.

Table 3.4

Eigenvalues of various order SSR model at 30% capacitor compensation for P_e = 0.9 p.u. at 0.9 power factor lagging and V_t = 1.0 p.u.

	26th order model	reduced 16th order model	reduced 14th order model
Mechanical modes	$-0.1818 \pm j298.18$ $-0.4938 \pm j203.59$ $-0.2513 \pm j160.64$ $-0.6705 \pm j127.02$ $-0.2810 \pm j99.136$ $-0.0031 \pm j8.4105$	$-0.4046 \pm j204.71$ $-0.2069 \pm j160.05$ $-0.2289 \pm j99.826$ $-0.0399 \pm j8.4284$	$-0.2723 \pm j200.37$ $-0.4052 \pm j157.16$ $-0.0229 \pm j8.4469$
Turbine and Governor	-0.1418 -4.5826 -3.1056 $-4.6721 \pm j0.5722$		
Stator and Network	$-7.0419 \pm j542.94$ $-5.5469 \pm j210.33$	$-7.0444 \pm j542.93$ $-5.6283 \pm j210.34$	$-7.0440 \pm j542.93$ $-5.6596 \pm j210.69$
Machine rotor	-8.6469 -31.876 -2.0220	-8.5228 -32.611 -2.2563	-8.5180 -32.627 -2.2569
Exciter and voltage regulator	-499.97 -101.94	-101.57	-101.56

Table 3.5

Eigenvalues of various order SSR model at 50% coapcitor compensation for P_e = 0.9 p.u. at 0.9 power factor lagging and V_t=1.0 p.u.

	26th order model	reduced 16th order model	reduced 14th order model
Mechanical modes	-0.1818±j298.18 +0.1237±j202.88 +0.2603±j161.38 -0.6829±j127.06 -0.3524±j99.345 -0.2327±j9.4692	+0.1033±j204.01 +0.2341±j161.72 -0.3053±j100.05 -0.2566±j9.4905	+0.0167±j200.32 +1.0147±j160.11 -0.2408±j9.5172
Turbine and governor	-0.1418 -3.8415 -3.5122 -4.8239±j0.2945		
Stator and Network	-7.0969±j591.27 -6.1493±j161.74	-7.0987±j591.27 -6.0584±j161.72	-7.0986±j591.27 -6.9236±j159.65
Machine rotor	-8.2324 -32.776 -1.9458	-8.3289 -32.776 -1.9458	-8.2283 -33.475 -2.1670
Exciter and voltage regulator	-499.97 -101.76	-101.76	-101.44

Table 3.6

Eigenvalues of various order SSR model at 80% capacitor compensation for P_e = 0.9 p.u. at 0.9 power factor lagging and V_t = 1.0 p.u.

	26th order model	reduced 16th order model	reduced 14th order model
Mechanical modes	−0.1818±j298.18 +0.0134±j202.91 −0.0967±j160.52 −0.5998±j126.95 +1.7178±j102.17 −0.7619±j11.662	+0.0125±j204.04 −0.0496±j159.93 +2.1999±j102.78 −0.7669±j11.682	−0.0409±j200.33 +0.2981±j156.59 −0.7572±j11.737
Turbine and governor	−0.1419 −3.4784±j0.5960 −4.9841±j0.0792		
Stator and Network	−7.1710±j648.08 −6.7654±j103.02	−7.1523±j648.08 −7.1328±j103.06	−7.1523±j648.08 −5.0848±j106.26
Machine rotor	−7.6295 −35.049 −1.7807	−7.5898 −35.594 −1.9481	−7.5873 −35.613 −1.9489
Exciter and voltage regulator	−499.97 −101.43	−101.15	−101.15

4. EXCITATION CONTROL DESIGN

4.1 Introduction

The main objective of the controller design is to stabilize all unstable modes over a wide range of power and capacitor compensation with minimum number of feedback signals.

For the multi-mode stabilization of torsional oscillations, the phase compensation power system stabilizer with single signal input is inadequate for the narrow frequency band sensitivity. It may also have detrimental effects on other torsional modes [17]. Multiple loop lead-lag compensation excitation control has also been designed [14], but remains to be improved.

In this chapter, the state regulator problem of control theory is applied, and the linear optimal excitation control is designed for the multiple torsional mode stabilization. It is a linear combination of many system feedback signals. Instead of the phase compensation, the linear combination of feedback signals according to the control law collectively ensures proper damping for all torsional modes.

In engineering practice, it is also desirable to have the minimum number of feedback signals which can be easily measured. Due to the complexity of the SSR problem, the order of the system model is usually very high and the linear optimal control designed usually requires a large number of feedback signals [17,18]. Suboptimal control alqorithms are avaiable in the control literature [29,30], but heavy computation is involved.

In this chapter, a different suboptimal excitation control design technique is presented. The linear optimal excitation control of SSR is designed in the usual way, but the controller is simplified by rejecting some feedback signals which have the least effect on the system damping, determined from an eigenvalue sensitivity analysis. Formulation will be given, suboptimal excitation control will be designed, and the results of both eigenvalue analysis and time domain simulation of the SSR control of a power system will be presented.

4.2 Linear Optimal Control

For the linear optimal excitation control design, let the state equation be,

$$[\dot{x}] = [A][x] + [B][u] \tag{4.1}$$

and a cost index be chosen as

$$J = \frac{1}{2}\int_0^\infty ([x]^T[Q][x] + [u]^T[R][u])dt \tag{4.2}$$

where $[x]$ is the state variable vector, $[u]$ the control vector, $[A]$ the system matrix, $[B]$ a control matrix, $[Q]$ a positive semi-definite weighting matrix, and $[R]$ a positive definite weighting matrix.

A Hamiltonian is formed by appending (4.1) to (4.2)

$$H = \frac{1}{2}([x]^T[Q][x] + [u]^T[R][u]) + [p]^T([A][x]+[B][u]) \tag{4.3}$$

where $[p]$ is the costate vector or Lagrange multipliers, and the optimal control can be found from $\partial H/\partial u$, resulting in

$$[u] = -[R]^{-1}[B]^T[p] \tag{4.4}$$

Let $$[p] = [K][x] \tag{4.5}$$

and assume a time-invariant system, $[K]$ must satify the following matrix Riccati equation

$$[K][A] + [A]^T[K] - [K][B][R]^{-1}[B]^T[K] + [Q] = 0 \tag{4.6}$$

From the state equation of [x] and the co-state equation of [p], a composite system matrix [M] becomes

$$[\,M\,] = \begin{bmatrix} [A] & -[B]\,[R]^{-1}\,[B]^T \\ -[Q] & -[A]^T \end{bmatrix} \tag{4.7}$$

There are 2n eigenvalues of matrix [M] for an n-th order system, and the eigenvalues are symmetrically distributed on the right and the left parts of the complex plane. Let the eigenvalue matrix be

$$[\,\Lambda\,] = \begin{bmatrix} \Lambda_I & \\ & \Lambda_{II} \end{bmatrix} , \quad [\,\Lambda_I] = -[\,\Lambda_{II}] \tag{4.8}$$

and the corresponding eigenvector matrix be

$$[\,X\,] = \begin{bmatrix} X_I & X_{III} \\ X_{II} & X_{IV} \end{bmatrix} \tag{4.9}$$

The Riccati matrix [K] may be computed from

$$[\,K\,] = [\,X_{II}]\,[\,X_I\,]^{-1} \tag{4.10}$$

where $[\,\Lambda_I\,]$ constitutes the n eigenvalues of [M] on the left hand side of the complex plane, which are the eigenvalues of the closed loop system matrix $[\,A_c\,]$, as the closed loop state equations may be written

$$\begin{aligned} [\,\dot{x}\,] &= [\,A\,][\,x\,] + [\,B\,][\,u\,] \\ &= (\,[A] - [B]\,[R]^{-1}\,[B]^T[K]\,)\,[x] \\ &= [\,A_c\,][\,x\,] \end{aligned} \tag{4.11}$$

4.3 Eigenvalue Sensitivity [31,32]

Consider the controlled system matrix A_c. For the i-th eigenvalue λ_i and eigenvector X_i, we have

$$A_c X_i = X_i \lambda_i \tag{4.12}$$

For the i-th eigenvalue λ_i and the eigenvector V_i of the transposed A_c, we have

$$A_c^T V_i = V_i \lambda_i \tag{4.13}$$

Taking the partial derivative of both sides of equation (4.12) with respect to a system parameter α gives

$$\frac{\partial A_c}{\partial \alpha} X_i + A_c\left(\frac{\partial X_i}{\partial \alpha}\right) = \lambda_i \left(\frac{\partial X_i}{\partial \alpha}\right) + \left(\frac{\partial \lambda_i}{\partial \alpha}\right) X_i \tag{4.14}$$

Premultiplying both sides of equation (4.14) by V_j^T results in

$$V_j^T \left(\frac{\partial A_c}{\partial \alpha}\right) X_i + V_j^T A_c\left(\frac{\partial X_i}{\partial \alpha}\right) = V_j^T \lambda_i \left(\frac{\partial X_i}{\partial \alpha}\right) + \left(\frac{\partial \lambda_i}{\partial \alpha}\right) V_j^T X_i \tag{4.15}$$

But

$$V_j^T A_c = V_j^T \lambda_j \tag{4.16}$$

Therefore equation (4.15) becomes

$$V_i^T \left(\frac{\partial A_c}{\partial \alpha}\right) X_i = \left(\frac{\partial \lambda_i}{\partial \alpha}\right) V_i^T X_i \tag{4.17}$$

or

$$\frac{\partial \lambda_i}{\partial \alpha} = \frac{V_i^T \left(\frac{\partial A_c}{\partial \alpha}\right) X_i}{(X_i, V_i)} \tag{4.18}$$

where (X_i, V_i) equals to $V_i^T \cdot X_i$, according to (4.12) and (4.16)

$$V_j^T X_i \begin{cases} \neq 0 & i = j \\ \\ = 0 & i \neq j \end{cases} \tag{4.19}$$

4.4 Reduced Order Controller via Eigenvalue Sensitivity Analysis [24]

Let the feedback matrix $[\, BR^{-1}B^TK \,]$ of (4.11) be simply written as $[\, F \,]$, and let ΔV_R fo the voltage regulator be the last state variable. The closed loop system matrix becomes

$$[\, A_c] = [\, A - F \,] \tag{4.20}$$

where

$$[\, F \,] = \begin{bmatrix} & [\, 0 \,] & \\ \\ f_{n1}, \ldots\ldots, & f_{nk}, \ldots\ldots, & f_{nn} \end{bmatrix} \tag{4.21}$$

Therefore, the eigenvalue shift of the controlled system is due to the change in the last row of $[\, F \,]$. Since not all the feedback elements , f_{ni}, $i=1,2,..,k,..,n$, contribute substantial damping to the system, those which have relatively small contribution may be neglected, which will not affect the overall performance of the controlled system.

Since

$$\frac{\partial A_c}{\partial f_{nk}} = \begin{bmatrix} & [\, 0 \,] & \\ \\ 0 \ldots 0 \ldots, & -1, & \ldots\ldots 0 \end{bmatrix} \tag{4.22}$$

therefore (4.18) becomes

$$\frac{\partial \lambda_i}{\partial f_{nk}} = \frac{-\, X_i^k \cdot V_i^n}{(X_i\ ,\ V_i)} \tag{4.23}$$

where X_i^k is the k-th element of the eigenvector X_i , and V_i^n is the n-th element of the eigenvector V_i .

When deleting a feedback element f_{nk} , $\Delta f_{nk} = -f_{nk}$, therefore

$$\Delta\lambda_i \simeq \frac{X_i^k \cdot V_i^n}{(X_i , V_i)} f_{nk} \tag{4.24}$$

By examining $\Delta\lambda_i$, i=1,2,....,n , one can decide which feedback elements of [F] in (4.21) can be deleted.

The total effect of deleting some feedback elements can be calculated from

$$\Delta\lambda_{i_{total}} \simeq \sum_d \frac{X_i^k \cdot V_i^n}{(X_i , V_i)} f_{nd} \tag{4.25}$$

where f_{nd}'s are those feedback control elements being eliminated. Of course, one has to check whether

$$Re (\lambda_i + \Delta\lambda_{i_{total}}) < 0 \quad i=1,2,....,n \tag{4.26}$$

in order to have a stable system, where λ_i , i=1,2,...,n , are the eigenvalue of the controlled system without deleting any feedback signals.

4.5 Examples of the Controller Design

Two examples of the SSR control design are given in this section using the reduced order one-machine infinite-bus models developed in Chapter 3. For the 14th order model, the state variables are

$$\begin{aligned}[x] = [&\Delta\omega_{IP},\Delta\theta_{IP},\Delta\omega_{LPB},\Delta\theta_{LPB},\Delta\omega,\Delta\delta,\Delta I_d,\Delta I_q,\Delta I_f,\Delta I_{kd}, \\ &\Delta I_{kq},\Delta V_{cd},\Delta V_{cq},\Delta V_R]^T\end{aligned} \tag{4.27}$$

For the excitation control design, [B] become a vector with only one non-zero element K_A/T_A associated with ΔV_R .

From earlier experience [18], the weighting matrices are chosen as

$$[\,Q\,] = \mathrm{diag}\,[\,5000,50,55000,50,3000,25;1000,1000,$$
$$0,5,5,1,1,0\,] \tag{4.28}$$
$$[\,R\,] = 1$$

After design, the control is substituted into the original 26th order full model whose state variables are

$$[\,x\,] = [\,\Delta\omega_1,\Delta\theta_1,\Delta\omega_2,\Delta\theta_2,\Delta\omega_3,\Delta\theta_3,\Delta\omega_4,\Delta\theta_4,\Delta\omega,\Delta\theta,\Delta\omega_6,\Delta\theta_6,\Delta a,\Delta P_{GV},$$
$$\Delta T_{HP},\Delta T_{IP},\Delta T_{LPA};\Delta I_d,\Delta I_q,\Delta I_f,\Delta I_{kd},\Delta I_{kq},\Delta V_{cd},\Delta V_{cq},$$
$$V_R,\ E_{fd}\,] \tag{4.29}$$

which corresponds to equations (2.41) and (2.42). Eigenvalue sensitivity technique is then applied. Typical eigenvalue shift due to individual state feedback is shown in Table 4.1.

Table 4.1

Typical value of the eigenvalue shift due to individual state feedback

Mechanical modes of the full order controlled system	Net eigenvalue shift due to the deletion of $f_{25,9}$
$-0.1836 \pm j298.18$	0.0
$-0.6618 \pm j203.32$	$+0.1182 \mp j0.0641$
$-0.1949 \pm j160.68$	$-0.1228 \mp j0.1891$
$-0.6980 \pm j127.08$	$-0.0033 \mp j0.0334$
$-0.2649 \pm j98.889$	$-0.1053 \mp j0.2758$
$-3.1529 \pm j4.8785$	$-0.5931 \mp j0.2181$

It is found that the state feedback of $\Delta\omega_{IP}$, $\Delta\theta_{IP}$, $\Delta\theta_{LPA}$, $\Delta\omega$, ΔI_{kq} , ΔV_{cd} , ΔV_{cq} do not have significant effect on the eigenvalues and hence may be deleted, resulting in a 7th order controller as follows

$$U_E = 918.63\Delta\omega_{LPB} - 46.159\Delta\delta + 214.58\Delta I_d - 23.06\Delta I_q$$
$$-200.67\Delta I_f - 198.67\Delta I_{kd} - 0.0558\Delta V_R \qquad (4.30)$$

With similiar procedures, an excitation control is also designed using the 16th order model. The state variables of the model are

$$[\ x\ ] = [\ \Delta\omega_{IP},\Delta\theta_{IP},\Delta\omega_{LPA},\Delta\theta_{LPA},\Delta\omega_{LPB},\Delta\theta_{LPB},\Delta\omega,\Delta\delta;$$
$$\Delta I_d,\Delta I_q,\Delta I_f,\Delta I_{kd},\Delta I_{kq},\Delta V_{cd},\Delta V_{cq},\Delta V_R\ ]\ , \qquad (4.31)$$

the weighting matrices are chosen as

$$[\ Q\ ] = \text{diag}[\ 500,0,10,1,600000,10,500,10;800,500,$$
$$0,0.5,0.5,1,1,0\ ] \qquad (4.32)$$
$$[\ R\ ] = 1$$

and the control U_E is found to be

$$U_E = 54.896\Delta\theta_{LPA} + 788.26\Delta\omega_{LPB} - 11.187\Delta\theta_{LPB} + 188.79\Delta I_d$$
$$-9.725\Delta I_q - 175.93\Delta I_f + 8.4749\Delta I_{kd} - 0.0404\Delta V_R \qquad (4.33)$$

The operating conditions for which the above controllers are designed are

electrical power	=	0.9 per unit
power factor	=	0.9 lagging
terminal voltage	=	1.0 per unit
capacitor compensation	=	60%

4.6 The Output Feedback Control

Although the state variables $\Delta\omega_{LPB}$, $\Delta\delta$, and $\Delta\omega_{LPA}$ of the mass-spring system can be processed by the torsional stress analyzer [33], electrical variables ΔI_d, ΔI_q, ΔI_{kd}^- can not be measured, and must be expressed in terms of measurable variables.

It is found that $\Delta\dot{\Psi}_{kq}$ is relatively small

$$\Delta\dot{\Psi}_{kq} \simeq 0$$

and (4.34)

$$\Delta I_{kq} \simeq \frac{X_{mq}}{X_{kq}} \Delta I_q$$

Since X_{mq}/X_{kq} is close to 1 for this particular case, the dynamic responses of ΔI_q and ΔI_{kq} as shown in Figure 4.1 are almost identical

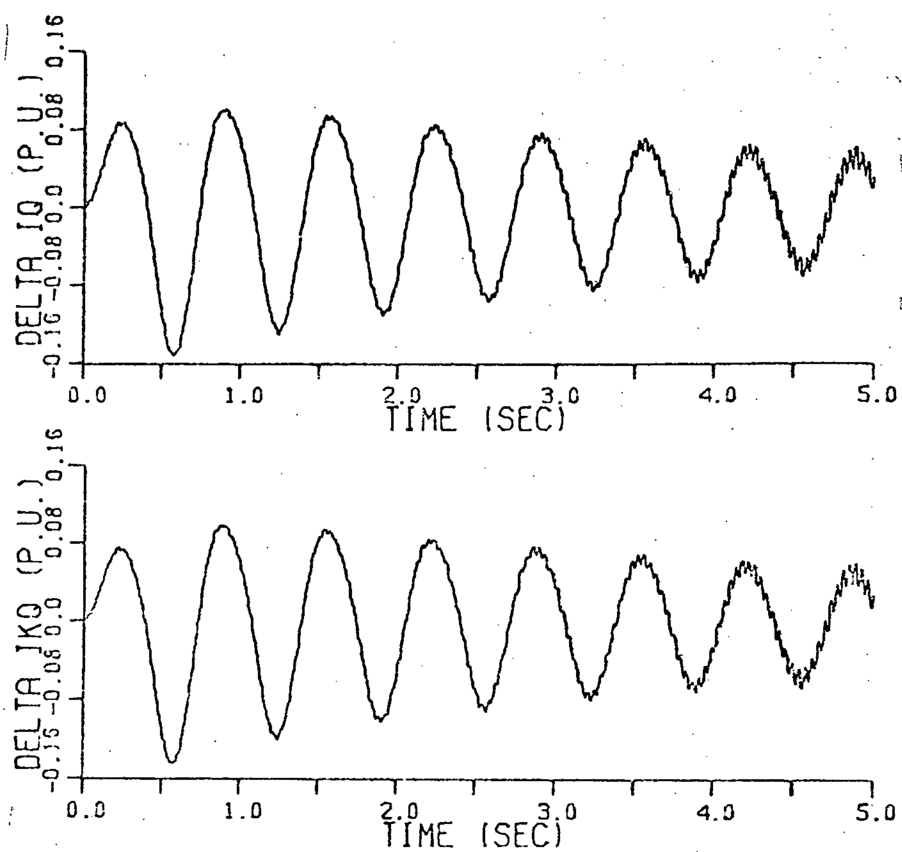

Figure 4.1 Dynamic responses of ΔI_q and ΔI_{kq}

Other equations are

$$
\begin{aligned}
P_e &\simeq \Psi_d I_q - \Psi_q I_d \\
Q_e &\simeq \Psi_d I_d - \Psi_q I_q \\
I_t^2 &= I_d^2 + I_q^2
\end{aligned}
\tag{4.35}
$$

which are linearized for the SSR studies. Therefore ΔI_d , ΔI_q , ΔI_{kd} , ΔI_f can be expressed in terms of the output variables ΔP_e , ΔQ_e , ΔI_t , ΔI_f according to the following relation

$$
\begin{bmatrix} \Delta P_e \\ \Delta Q_e \\ \Delta I_f \\ \Delta I_t \end{bmatrix}
=
\begin{bmatrix}
(X_q - X_d) I_{qo} & ((X_q - X_d - \frac{X_{mq}^2}{X_{kq}}) I_{do} + E_{fdo}) & I_{qo} X_{md} & I_{qo} X_{md} \\
(E_{fdo} - 2X_d I_{do}) & -(2X_q - \frac{X_{mq}^2}{X_{kq}}) I_{qo} & I_{do} X_{md} & I_{do} X_{md} \\
 & & 1 & \\
I_{do}/I_{to} & I_{qo}/I_{to} & &
\end{bmatrix}
\begin{bmatrix} \Delta I_d \\ \Delta I_q \\ \Delta I_f \\ \Delta I_{kd} \end{bmatrix}
\tag{4.36}
$$

Applying (4.36), the simplified controller of the 14th order model design of (4.30) becomes

$$
\begin{aligned}
U_E = {} & 918.63\Delta\omega_{LPB} - 46.159\Delta\delta - 145.46\Delta P_e - 68.665\Delta Q_e \\
& + 160.88\Delta I_t - 1.9982\Delta I_f - 0.0558\Delta V_R
\end{aligned}
\tag{4.37}
$$

which has seven measurable feedback signals, and that of the 16th order model design of (4.33) becomes

$$
\begin{aligned}
U_E = {} & 54.896\Delta\theta_{LPA} + 788.28\Delta\omega_{LPB} - 11.187\Delta\theta_{LPB} - 118.85\Delta P_e \\
& -64.489\Delta Q_e + 137.89\Delta I_t - 1.0512\Delta I_f - 0.0404\Delta V_R
\end{aligned}
\tag{4.38}
$$

which has eight measurable feedback signals.

4.7 Eigenvalue Analysis of the Simplified Controllers

The excitation controls of the 16th order model and 14th order model design are substituted into the linearized 26th order full model for eigenvalue analysis, for a wide range compensation of X_c/X_L from 10% to 80%, and for three operating conditions of P_e equal to 0.5, 0.9, and 1.25 per unit. The system with either one of these two controls under all conditions are stable. Typical results are given in Tables 4.2, 4.3, and 4.4 . Note that the control designed for the 14th order model not only stabilizes mode 3 and mode 4, but also provides damping to mode 1 which is not included in the model for the design.

4.8 Dynamic Performance Test using Nonlinear Model

The simplified controllers are also substituted into the nonlinear 26th order full model derived in Chapter 2 for dynamic performance test. A pulsed torque disturbance of 20% for 0.2 second is assumed for the system at various compensation and operating conditions. Typical responses of the system without and with control of the 14th order model design, at 0.9 per unit generator load and 50% capacitor compensation, are shown in Figures 4.2 and 4.3 respectively.

Although some responses of the system without control are unstable, responses of the system with control are all stable. Note that all responses are in per unit except the torque angle which is in degree. The speed response is the deviation from its steady state value.

Table 4.2

Typical mechanical modes of the system with and without control at normal load (P_e = 0.9 p.u., Q_e = 0.4359 p.u., V_t = 1.0 p.u.)

Compensation	Without the excitation control	With a control designed for the 16th order	With a control designed for the 14th order
30%	-0.1818±j298.18	-0.1819±j298.18	-0.1818±j298.18
	-0.4938±j203.60	-1.2264±j201.18	-0.8842±j201.52
	-0.2513±j160.64	-0.3396±j160.39	-0.2672±j160.45
	-0.6705±j127.02	-0.7310±j127.15	-0.6927±j127.09
	-0.2811±j99.136	-0.7864±j99.290	-0.4608±j99.295
	-0.0031±j8.4105	-1.3534±j5.1525	-1.3517±j6.3035
50%	-0.1818±j298.18	-0.1819±j298.18	-0.1818±j298.18
	+0.1237±j202.87	-0.4237±j203.56	-0.4554±j203.44
	+0.2603±j161.38	-0.6495±j160.11	-0.4192±j160.36
	-0.6828±j127.05	-0.7958±j127.23	-0.7322±j127.16
	-0.3528±j99.345	-1.0005±j99.479	-0.5894±j99.490
	-0.2327±j9.4692	-1.7884±j6.0755	-1.6931±j7.1144
60%	-0.1818±j298.18	-0.1819±j298.18	-0.1818±j298.18
	+0.0612±j202.88	-0.4547±j203.32	-0.4526±j203.22
	+0.0908±j160.45	-0.5202±j161.06	-0.3562±j160.72
	-0.6947±j127.23	-0.8516±j127.37	-0.7674±j127.25
	-0.4162±j99.567	-1.1792±j99.678	-0.6892±j99.674
	-0.3773±j10.099	-2.0708±j6.5702	-1.9159±j7.5326
80%	-0.1818±j298.18	-0.1819±j298.19	-0.1818±j298.18
	-0.0134±j202.89	-0.5034±j203.17	-0.4788±j203.09
	-0.0967±j160.52	-0.3236±j160.68	-0.2693±j160.58
	-0.5998±j126.94	-0.2165±j127.36	-0.2864±j127.16
	+1.7178±j102.17	-1.1561±j101.12	-0.6186±j100.85
	-0.7619±j11.662	-2.8558±j7.5796	-2.5196±j8.2862

Table 4.3

Typical mechanical modes of the system with and without control at light load (P_e = 0.5 p.u., Q_e = 0.4359 p.u., V_t = 1.0 p.u.)

Compensation	Without the Excitation control	With a control designed for the 16th order	With a control designed for the 14th order
30%	-0.1818±j298.18	-0.1819±j298.18	-0.1819±j298.18
	-0.1624±j203.39	-0.6431±j203.39	-0.4097±j201.66
	-0.2079±j160.64	-0.2565±j160.45	-0.2110±j160.50
	-0.6629±j127.02	-0.7198±j127.11	-0.6883±j127.07
	-0.2178±j99.147	-0.6132±j99.198	-0.3883±j99.227
	-0.4313±j8.4705	-1.4887±j5.8854	-1.3734±j6.4130
50%	-0.1818±j298.18	-0.1819±j298.18	-0.1819±j298.18
	+0.0503±j202.88	-0.5279±j203.59	-0.5680±j203.47
	+0.3037±j160.06	-0.3573±j160.11	-0.1995±j160.34
	-0.6665±j127.05	-0.7922±j127.16	-0.7302±j127.12
	-0.2474±j99.356	-0.7957±j99.309	-0.4974±j99.381
	-0.6297±j9.4819	-1.9004±j6.6909	-1.7489±j7.1128
60%	-0.1818±j298.18	-0.1819±j298.18	-0.1819±j298.18
	+0.0138±j202.88	-0.4872±j203.39	-0.4972±j203.38
	-0.0050±j160.42	-0.7074±j160.90	-0.4829±j160.56
	-0.6586±j127.11	-0.8700±j127.28	-0.7748±j127.20
	-0.2655±j99.553	-0.9639±j99.425	-0.5871±j99.520
	-0.7548±j10.082	-2.1637±j7.1201	-1.9926±j9.4656
80%	-0.1818±j298.18	-0.1818±j298.18	-0.1819±j298.18
	-0.0135±j202.91	-0.4812±j203.26	-0.4728±j203.17
	-0.1284±j160.52	-0.3631±j160.61	-0.3139±j160.59
	-0.6624±j126.94	-0.2603±j127.42	-0.3162±j127.19
	+1.7579±j101.46	-1.3391±j100.52	-0.6494±j100.47
	-1.0877±j11.568	-2.9051±j7.9656	-2.6895±j8.0386

Table 4.4

Typical mechanical modes of the system with and without control at heavy load (P_e = 1.25 p.u., Q_e = 0.4359 p.u., V_t = 1.0 p.u.)

Compensation	Without the excitation control	With a control designed for the 16th order	With a control designed for the 14th order
30%	−0.1818±j298.18 −0.8632±j203.72 −0.2907±j160.63 −0.6774±j127.02 −0.3384±j99.104 +0.4213±j8.1027	−0.1819±j298.18 −1.5884±j201.03 −0.3915±j160.33 −0.7369±j127.17 −0.8755±j99.329 −1.4984±j4.7420	−0.1819±j298.18 −1.1821±j201.42 −0.3036±j160.42 −0.6952±j127.11 −0.4942±j99.318 −1.5920±j6.4917
50%	−0.1818±j298.18 +0.1881±j202.89 +0.2020±j161.68 −0.6981±j127.06 −0.4477±j99.318 +0.1360±j9.2235	−0.1819±j298.18 −0.3394±j203.55 −0.8504±j160.10 −0.7978±j127.26 −1.1084±j99.570 −1.8497±j5.9294	−0.1819±j298.19 −0.3682±j203.44 −0.5762±j160.37 −0.7343±j127.17 −0.6348±j99.541 −1.8564±j7.5255
60%	−0.1818±j298.18 +0.1031±j202.89 +0.1726±j160.49 −0.7293±j127.13 −0.5537±j99.546 −0.0402±j9.8917	−0.1819±j298.18 −0.4175±j203.29 −0.4076±j161.16 −0.8409±j127.41 −1.2920±j99.823 −2.1070±j6.5627	−0.1819±j298.18 −0.4098±j203.19 −0.2738±j160.83 −0.7656±j127.28 −0.7407±j99.753 −2.0503±j8.0835
80%	−0.1818±j298.18 +0.0373±j202.91 −0.0687±j160.52 −0.5800±j126.95 +1.6687±j102.81 −0.4977±j11.552	−0.1819±j298.18 −0.5021±j203.12 −0.2926±j160.67 −0.1939±j127.33 −0.9919±j101.47 −2.8669±j7.9327	−0.1819±j298.18 −0.4692±j203.05 −0.2361±j160.58 −0.2693±j127.14 −0.5752±j101.08 −2.6189±j9.2738

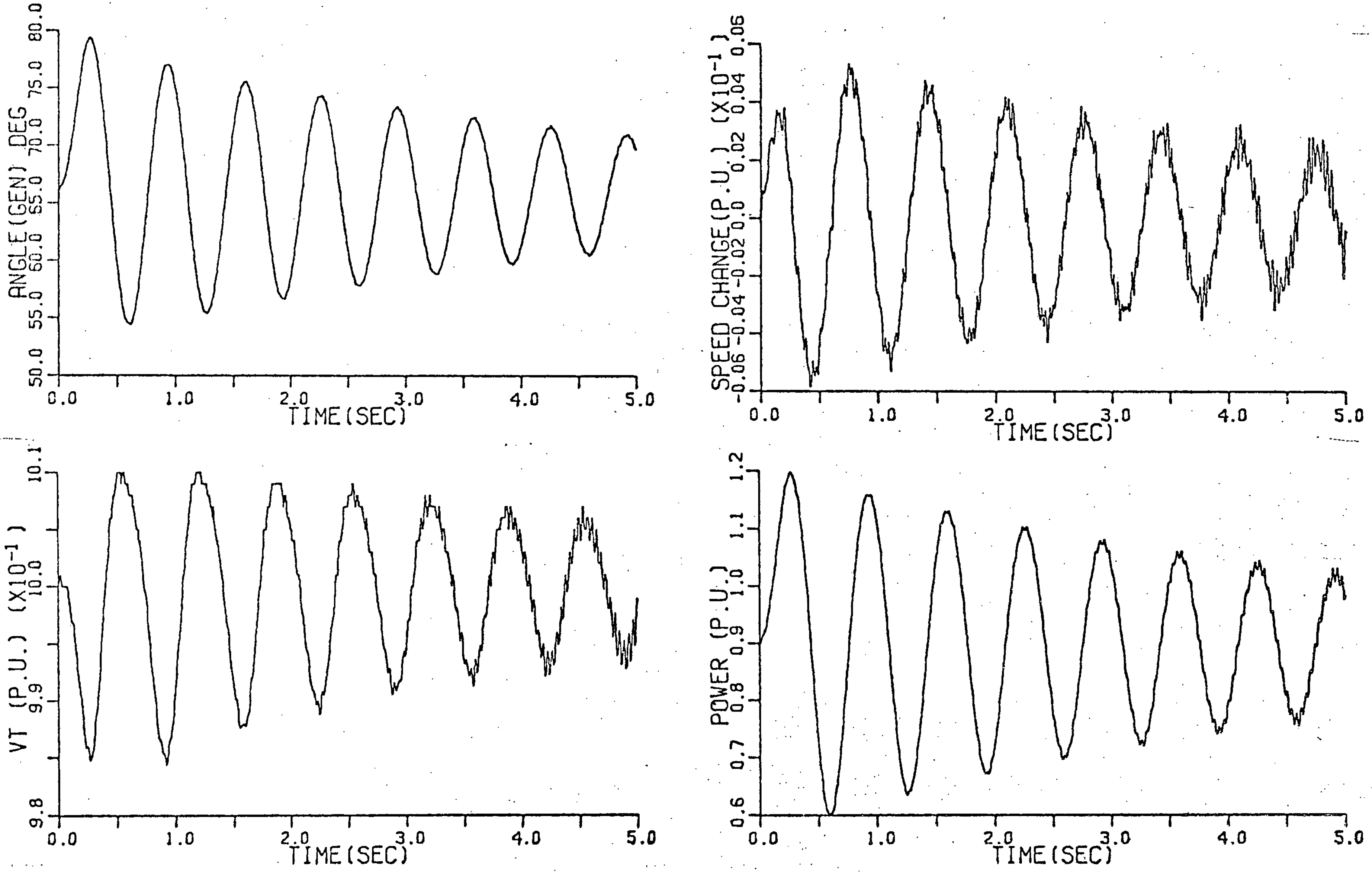

Figure 4.2 Dynamic responses of the power system without control

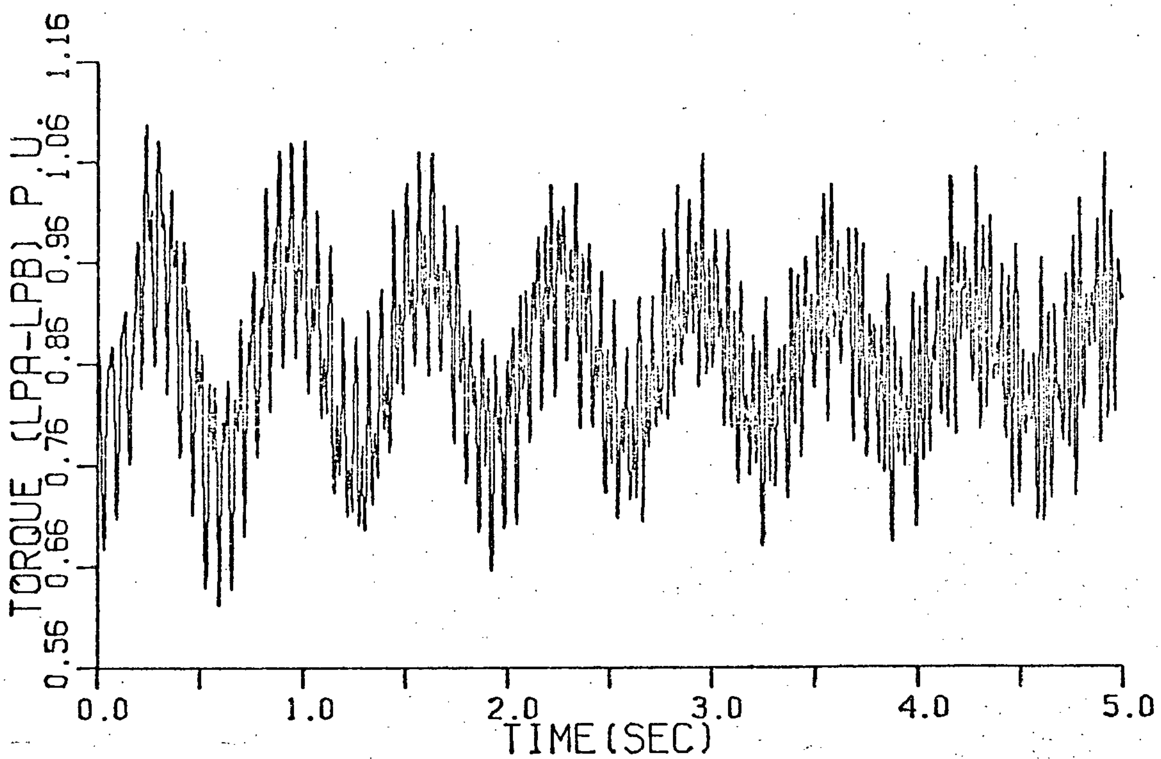

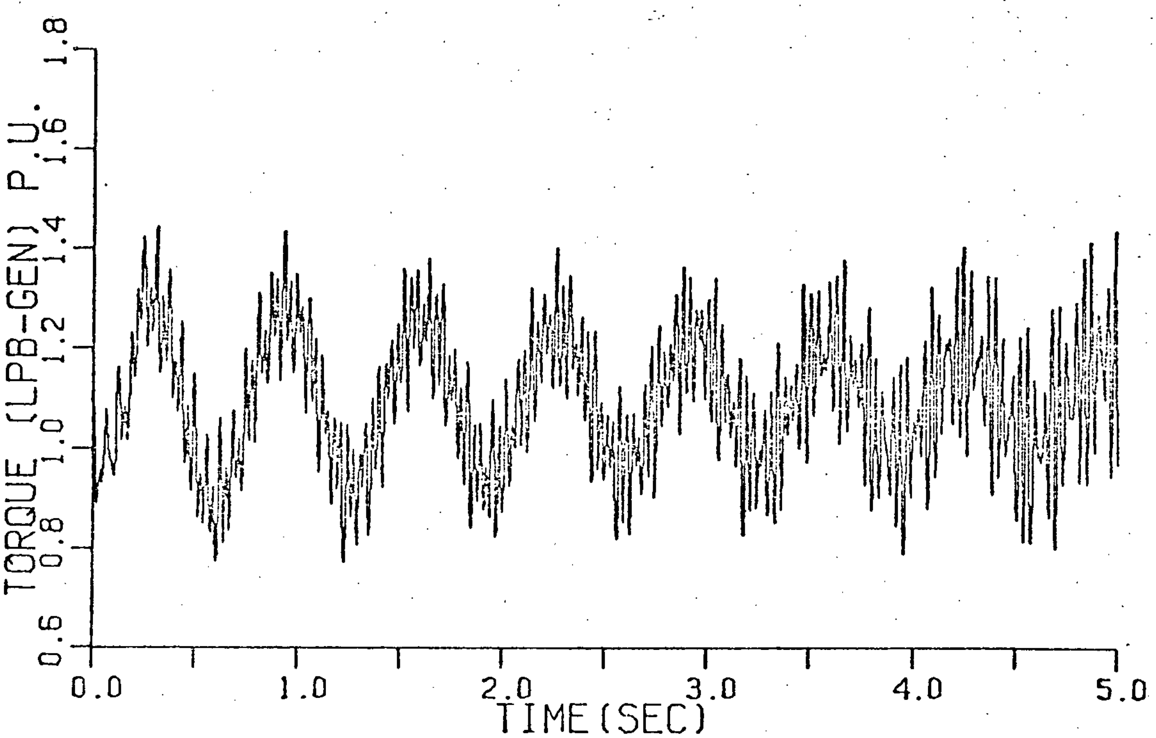

Figure 4.2 (continued)

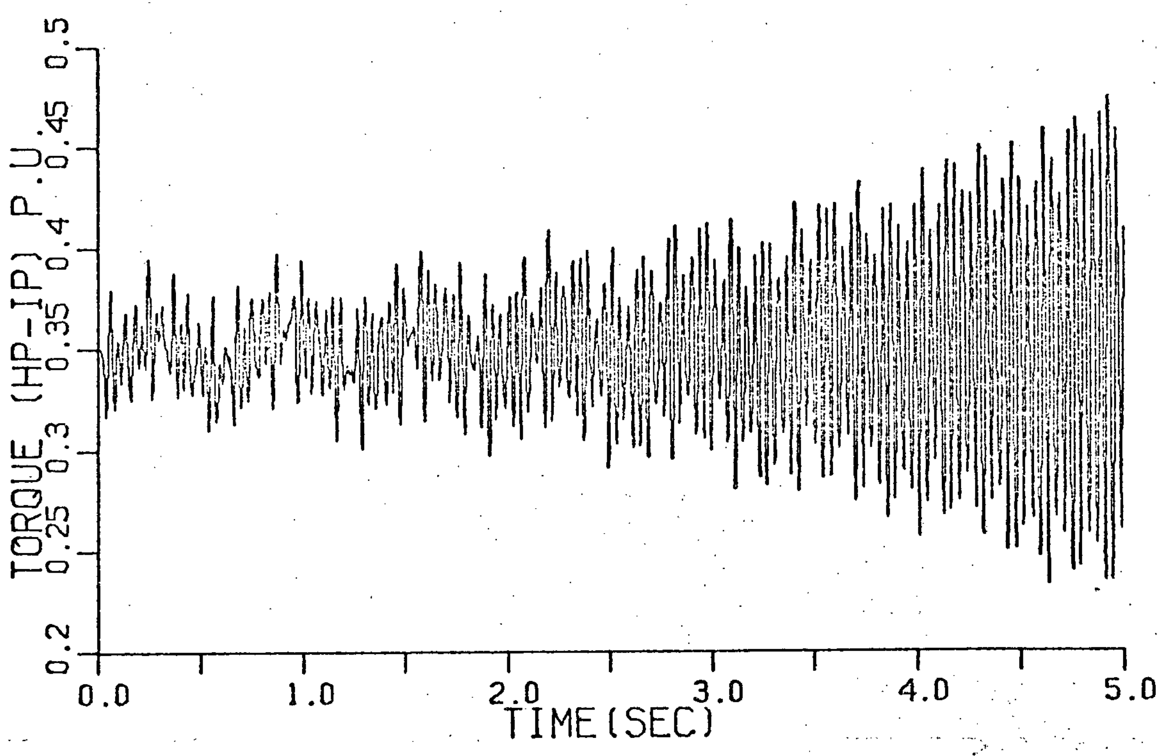

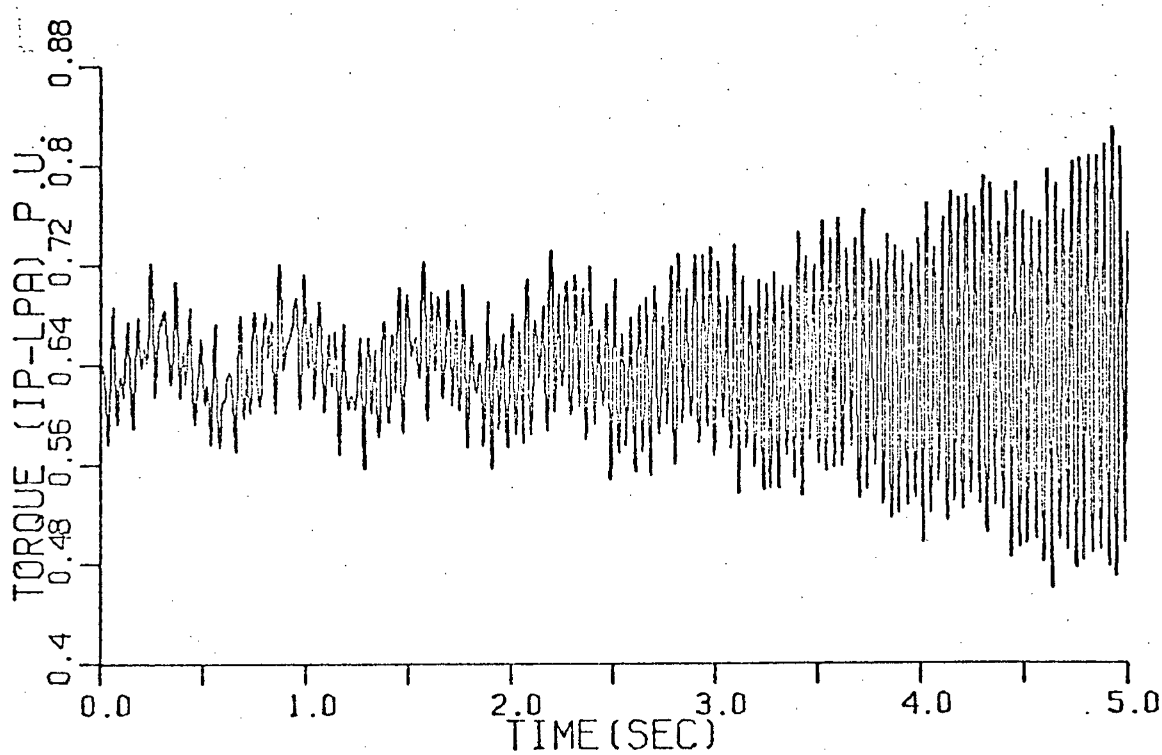

Figure 4.2 (continued)

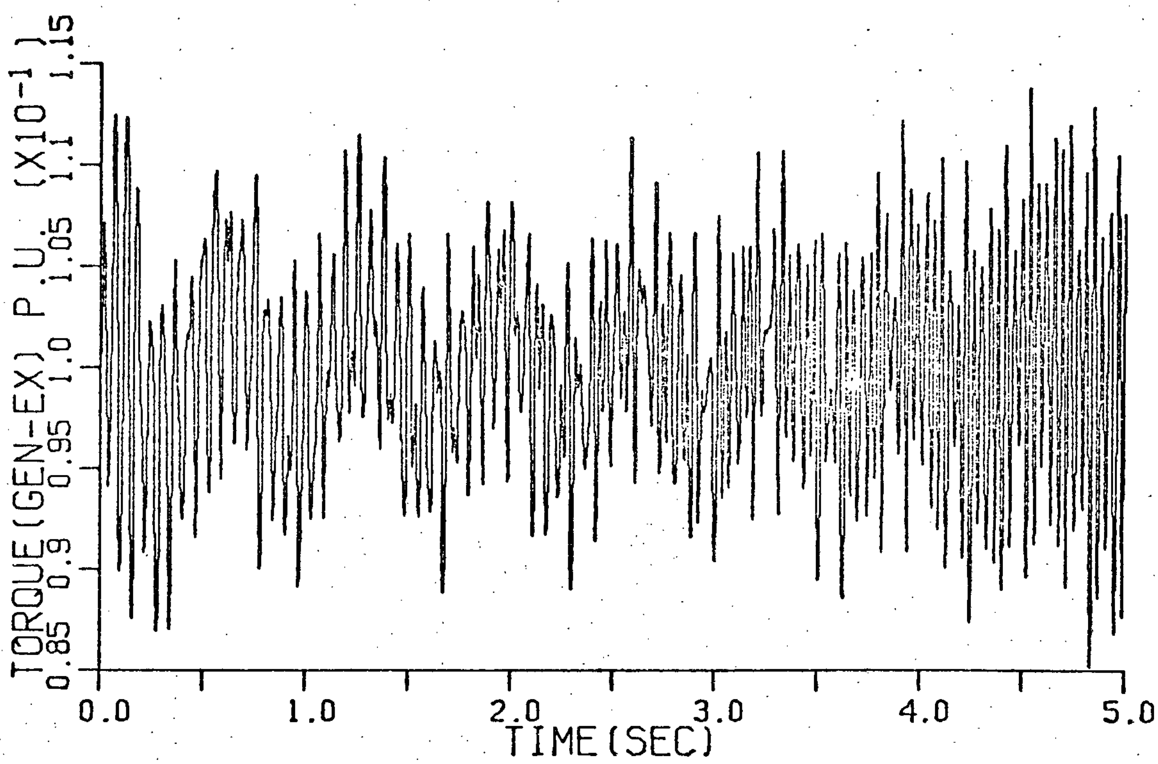

Figure 4.2 (continued)

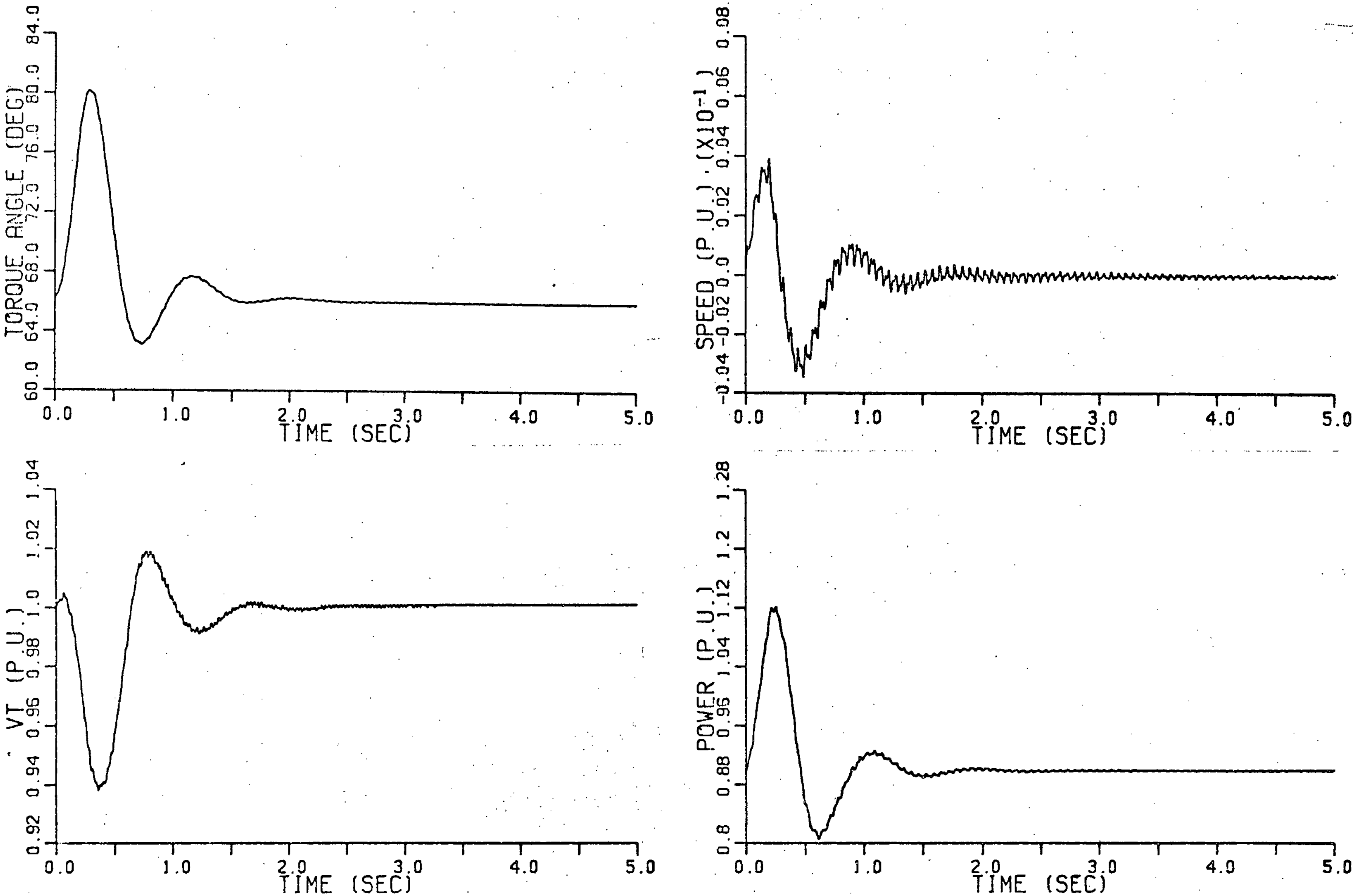

Figure 4.3 Dynamic responses of the power system with control.

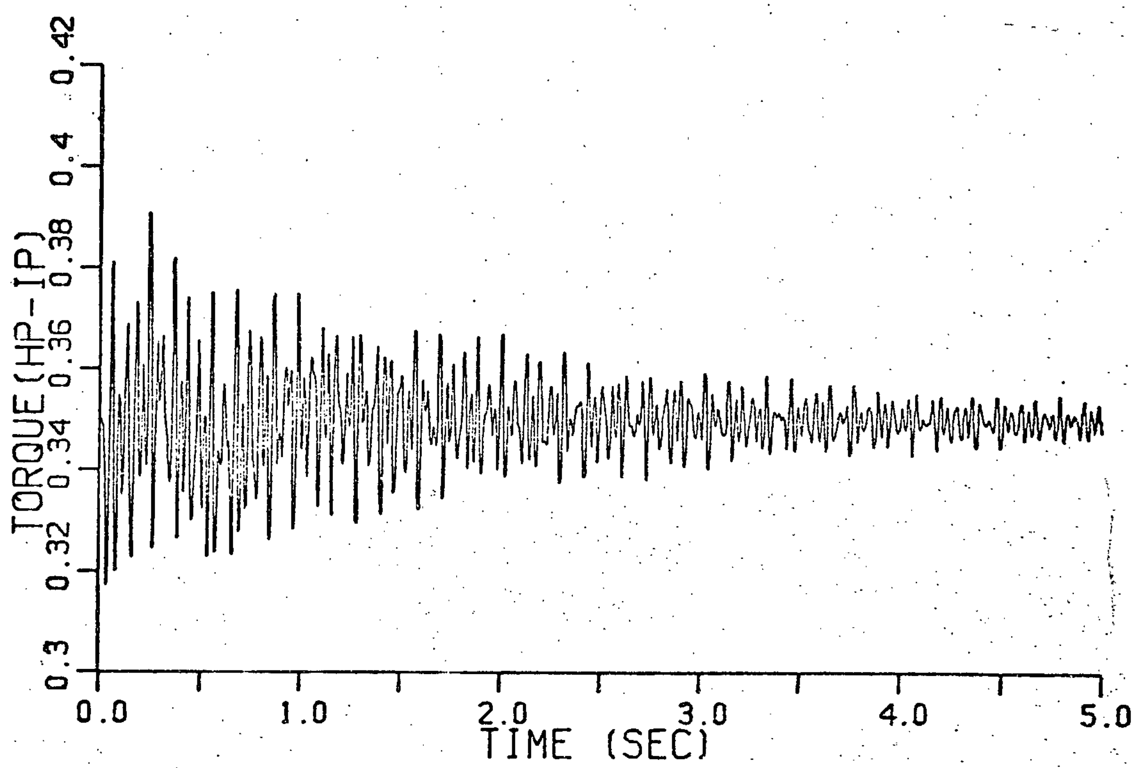

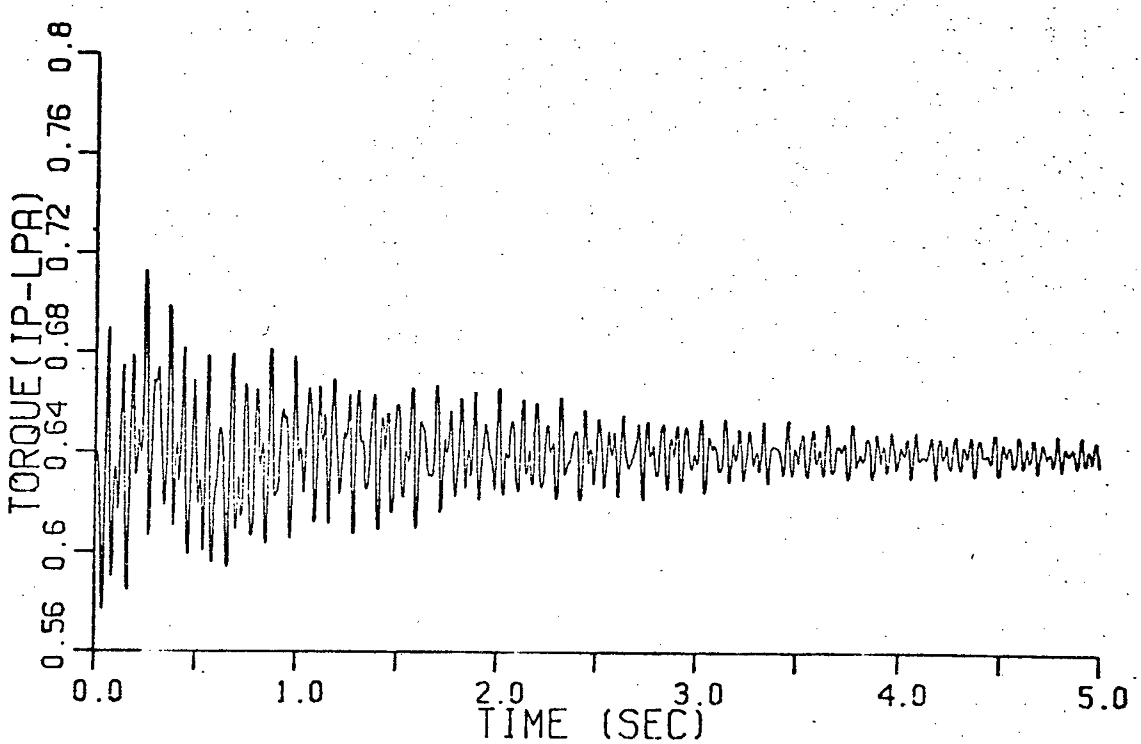

Figure 4.3 (continued)

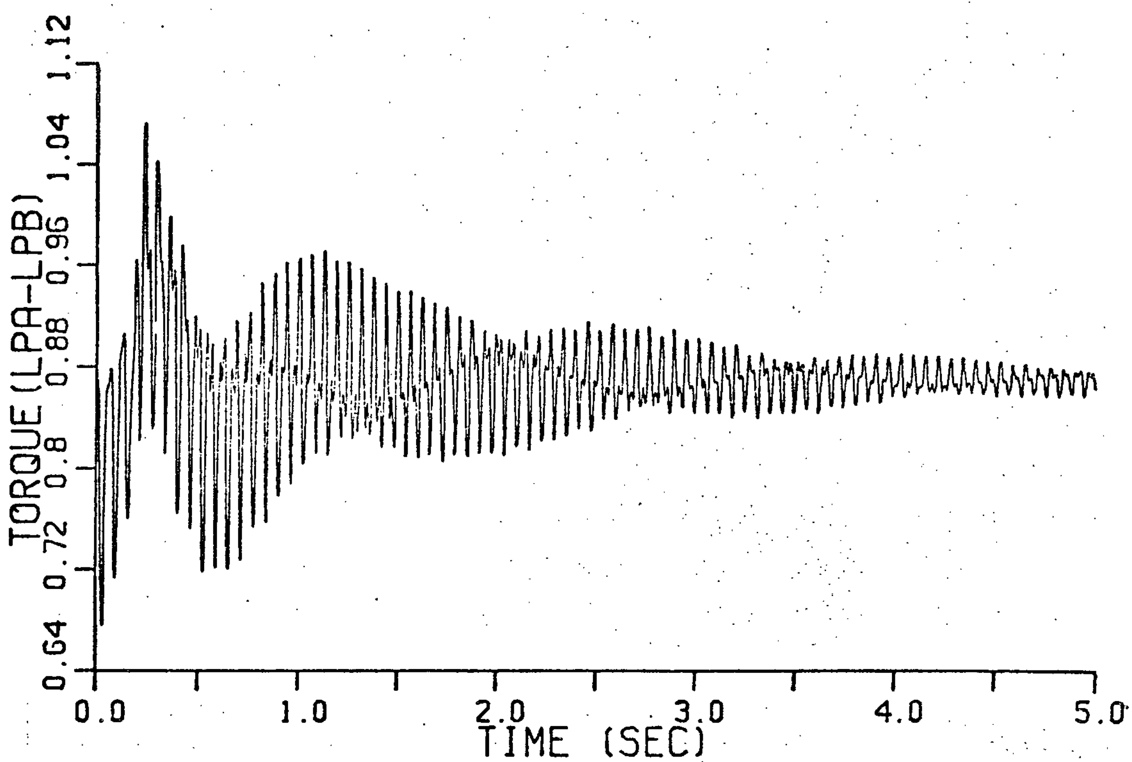

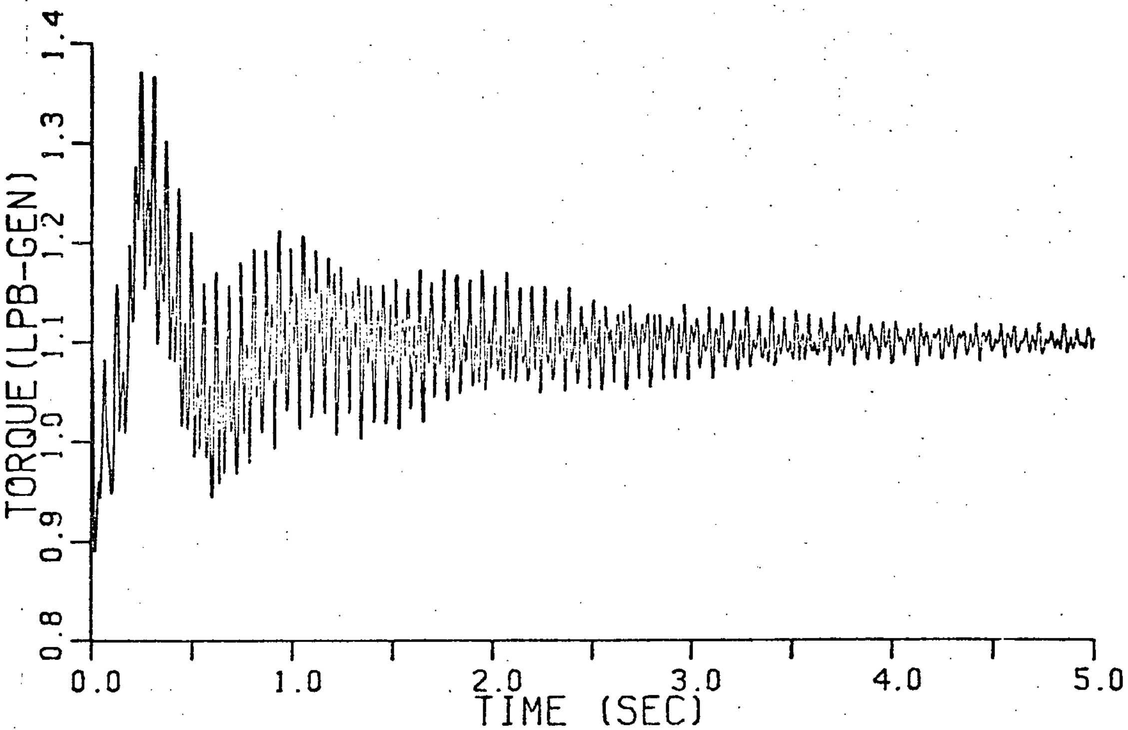

Figure 4.3 (continued)

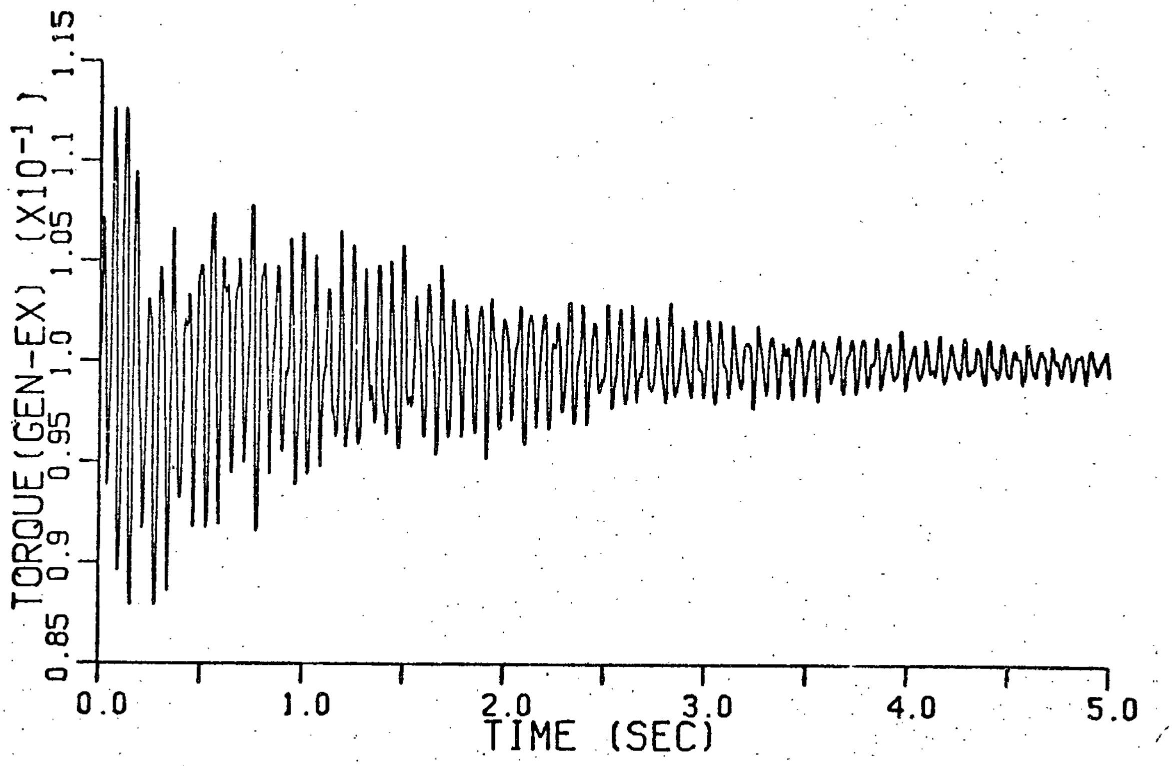

Figure 4.3 (continued)

4.9 The Control Signal

The control signal U_E of the 14th order model design and its frequecy spectrum from Fourier analysis are shown in Figures 4.4 and 4.5 respectively. There are four significant peaks at 1.15 Hz, 15.7 Hz , 25.6 Hz , and 32.3 Hz in the spectrum, which correspond to mode 0, mode 1, mode 3, and mode 4 of the generator mass-spring system respectively. The stabilizing effects on all mode of oscillations of this design are well coordinated.

Although the output feedback excitation control of SSR proves very effective for a single machine system, its effectiveness on multi-machine system is still unknown. The investigation of SSR control of multi-machine system with excitation control will be continued in the subsequent chapter.

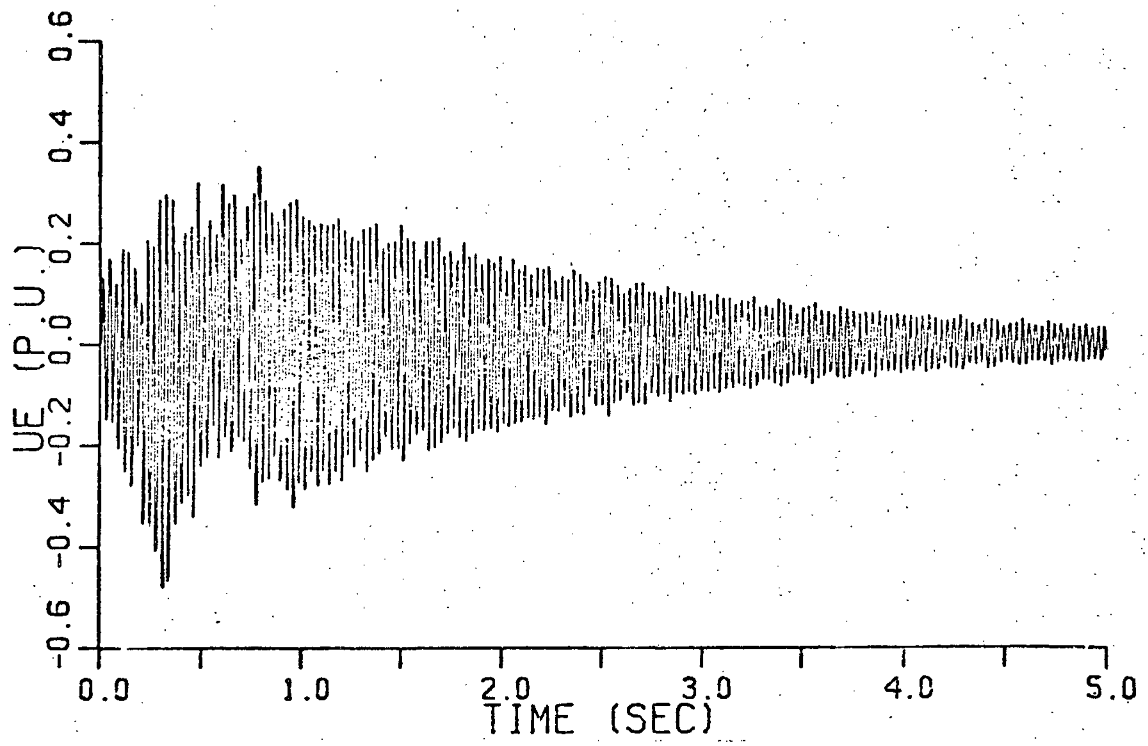

Figure 4.4 The control signal

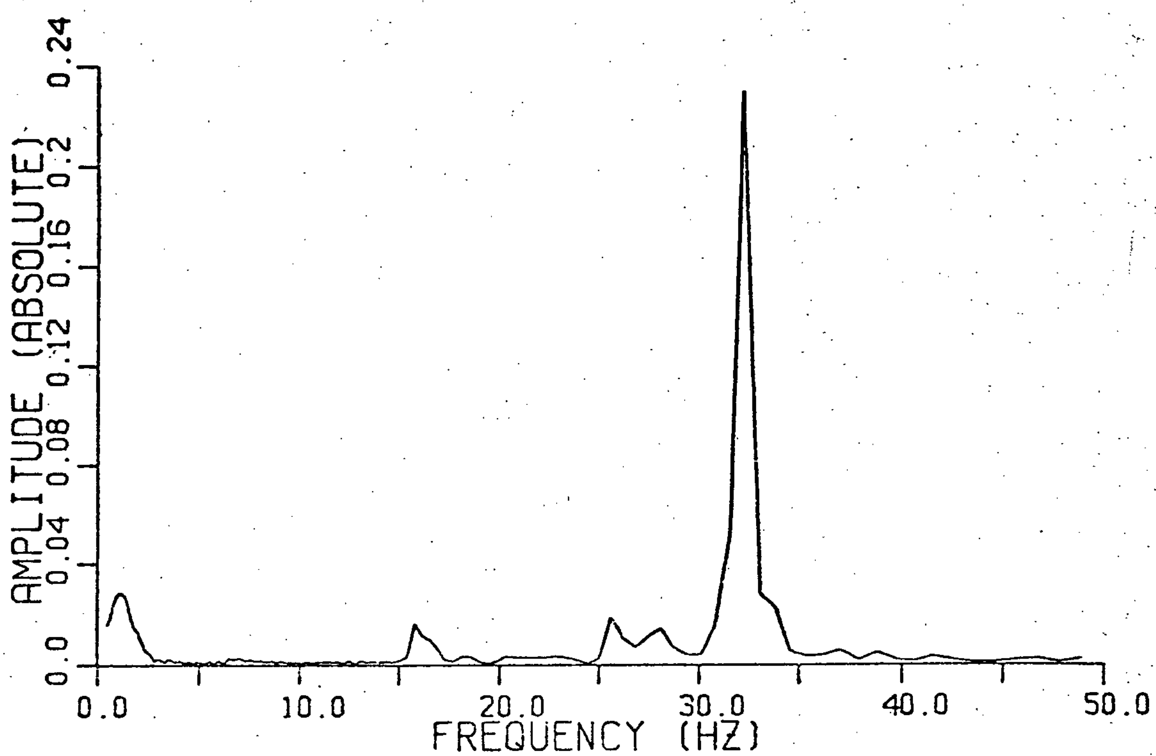

Figure 4.5 The frequency spectrum of the control signal

5 MULTI-MACHINE SSR STUDIES

5.1 Introduction

The SSR literatures so far are dealing with the torsional oscillations and counter measures of single generating unit possibly for two reasons: one, it has been considered as a local problem, two, it is difficult to deal with a very high order multi-machine system.

In this chapter, the multi-machine SSR problem will be examined, and excitation control of SSR will be developed. Two working examples will be given: a two-machine system and a three-machine system. Two factors make SSR studies in a multi-machine system different from that of a single machine system. First, more than one electrical resonance frequency may exist for the series-capacitor-compensated multiple transmission lines. Second, the torsional interaction of the mass-spring systems and the dynamic interaction of the low frequency oscillations between machines may exist. Therefore, the strategy of controller design depends very much upon the degree of interaction between machines.

The procedures of the multi-machine SSR studies are as follows: first, the system is given an eigenvalue analysis to find the effect of other capacitor-compensated lines not directly connected to a particular machine on the torsional modes of that machine. Second, the torsional interacting effects of other machines on the individual systems are examined. Third, excitation controls of SSR are designed, using the techniques developed in the previous chapters, for the machines with unstable torsional modes. Finally, the system with controller is evaluated using eigenvalue analysis and computer simulation test using the nonlinear power system model.

5.2 A Two-machine System and a Three-machine System

A two-machine system for the SSR studies is shown in Figure 5.1 with components listed in Table 5.1 and data given in Appendix II. As for the operating conditions, the conditions of machine 1 are fixed (i.e. P_{e1} = 0.9 p.u. , P.F. = 0.9 lagging , V_{t1} = 1.0 p.u.) and these of machine 2 vary with the compensation level (10% - 80%). The operating conditions of all buses other than the terminal bus of machine 1 are calculated for various compensation levels.

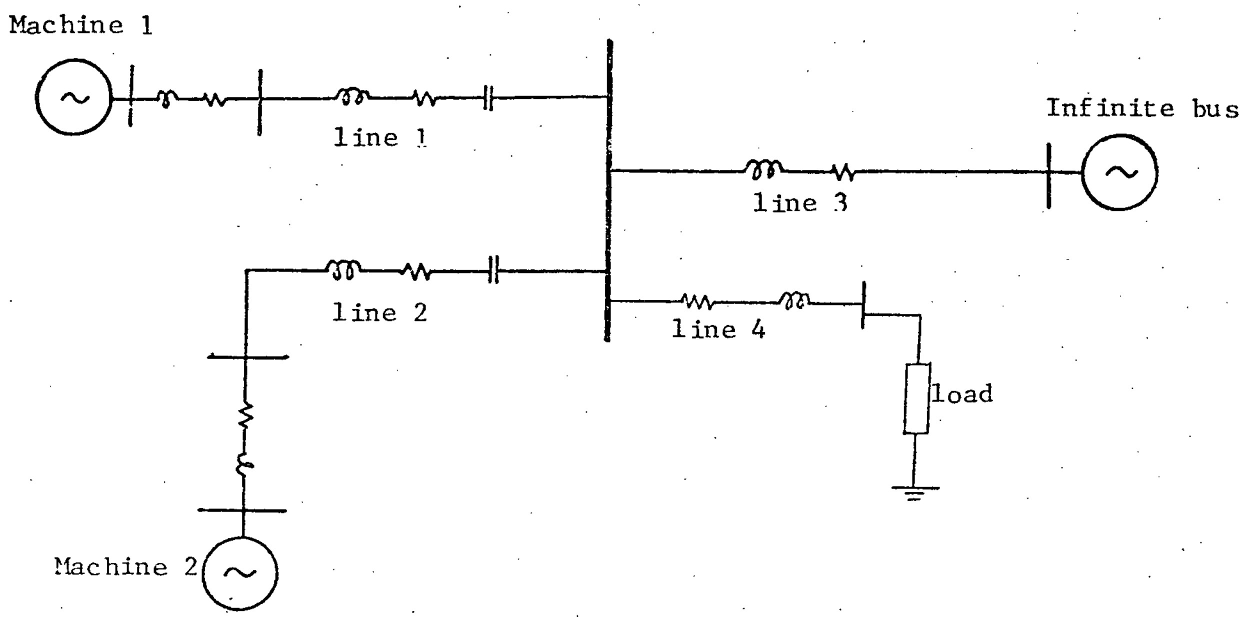

Figure 5.1 A two-machine power system.

Table 5.1

Summary of the components and number of state in the two-machine system

	system component		No. of state
Machine 1	six mass-spring system		12
	five-winding generator model		5
	second order excitation system		2
Machine 2	five mass-spring system		10
	five-winding generator model		5
	second order excitation system		2
Transmission system	Line No.	capacitor compensated	6
	1	yes	
	2	yes	
	3 and 4	no	
		Total No. of state	42

A three-machine system for SSR studies is shown in Figure 5.2 with components listed in Table 5.2 and data given in Apprendix III. Three base cases are studied:

1) 50% compensation for all lines, except no compensation for line 7.
2) 60% compensation for all lines, except no compensation for line 7.
3) The compensation of line 1 and 5 is 40%, that of lines 3,4,6,and 8 is 70%, and that of line 9 is 35%. No compensation for line 7.

In addition to the three base case studies, line compensation is also varied one at a time in the range of 30% to 70% for further studies. Operating conditions of the three base case studies are given in Table 5.3 .

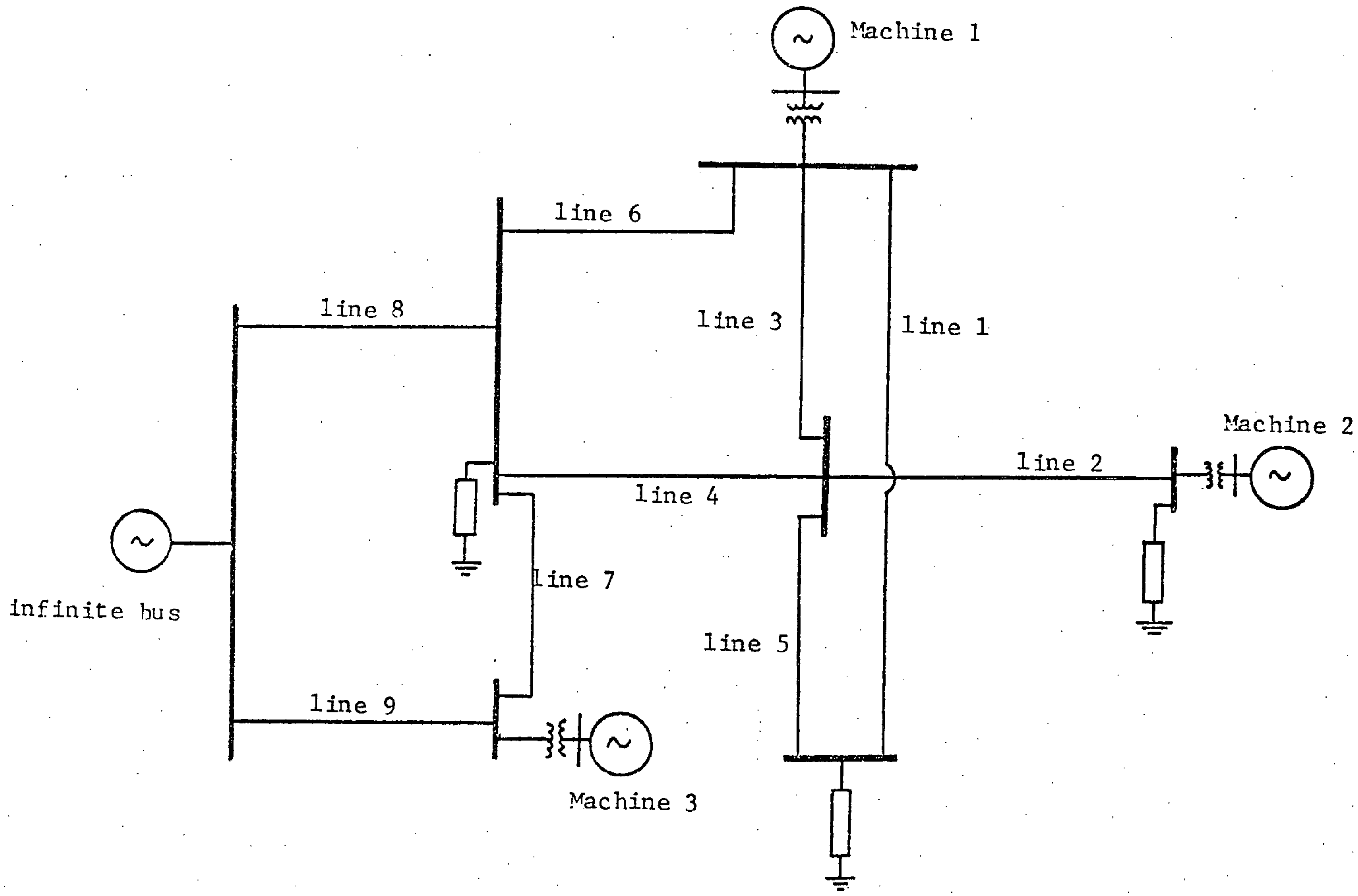

Figure 5.2 A three-machine power system.

Table 5.2

Summary of the components and number of state in the three-machine system

	system component		No. of state
Machine 1	six mass-spring system		12
	five-winding generator model		5
	second order excitation system		2
Machine 2	five mass-spring system		10
	five-winding generator model		5
	second order excitation system		2
Machine 3	four mass-spring system		8
	five-winding generator model		5
	second order excitation system		2
Transmission system	Line No.	capacitor compensated	28
	1 to 6	yes	
	7	no	
	8 to 9	yes	
		Total No. of state	79

Table 5.3

Various machine operating conditions in the three-machine system

		Machine 1	Machine 2	Machine 3
base case 1	P_e	0.9	0.9068	0.5
	Q_e	0.3359	0.3408	0.2744
	V_t	$1.0 \angle -3.12^\circ$	$1.0 \angle 0^\circ$	$1.0 \angle -13.6^\circ$
base case 2	P_e	0.9	0.9056	0.5
	Q_e	0.3071	0.3196	0.2602
	V_t	$1.0 \angle -2.38^\circ$	$1.0 \angle 0^\circ$	$1.0 \angle -11.48^\circ$
base case 3	P_e	0.9	0.9086	0.5
	Q_e	0.3076	0.3799	0.2627
	V_t	$1.0 \angle -4.56^\circ$	$1.0 \angle 0^\circ$	$1.0 \angle -11.32^\circ$

5.3 Prelimary Study of the two-machine System

From full model eigenvalue analysis of the two-machine system over a wide range of capacitor compensation, five unstable modes of the system are identified and given in Table 5.4 . Typical mechanical modes of the system are shown in Table 5.5 . The effect of capacitor compensation on the torsional modes of the machine not directly connected to that transmission line is also investigated. Typical results as manifested by the variation of real parts of the eigenvalues of particular torsional modes are shown in Figures 5.3 through 5.6 . The natural frequencies also change slightly. Therefore, for a multi-machine system with multiple capacitor-compensated-lines, more than one condition at which SSR may occur.

Table 5.4

Unstable modes of the two-machine system

Machine 1	mode 3 (25.5 Hz.)
	mode 4 (32.3 Hz.)
Machine 2	mode 0 (1-2 Hz.)
	mode 2 (24.0 Hz.)
	mode 3 (30.2 Hz.)

Interaction between machines' torsional modes is obviously an important factor to be considered in the SSR controller design. If the interaction between machines is significant it must be considered, otherwise, the controller can be designed one machine at a time.

The torsional interaction between machines are investigated as follows:

1) Find the eigenvalues from the full model of the system.

2) Find the eigenvalues of the reduced order models that the mass-spring system of one machine is represented in detail and the mass-spring system of the other is lumped into one mass.

3) Compare the results of steps 1) and 2). Any significant change in the torsional modes indicates the existence of interaction. Otherwise, the interaction between machines is insignificant.

Typical results for the two-machine system are shown in Table 5.6 . Although there are slight changes in the torsional modes between steps 1) and 2) especially when two mode frequencies are close, these interactions are not strong enough to make the unstable modes stable or vice versa. Therefore, the interaction between the two machines' torsional modes is insignificant.

Table 5.5

Typical mechanical modes of the two-machine system

Line compensation	Machine 1	Machine 2
Line 1 70% Line 2 70%	$-1.2096\pm j298.18$ $+0.1503\pm j203.02$ $-0.2213\pm j160.46$ $-0.7152\pm j127.08$ $-0.6302\pm j99.416$ $-0.9949\pm j10.242$	$-0.1215\pm j276.41$ $+0.0862\pm j189.96$ $+0.3546\pm j151.55$ $-0.2503\pm j102.42$ $-0.1677\pm j6.8353$
Line 1 70% Line 2 30%	$-1.2224\pm j298.18$ $+0.1073\pm j202.87$ $+0.1379\pm j160.88$ $-0.7183\pm j127.08$ $-0.6550\pm j99.429$ $-0.6239\pm j10.422$	$-0.1215\pm j276.41$ $+0.1396\pm j189.81$ $-0.2186\pm j151.65$ $-0.2048\pm j102.26$ $+0.3318\pm j6.6557$
Line 1 50% Line 2 50%	$-1.2066\pm j298.18$ $+0.0610\pm j202.91$ $-0.5470\pm j160.75$ $-0.7039\pm j99.204$ $-0.6625\pm j9.3108$	$-0.1215\pm j276.41$ $+0.1352\pm j189.97$ $-0.1927\pm j151.52$ $-0.0119\pm j6.5236$
Line 1 50% Line 2 70%	$-1.1997\pm j298.18$ $-0.0383\pm j203.38$ $-0.4321\pm j160.95$ $-0.7027\pm j127.04$ $-0.5727\pm j99.211$ $-0.9671\pm j9.3253$	$-0.1215\pm j276.41$ $-0.0467\pm j189.98$ $-0.0619\pm j151.68$ $-0.2159\pm j102.27$ $-0.1467\pm j6.6456$

Table 5.6

Typical mechanical modes of the two-machine system using different models for the investigation of torsional interaction between machines

		M1 : detail M2 : detail	M1 : detail M2 : one mass	M1 : one mass M2 : detail
Line 1 60%	Machine 1 (M1)	-1.2143±j298.18	-1.2143±j298.18	
		+0.1296±j202.87	+0.1303±j202.87	
		-0.5487±j161.02	-0.5472±j160.01	
		-0.7096±j127.05	-0.7095±j127.05	
		-0.6088±j99.282	-0.6179±j99.299	
		-0.6064±j9.7300	-0.6064±j9.730	-0.5022±j9.7802
Line 2 40%	Machine 2 (M2)	-0.1215±j276.41		-0.1215±j276.41
		-0.0295±j189.95		-0.0296±j189.95
		-0.1843±j151.52		-0.1850±j151.52
		-0.1887±j102.18		-0.1797±j102.16
		-0.0831±j6.4809	-0.0799±j6.5063	-0.0623±j6.4929
Line 1 70%	Machine 1 (M1)	-1.2194±j298.18	-1.2914±j298.18	
		+0.0714±j202.87	+0.0718±j202.87	
		+0.1326±j160.77	+0.1228±j160.78	
		-0.7167±j127.08	-0.7167±j127.07	
		-0.6448±j99.411	-0.6612±j99.438	
		-0.6822±j10.288	-0.6944±j10.313	-0.5805±j10.351
Line 2 40%	Machine 2 (M2)	-0.1215±j276.41		-0.1215±j276.41
		-0.0509±j189.95		-0.0509±j189.96
		-0.1115±j151.62		-0.1058±j151.96
		-0.1970±j102.25		-0.1807±j102.23
		-0.1094±j6.7660	-0.1065±j6.7949	-0.0885±j6.7772

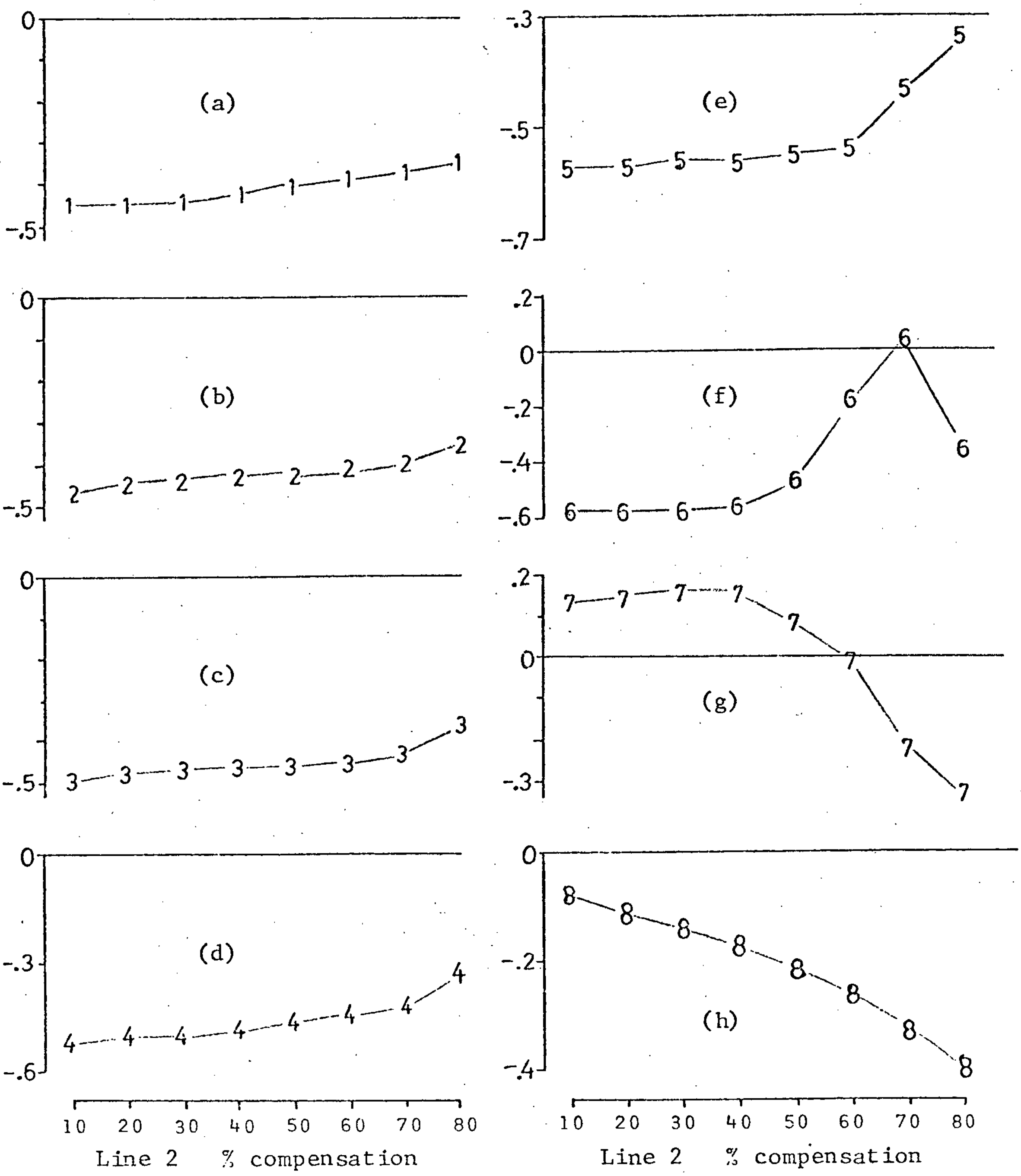

Figure 5.3 Variation of the real part of mode 3 (160 rad/sec.) of machine 1 (vertical axis) as line 2's capacitor changes and line 1's capacitor kept constant at (a) 10%, (b) 20%, (c) 30%, (d) 40%, (e) 50%, (f) 60%, (g) 70%, (h) 80% compensation.

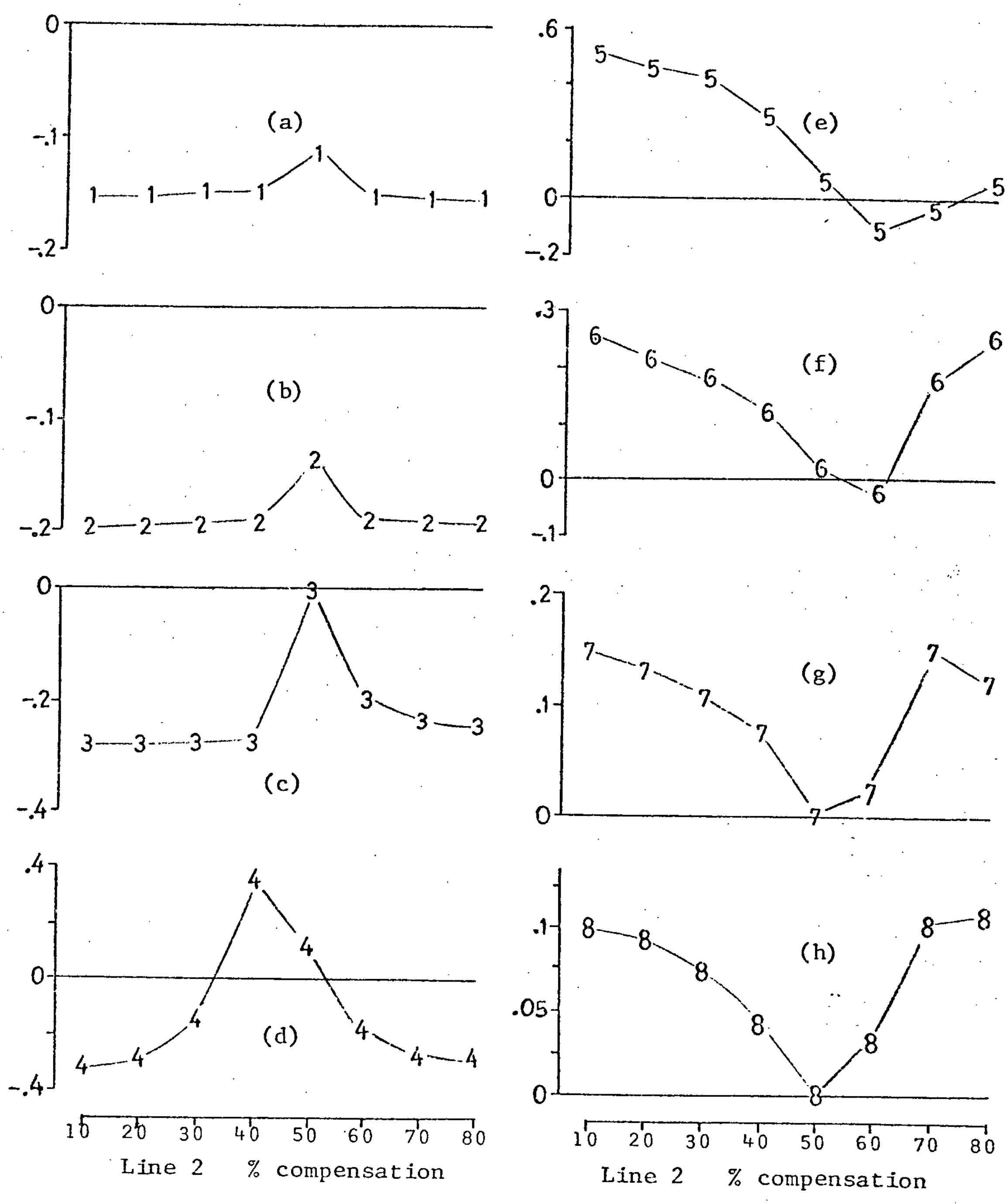

Figure 5.4 Variation of the real part of mode 4 (203 rad/sec.) of machine 1 (vertical axis) as line 2's capacitor changes and line 1's capacitor kept constant at (a) 10%, (b) 20%, (c) 30%, (d) 40%, (e) 50%, (f) 60%, (g) 70%, (h) 80% compensation.

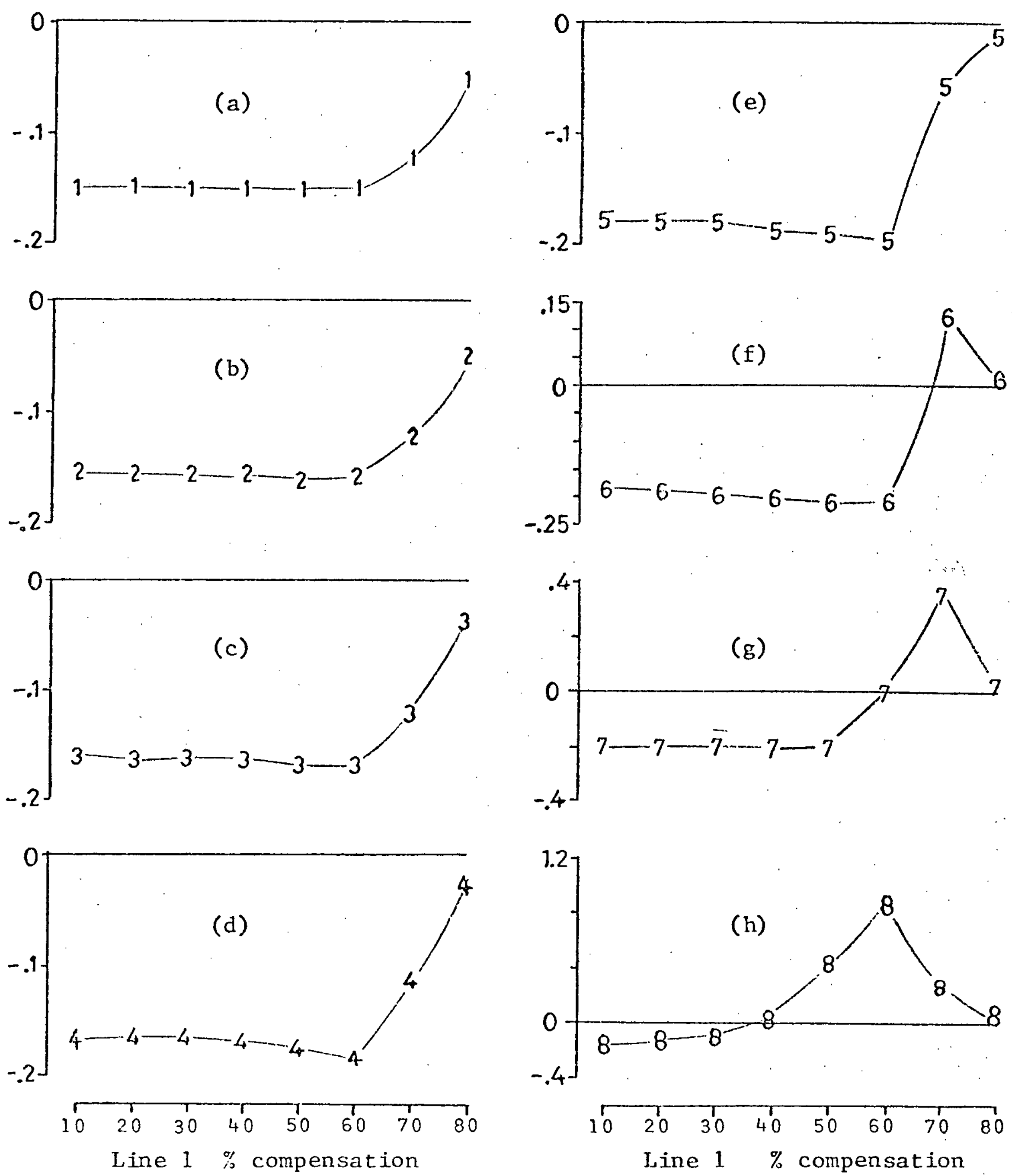

Figure 5.5 Variation of the real part of mode 2 (151 rad/sec) of machine 2 (vertical axis) as line 1's compensation changes and line 2's capacitor kept constant at (a) 10%, (b) 20%, (c) 30%, (d) 40%, (e) 50%, (f) 60%, (g) 70%, (h) 80% compensation.

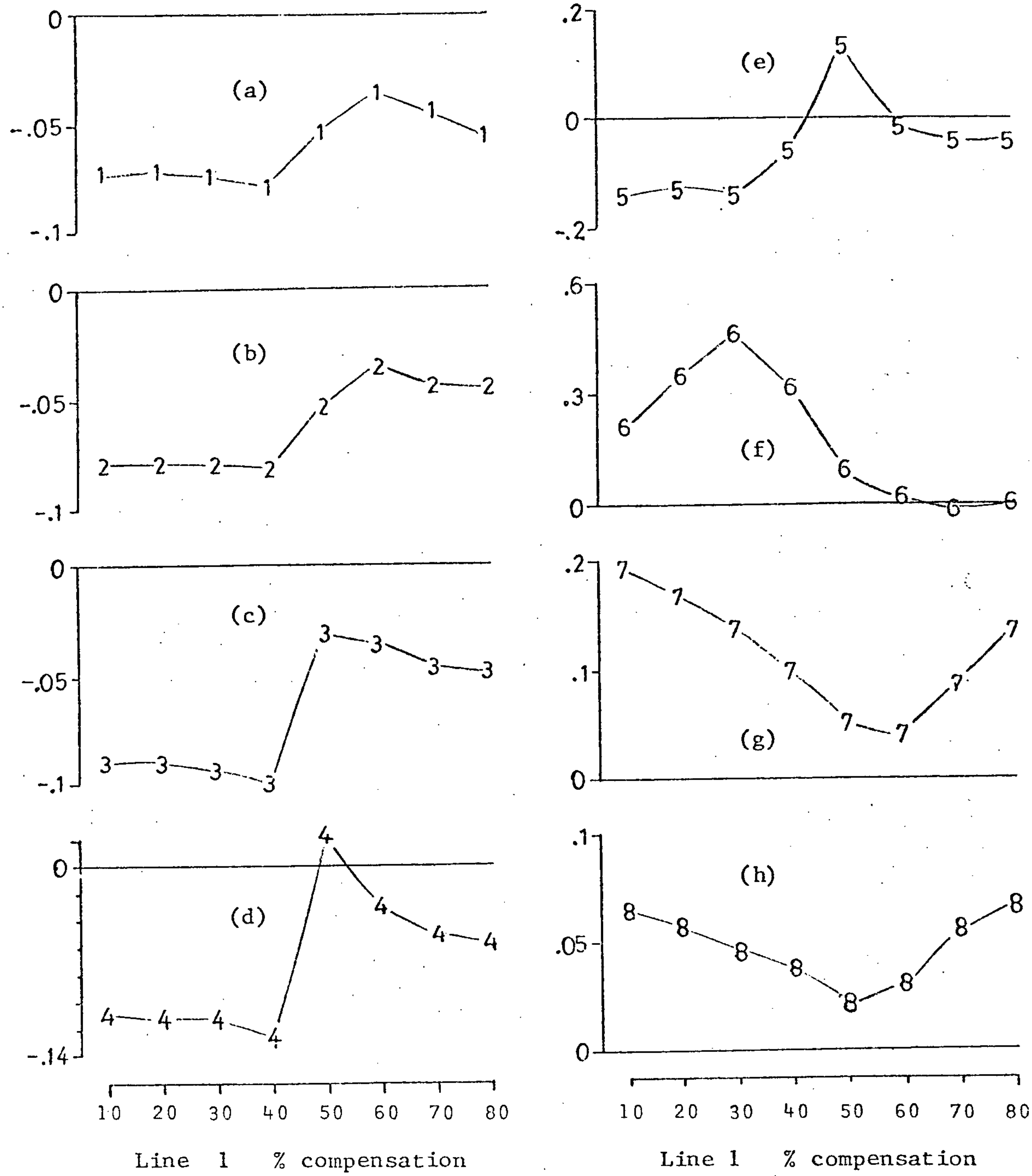

Figure 5.6 Variation of the real part of mode 3 (190 rad/sec.) of machine 2 (vertical axis) as line 1's capaciotr changes and line 2's capacitor kept constant at (a) 10%, (b) 20%, (c) 30%, (d) 40%, (e) 50%, (f) 60%, (g) 70%, (h) 80% compensation.

5.4 Preliminary Study of the Three-machine System

Again from the full model eigenvalue analysis of the three-machine system over a wide range of capacitor compensation, six unstable modes of the system are identified, and they are given in Table 5.7 . Typical mechanical modes of the system are given in Table 5.8 .

The interacting effect of torsional modes for the system is also investigated using the same procedures as described in section 5.3 . The results are shown in Table 5.9 , which also suggest that interaction between machine's torsional modes is insignificant.

Table 5.7

Unstable modes of the three-machine system

Machine 1	mode 1 (15.7 Hz.) mode 4 (32.3 Hz.)
Machine 2	mode 0 (1-2 Hz.) mode 1 (16.2 Hz.) mode 2 (24.0 Hz.) mode 3 (30.2 Hz.)
Machine 3	none

Table 5.8

Typical mechanical modes of the three-machine system

Line compensation	Machine 1	Machine 2	Machine 3
Line 1 60% Line 2 70% Line 3-9 60% (except 7)	-0.1818±j298.18 +0.2653±j203.29 -0.2753±j160.70 -0.6612±j127.04 -0.2455±j99.456 -1.7915±j10.363	-0.1214±j276.41 -0.0644±j189.99 +0.0832±j151.81 +0.2785±j102.65 +1.3101±j10.175	-0.1336±j353.25 -0.1336±j190.17 -0.7337±j167.73 -3.2331±j17.474
Line 1-8 50% (except 7) Line 9 30%	-0.1818±j298.18 -0.2359±j203.20 -0.2283±j160.66 -0.6773±j127.02 -0.2707±j99.224 -1.1930±j9.8449	-0.1215±j276.41 +0.1086±j189.99 -0.0544±j151.58 -0.3096±j102.66 +0.6526±j8.8284	-0.1344±j353.24 -0.2284±j190.11 -0.7334±j167.73 -3.1623±j17.262
Line 1-3 50% Line 4 30% Line 5-9 50% (except 7)	-0.1818±j298.18 +0.0608±j203.34 -0.3752±j160.63 -0.6427±j126.99 +0.1309±j99.502 -0.9892±j10.472	-0.1214±j276.41 -0.0549±j189.84 +0.1253±j151.93 -0.4555±j102.56 +0.2684±j8.7070	-0.1334±j353.24 -0.1776±j190.28 -0.7326±j167.73 -3.3444±j17.589
Line 1,5 40% Line 9 35% Line 2-4,6,8 70%	-0.1818±j298.18 +0.2653±j203.29 -0.2753±j160.70 -0.6612±j127.04 -0.2455±j99.456 -1.7915±j10.363	-0.1214±j276.41 -0.0644±j189.99 +0.0832±j151.81 +0.2785±j102.65 +1.3101±j10.175	-0.1336±j353.24 -0.1631±j190.17 -0.7337±j167.73 -3.2331±j17.474

Table 5.9

Typical mechanical modes of the three-machine system using different models for the investigation of torsional interaction between machines

	M1 : detail M2 : detail M3 : detail	M1 : one mass M2 : detail M3 : detail	M1 : detail M2 : one mass M3 : detail	M1 : detail M2 : detail M3 : one mass	M1 : one mass M2 : one mass M3 : detail	M1 : one mass M2 : detail M3 : one mass	M1 : detail M2 : one mass M3 : one mass
Machine 1 (M1)	-0.182±j298.2		-0.182±j298.2	-0.182±j298.2			-0.182±j298.2
	+0.265±j203.3		+0.253±j203.3	+0.266±j203.3			+0.253±j203.3
	-0.275±j160.7		-0.270±j160.7	-0.275±j160.7			-0.270±j160.7
	-0.661±j127.0		-0.661±j127.0	-0.661±j127.0			-0.661±j127.0
	-0.245±j99.46		-0.412±j99.45	-0.245±j99.46			-0.411±j99.45
	-1.792±j10.36	-1.818±j10.41	-1.805±j10.40	-1.792±j10.36	-1.834±j10.45	-1.818±j10.41	-1.805±j10.40
Machine 2 (M2)	-0.121±j276.4	-0.121±j276.4		-0.121±j276.4		-0.121±j276.4	
	-0.064±j189.9	-0.067±j189.9		-0.013±j190.0		-0.014±j190.0	
	+0.083±j151.8	+0.080±j151.8		+0.083±j151.8		+0.081±j151.8	
	+0.278±j102.6	+0.414±j102.6		+0.278±j102.6		+0.413±j102.6	
	+1.310±j10.18	+1.327±j10.20	+1.331±j10.25	+1.310±j10.18	+1.350±j10.27	+1.327±j10.20	+1.332±j10.25
Machine 3 (M3)	-0.134±j353.2	-0.134±j353.2	-0.134±j353.2		-0.134±j353.2		
	-0.163±j190.2	-0.161±j190.2	-0.216±j190.1		-0.216±j190.1		
	-0.734±j167.7	-0.734±j167.7	-0.734±j167.7		-0.734±j167.7		
	-3.233±j17.47	-3.233±j17.47	-3.234±j17.48	-3.248±j17.51	-3.235±j17.47	-3.248±j17.51	-3.249±j17.51

5.5 Controller Design Considerations of Multi-machine SSR System

Although the controller design using the full model, which accounts for all natural frequencies in the electrical system and torsional interaction between machines, could be the best, it often results in a high order controller. Since the torsional interaction between machines according to the foregoing studies is insignificant, an alternative method using a reduced order model for the design is developed. The original system is divided into several one-machine systems, and the controller is designed one at a time. Two general steps are as follows:

1) Choose an appropriate one-machine system model by retaining one of the transmission lines directly connected to the machine, which has the largest steady current and hence the strongest torsional interacting effect between the electrical and mechanical systems.

2) Modify the line by adding some impedance so that the critical electrical frequency for the line with compensation as viewed from the machine will not change.

When the multi-machine system is divided into several one-machine systems, the dynamic interaction between machines has been neglected. But these interactions depend very much upon the tie lines between machines. For a strong tie line , strong interaction may exist. Therefore, the controllers designed for individual one-machine systems must be coordinated. An iterative scheme as shown in Figure 5.7 may be applied to adapt the designed controllers so that all dampings of the mechanical modes in the system are coordinated.

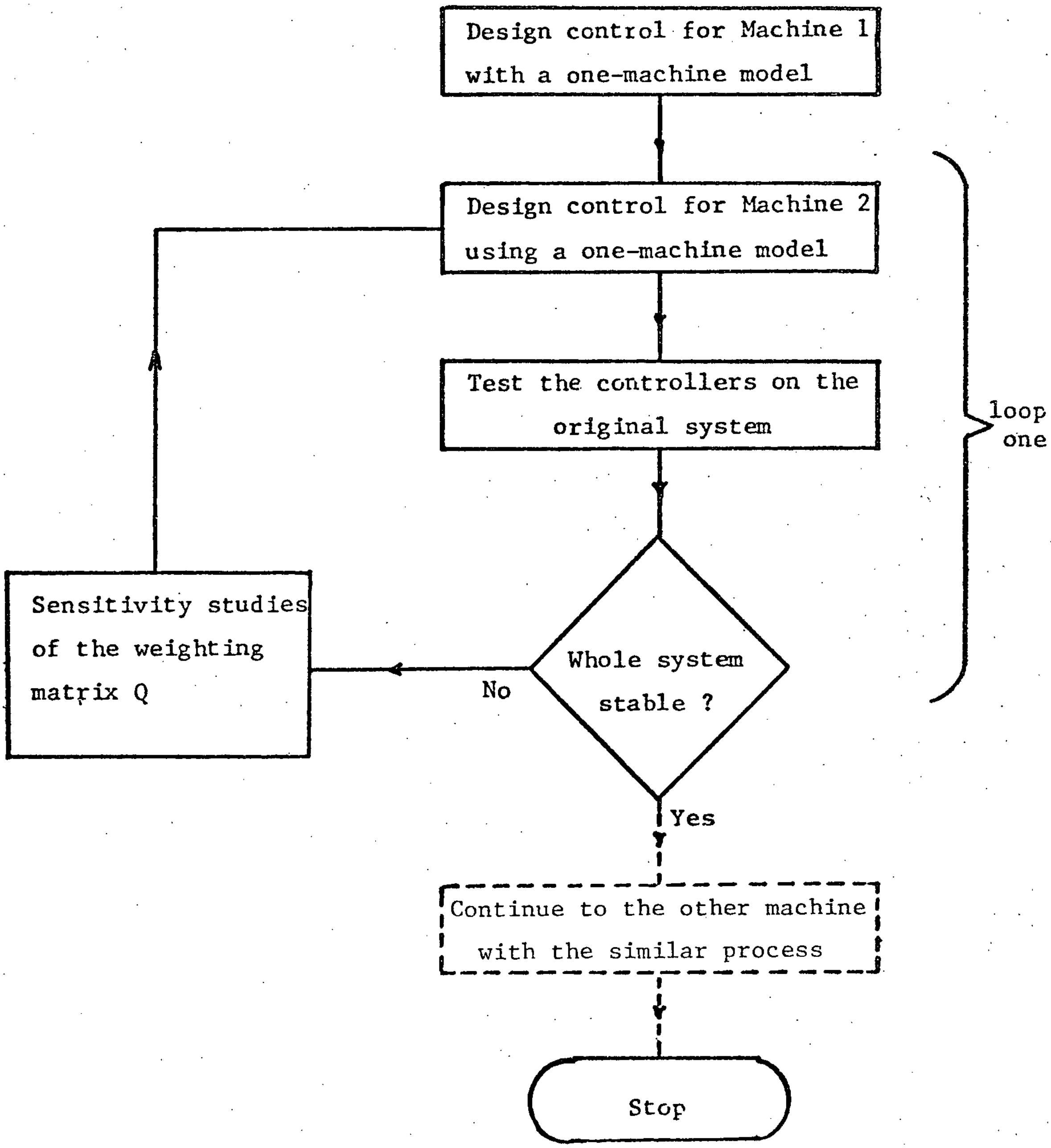

Figure 5.7 Iterative scheme for adapting controller into the original system.

5.6 Controllers Design and Test of the Two-Machine System

The two-machine system is divided into two one-machine infinite-bus system models for the controller design as follows:

1) The natural frequencies of either one of the two transmission lines for a wide range of capacitor compensation are determined by setting the capacitor compensation of the other line to zero.

2) The rest of the system is replaced by an equivalent impedance, X_{E1} or X_{E2} as shown in Figure 5.8(a) or (b) respectively, such that each system will have the same electrical natural frequencies as determined in step 1).

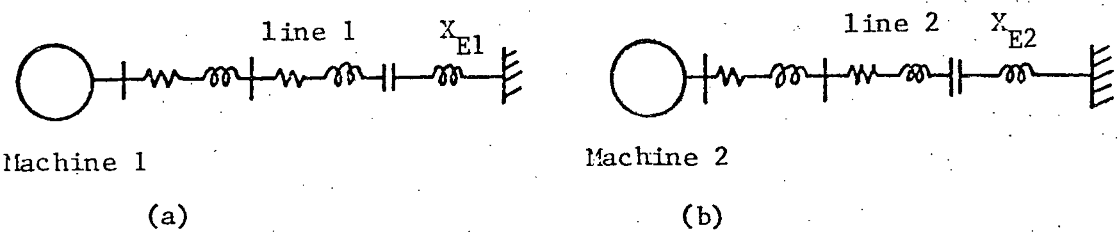

Figure 5.8 Two subsystems resulted from the two-machine system.

For machine 1 of Figure 5.8(a), X_{E1} is found to be 0.1 p.u. . Since the operating conditions, the machine and transmission line parameters of the system given in Appendix II are almost the same as that of the one-machine system studied in the previous chapters, the same controller in Equation (4.37) will be applied without change.

For machine 2 of Figure 5.8(b), X_{E2} is 0.11 p.u. , and the average operating conditions are

$$P_{e2} = 0.8 \text{ p.u.} \quad , \quad Q_{e2} = 0.4 \text{ p.u.} \quad , \quad V_{t2} = 0.9 \text{ p.u.}$$

Applying the mass-spring equivalencing technique developed in Chapter 3, the mass-spring system of machine 2 is reduced to a three-mass equivalent retaining only modes 2 and 3. The mode shapes of the original and the equivalent system are shown in Figure 5.9. Including the electrical system, a reduced 14th order model is obtained. The state variables are

$$[x_2] = [\Delta\omega_{IP2}, \Delta\theta_{IP2}, \Delta\omega_{LPB2}, \Delta\theta_{LPB2}, \Delta\omega_{Gen2}, \Delta\delta_{Gen2}, \Delta I_{d2}, \Delta I_{q2},$$
$$\Delta I_{f2}, \Delta I_{kd2}, \Delta I_{kq2}, \Delta V_{cd2}, \Delta V_{cq2}, \Delta V_{R2}] \quad (5.1)$$

Using the 14th order model, an excitation control is designed using the linear optimal control laws and eigenvalue sensitivity technique developed in Chapter 4, resulting an 8th order controller.

The weighting matrices are

$$[R] = 1$$
$$[Q] = \mathrm{diag}[5000, 50, 50000, 50, 100, 25; 100, 100,$$
$$0, 50, 50, 1, 1, 0] \quad (5.2)$$

The state feedback control after the eigenvalue sensitivity analysis results in

$$U_{E2} = 633.82\Delta\omega_{LPB2} + 35.559\Delta\theta_{LPB2} - 56.804\Delta\delta_{Gen2} + 56.63\Delta I_{d2}$$
$$+ 12.453\Delta I_{q2} - 56.089\Delta I_{f2} - 52.01\Delta I_{kd2} - 0.214\Delta V_{R2} \quad (5.3)$$

Applying (4.37), the state feedback control of (5.3), in terms of output variables, becomes

$$U_{E2} = 633.83\Delta\omega_{LPB2} + 35.559\Delta\theta_{LPB2} - 56.804\Delta\delta_{Gen2} - 17.481\Delta P_{e2}$$
$$-27.287\Delta Q_{e2} - 4.0792\Delta I_{f2} + 29.981\Delta I_{t2} - 0.214\Delta V_{R2} \quad (5.4)$$

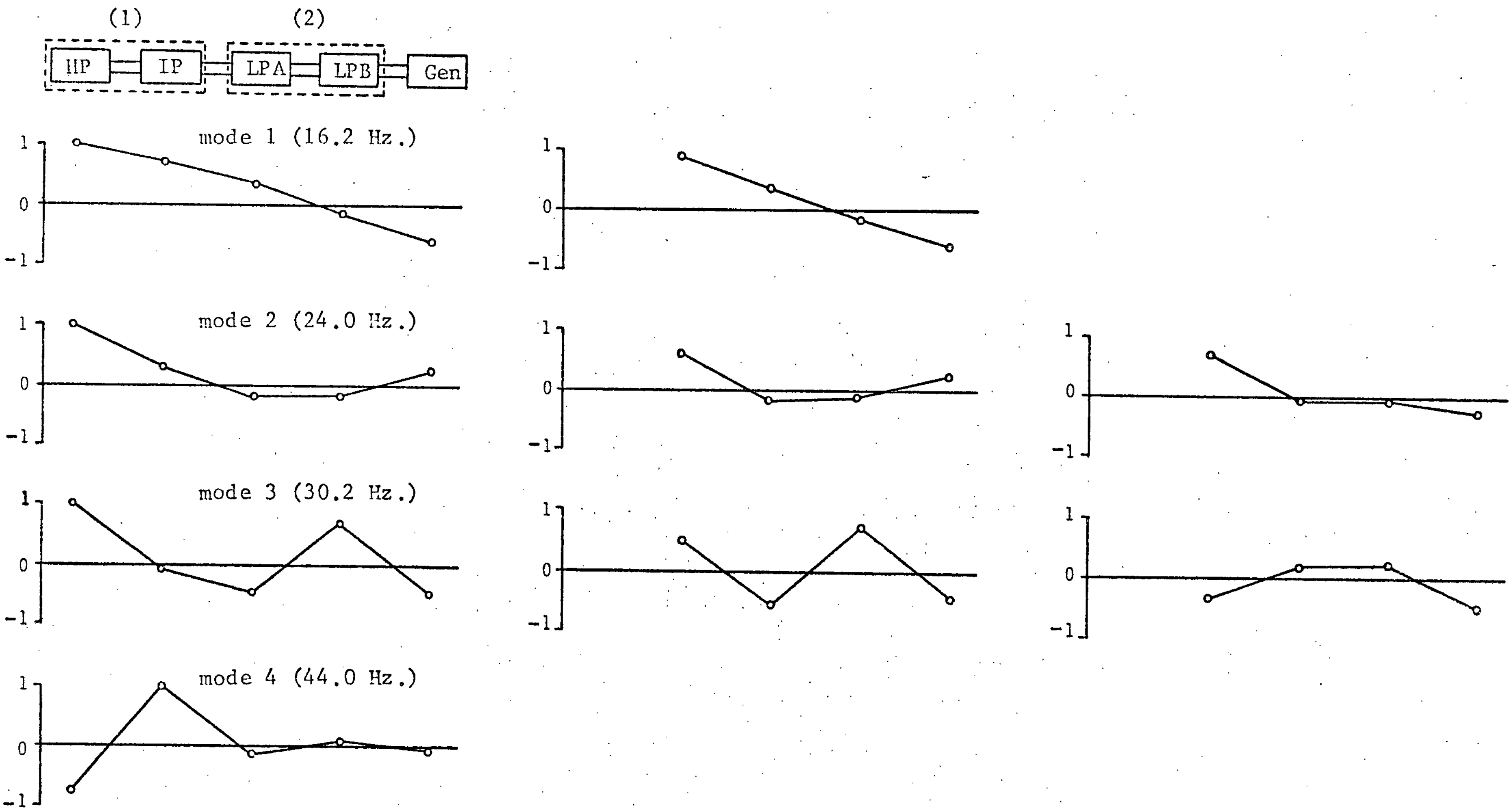

(a) Five mass-spring system

(b) Four mass-spring system

(c) Three mass-spring system

Figure 5.9 Mode shapes of the original and equivalent systems for machine 2 in the two-machine system.

5.6.1 Testing of Controllers Using Eigenvalue Analysis

After the controller design, eigenvalues of the two-machine system are analyzed in the sequence as shown in Table 5.10 .

Table 5.10

Testing sequence for the two-machine system

	Machine 1	Machine 2
1	with control	without control
2	without control	with control
3	with control	with control

The first two tests are used to examine the effect of the controller designed for one machine on the other machine, typical results are shown in columns 2 and 3 of Table 5.11 . It was found that the damping provided by the controller to the torsional modes of the other machine is insignificant. However, the effect of the controller on mode 0 of the other machine is noticable. It may give positive or negative damping to the other machine, depending on the operating conditions.

With both controllers applied to machines 1 and 2, all unstable modes are stabilized over the entire range of capacitor compensation. Typical results are shown in column 4 of Table 5.11 . Note that the controllers provide substantial amount of damping to mode 1 of both machines even though they are not considered in the controller design.

Although the effect of controller on mode 0 of the other machine is noticable, it is not significant due to the weak tie lines between the machines. Therefore, each control can be separately designed and the iterative scheme presented in Figure 5.7 is not necessary.

Table 5.11

Typical mechanical modes of the two-machine system without and with control

		M1 without M2 without	M1 with M2 without	M1 without M2 with	M1 with M2 with
Line 1 50% , Line 2 30%	Machine 1 (M1)	$-1.2128 \pm j298.18$	$-1.2129 \pm j298.18$	$-1.2128 \pm j298.18$	$-1.2129 \pm j298.18$
		$+0.4186 \pm j202.99$	$-0.9341 \pm j203.25$	$+0.3826 \pm j203.00$	$-0.9107 \pm j203.19$
		$-0.5580 \pm j160.73$	$-0.5254 \pm j160.51$	$-0.5551 \pm j160.73$	$-0.5249 \pm j160.51$
		$-0.7047 \pm j127.03$	$-0.7329 \pm j127.10$	$-0.7047 \pm j127.03$	$-0.7328 \pm j127.10$
		$-0.5844 \pm j99.199$	$-0.7476 \pm j99.349$	$-0.5813 \pm j99.203$	$-0.7429 \pm j99.351$
		$-0.4836 \pm j9.2996$	$-1.9182 \pm j7.9942$	$-0.5765 \pm j9.4304$	$-2.2889 \pm j8.5922$
	Machine 2 (M2)	$-0.1214 \pm j276.41$	$-0.1214 \pm j276.41$	$-0.1223 \pm j276.41$	$-0.1223 \pm j276.41$
		$-0.0318 \pm j190.02$	$-0.0621 \pm j190.02$	$-0.4476 \pm j189.17$	$-0.3403 \pm j189.15$
		$-0.1690 \pm j151.46$	$-0.1665 \pm j151.46$	$-0.1992 \pm j151.06$	$-0.2045 \pm j151.07$
		$-0.1711 \pm j102.11$	$-0.1700 \pm j102.11$	$-0.6437 \pm j102.06$	$-0.6434 \pm j102.23$
		$-0.0261 \pm j6.3218$	$-0.2053 \pm j5.7251$	$-2.4631 \pm j5.8497$	$-2.4449 \pm j4.7145$
Line 1 70% , Line 2 70%	Machine 1 (M1)	$-1.2096 \pm j298.18$	$-1.2096 \pm j298.18$	$-1.2096 \pm j298.18$	$-1.2098 \pm j298.18$
		$+0.1503 \pm j203.02$	$-0.4857 \pm j203.03$	$+0.1422 \pm j203.01$	$-0.4790 \pm j203.01$
		$-0.2213 \pm j160.46$	$-0.4882 \pm j160.52$	$-0.2893 \pm j160.53$	$-0.5114 \pm j160.52$
		$-0.7152 \pm j127,08$	$-0.7699 \pm j127.19$	$-0.7116 \pm j127.11$	$-0.7673 \pm j127.21$
		$-0.6302 \pm j99.416$	$-0.8320 \pm j99.550$	$-0.6115 \pm j99.439$	$-0.8113 \pm j99.565$
		$-0.9949 \pm j10.246$	$-3.0374 \pm j9.0538$	$-0.9926 \pm j10.613$	$-2.7396 \pm j9.9798$
	Machine 2 (M2)	$-0.1215 \pm j276.41$	$-0.1215 \pm j276.41$	$-0.1221 \pm j276.41$	$-0.1221 \pm j276.41$
		$+0.0862 \pm j189.96$	$+0.0779 \pm j189.95$	$-1.2334 \pm j189.43$	$-1.1587 \pm j189.43$
		$+0.3546 \pm j151.51$	$+0.2397 \pm j151.80$	$-0.8976 \pm j151.13$	$-1.0465 \pm j150.77$
		$-0.2503 \pm j102.42$	$-0.2336 \pm j102.41$	$-1.0867 \pm j102.52$	$-1.0463 \pm j102.55$
		$-0.1677 \pm j6.8352$	$-0.0079 \pm j6.0831$	$-2.3147 \pm j6.8506$	$-2.2604 \pm j5.4211$

5.6.2 Dynamic Performance Test of the Two-machine System

The controller designs in (4.38) and (5.4) are substituted into the nonlinear two-machine system model for dynamic performance test. A three-phase fault for 0.075 second is assumed at the load bus as shown in Figure 5.10. Typical responses of the system with 50% compensation for both lines 1 and 2 without control are shown in Figures 5.11 and 5.12, and those with control in Figures 5.13 and 5.14 respectively.

For the system without control, most responses of the machines are either oscillatory or unstable. However, all responses of the system with excitation control are stable and all oscillations are damped out within 5 seconds.

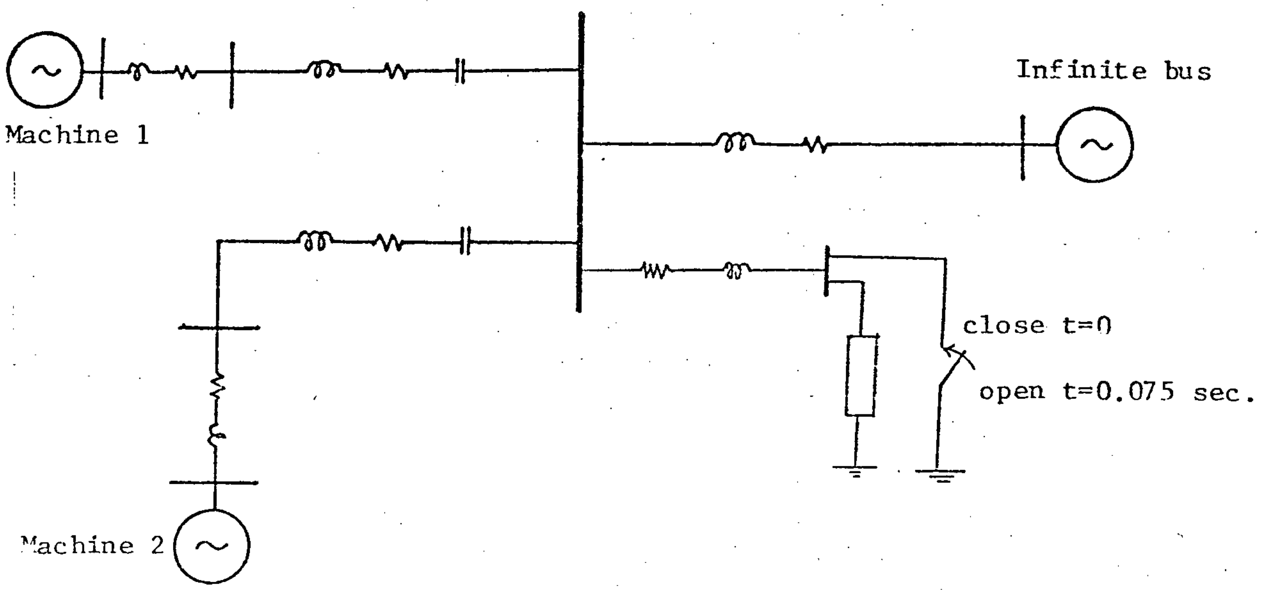

Figure 5.10 The two-machine system subjected to disturbance.

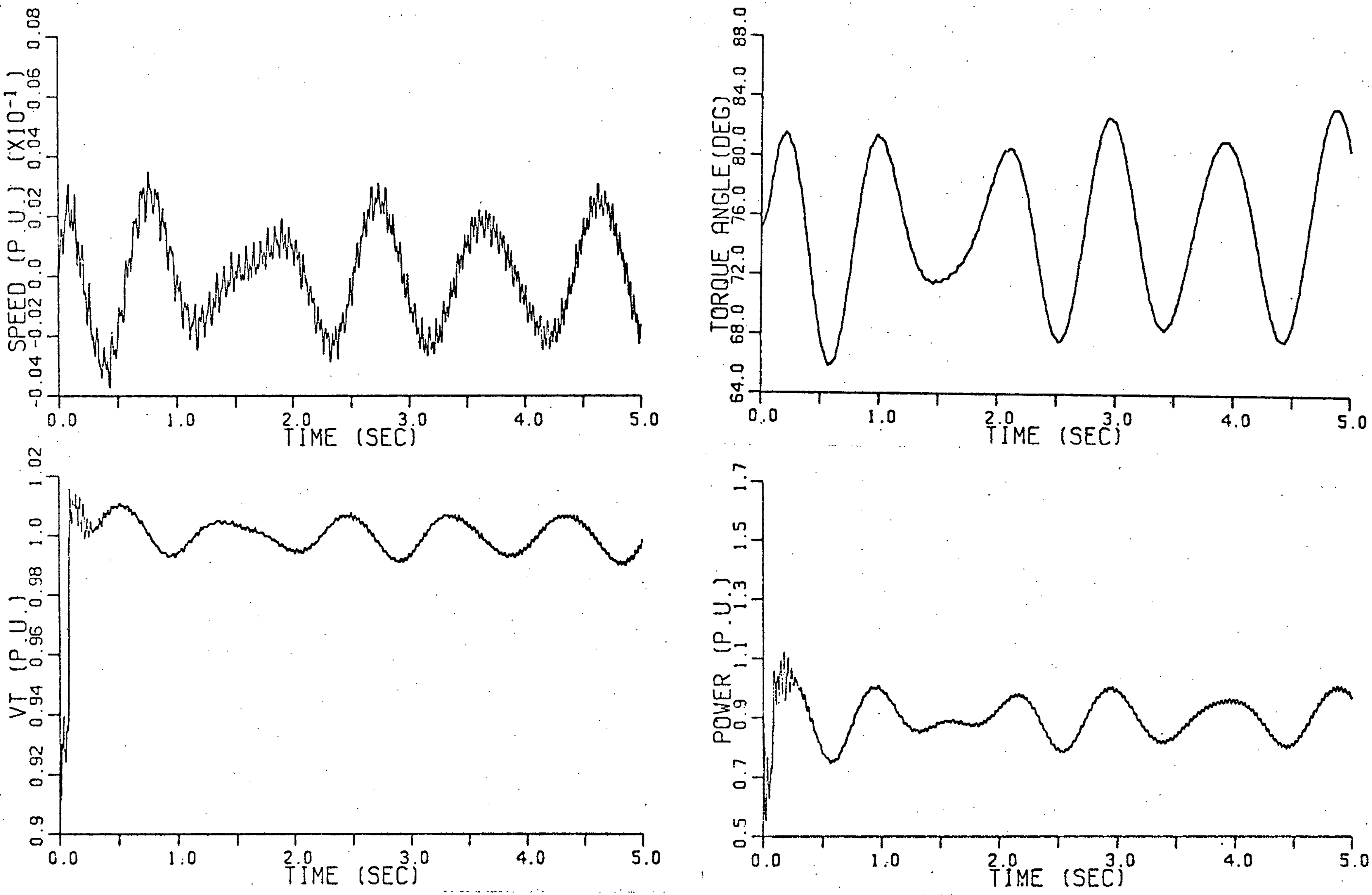

Figure 5.11 Typical responses of machine 1 in the two-machine system without control.

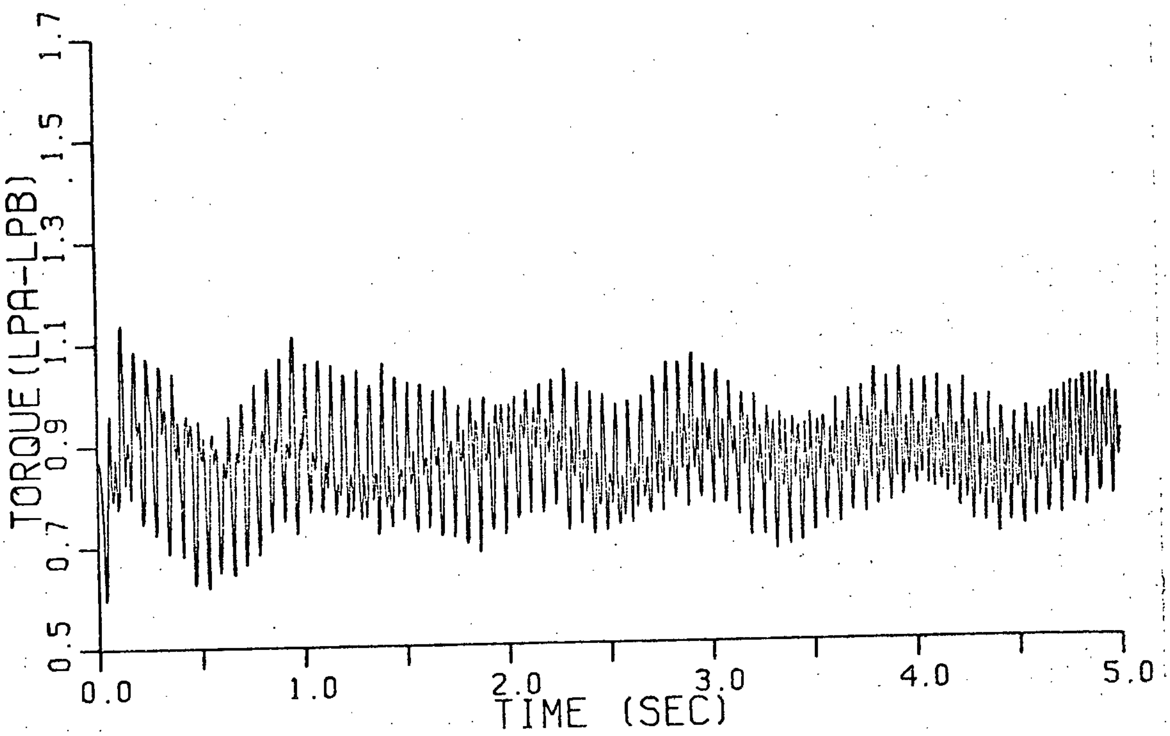

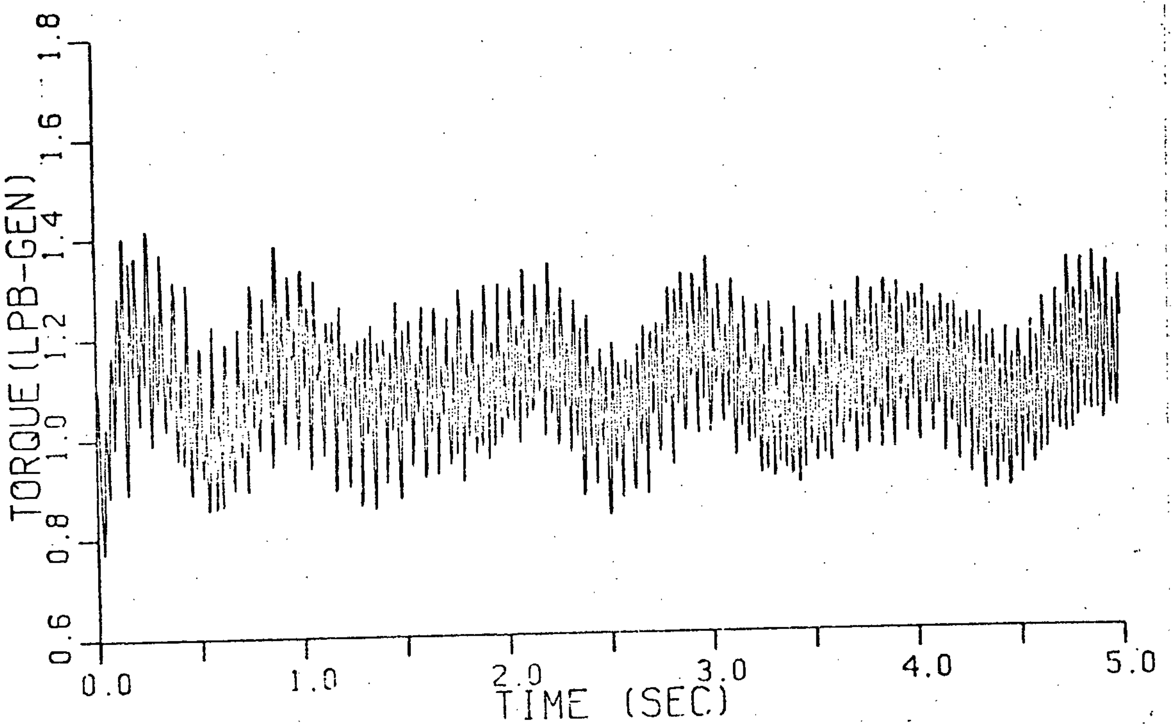

Figure 5.11 (continued)

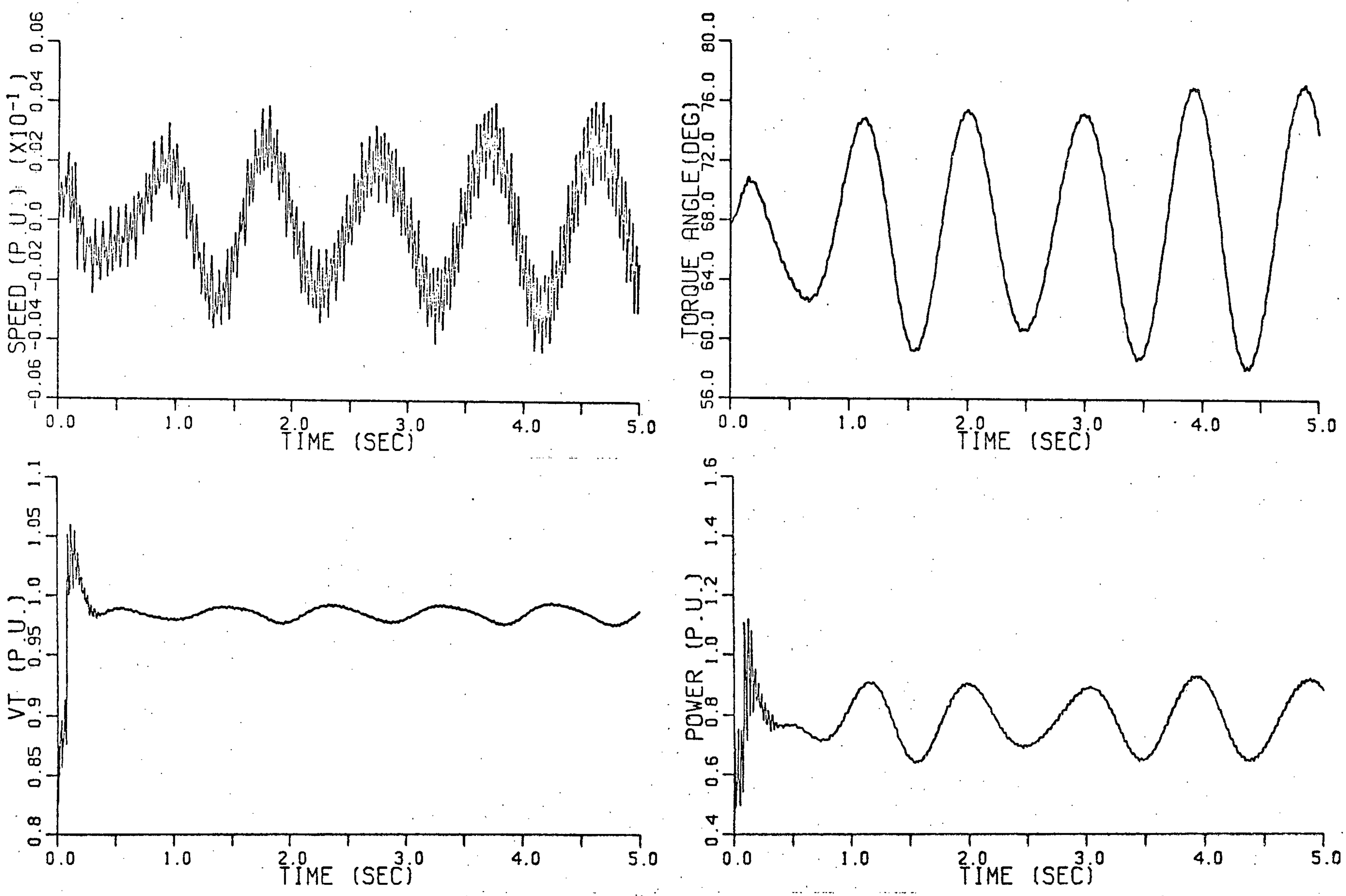

Figure 5.12 Typical responses of machine 2 in the two-machine system with control

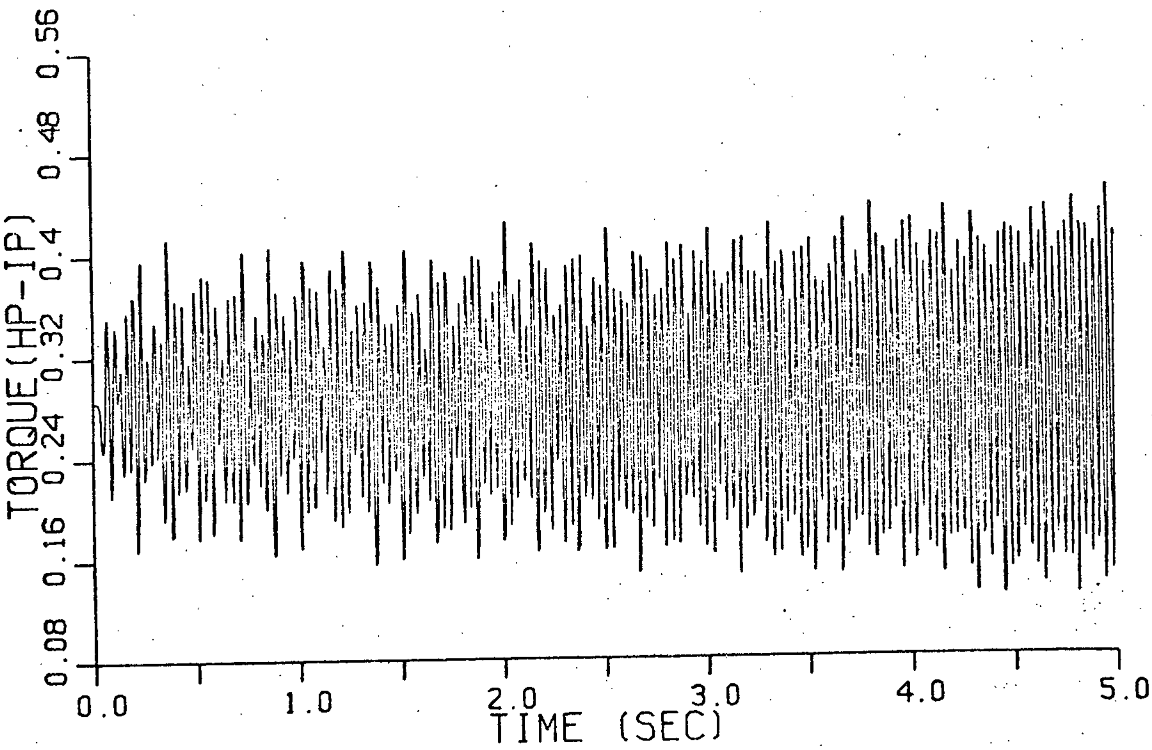

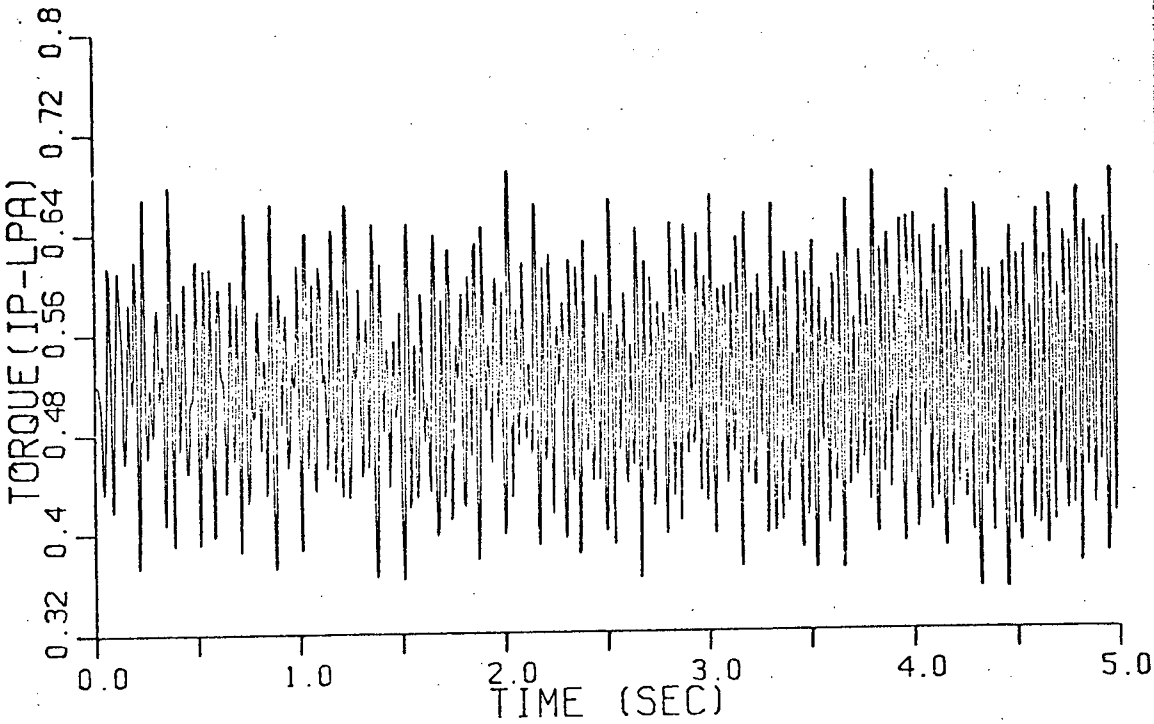

Figure 5.12 (continued)

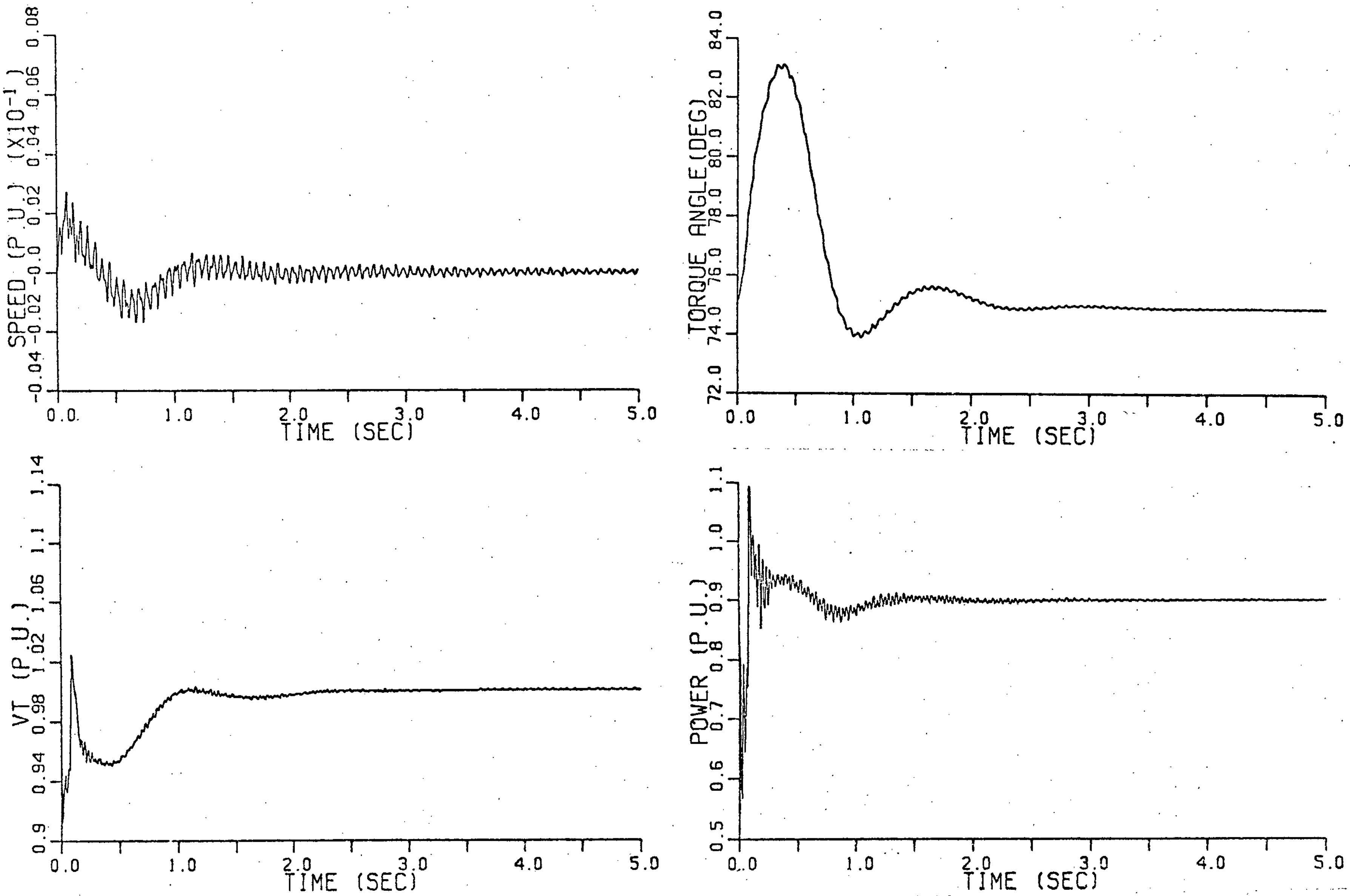

Figure 5.13 Typical responses of machine 1 in the two-machine system with control.

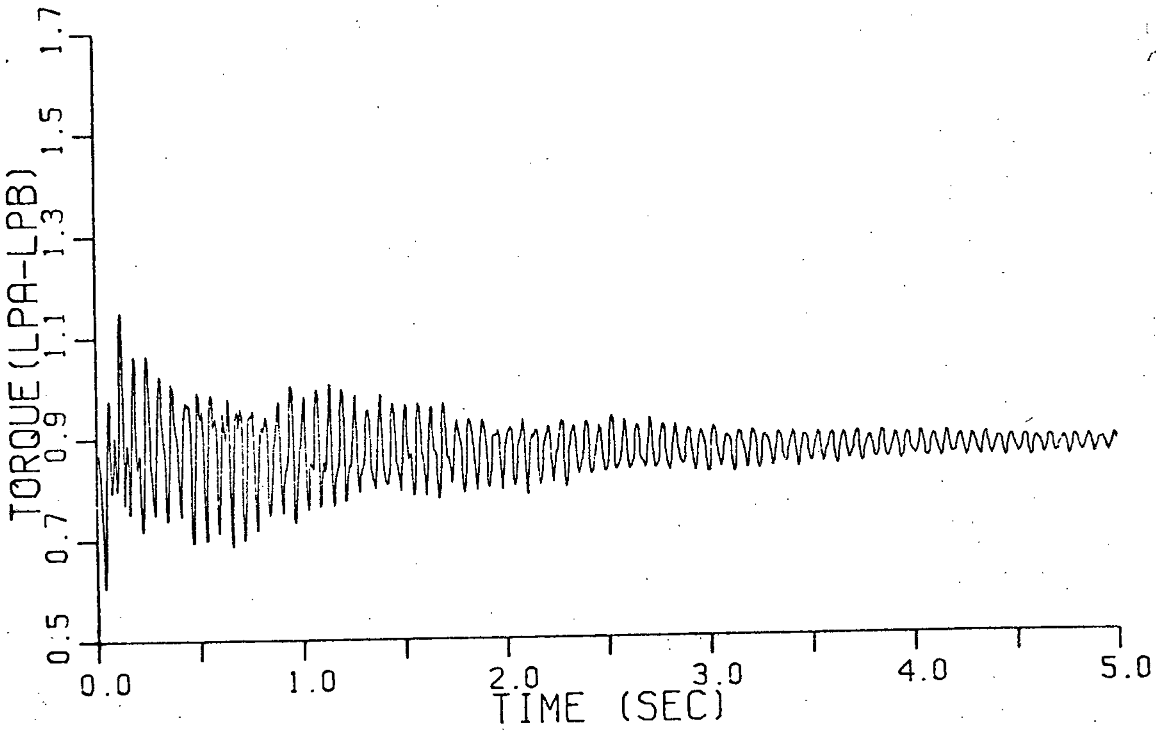

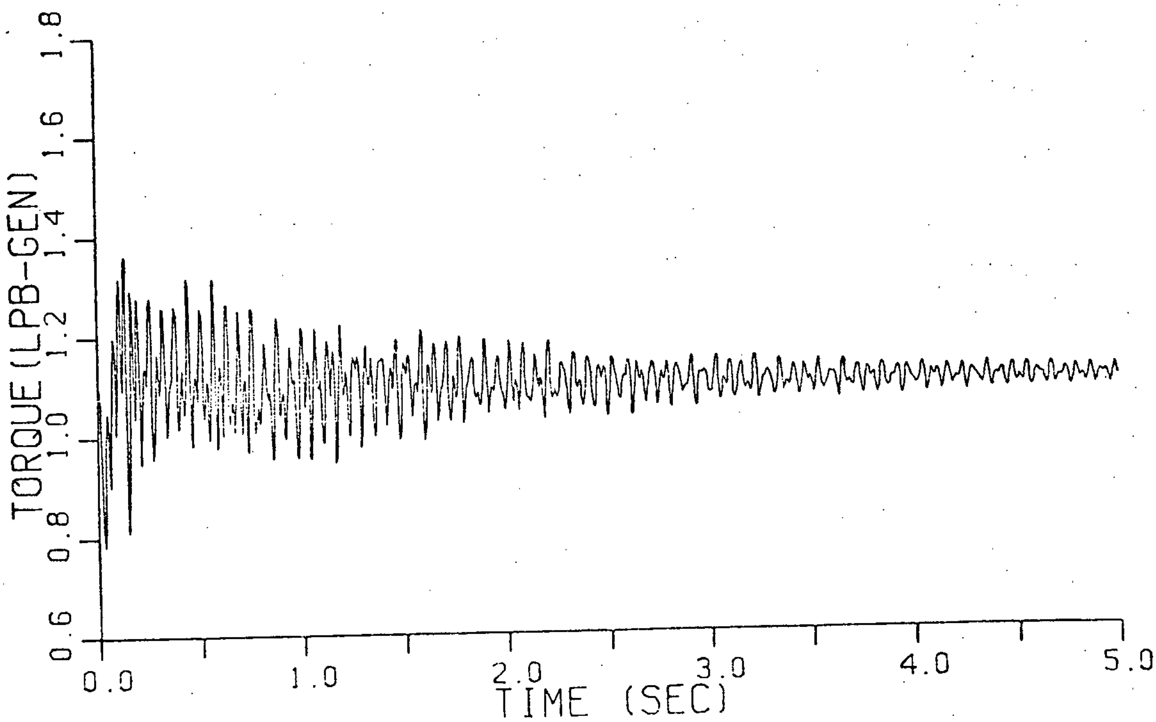

Figure 5.13 (continued)

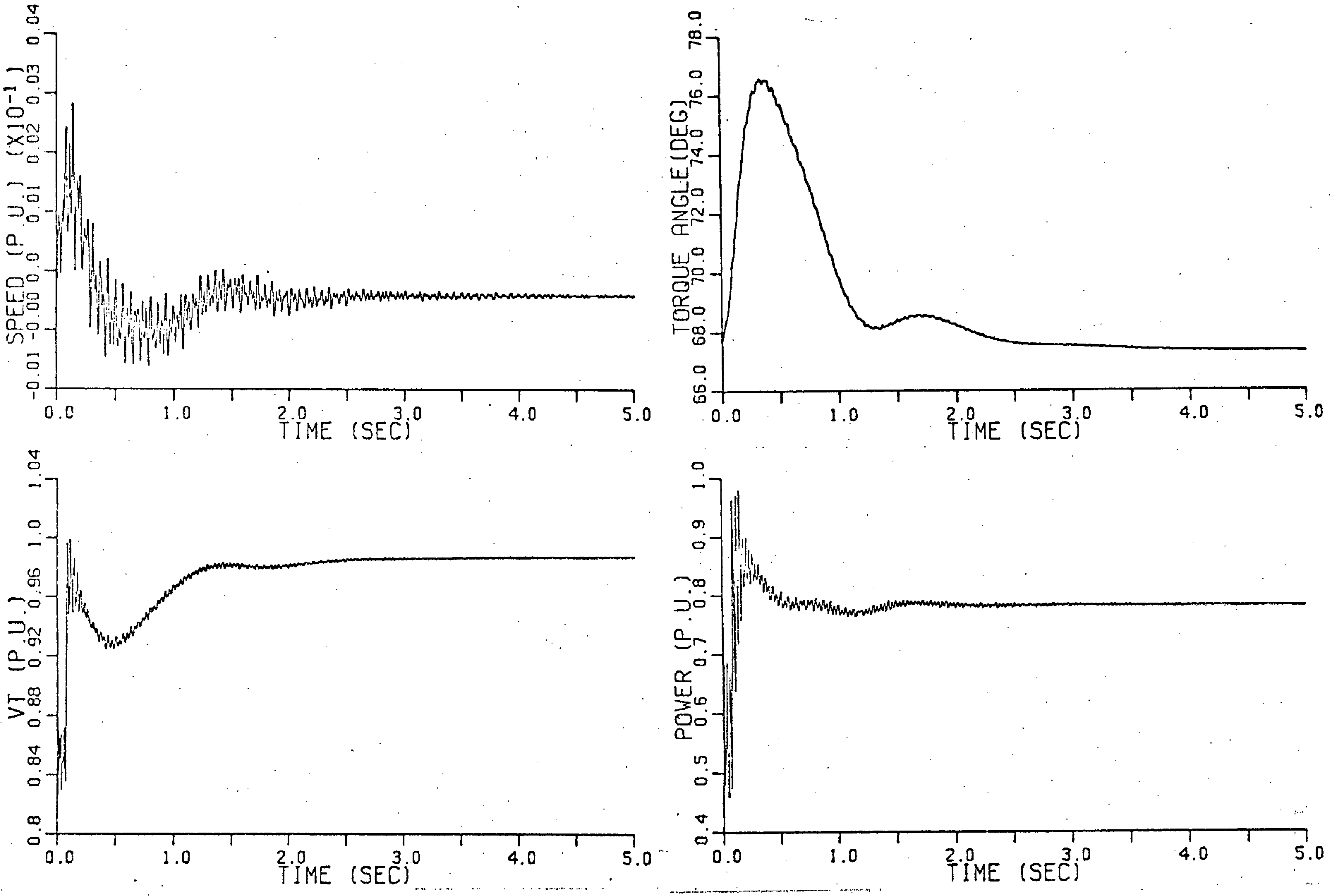

Figure 5.14 Typical responses of machine 2 in the two-machine system with control.

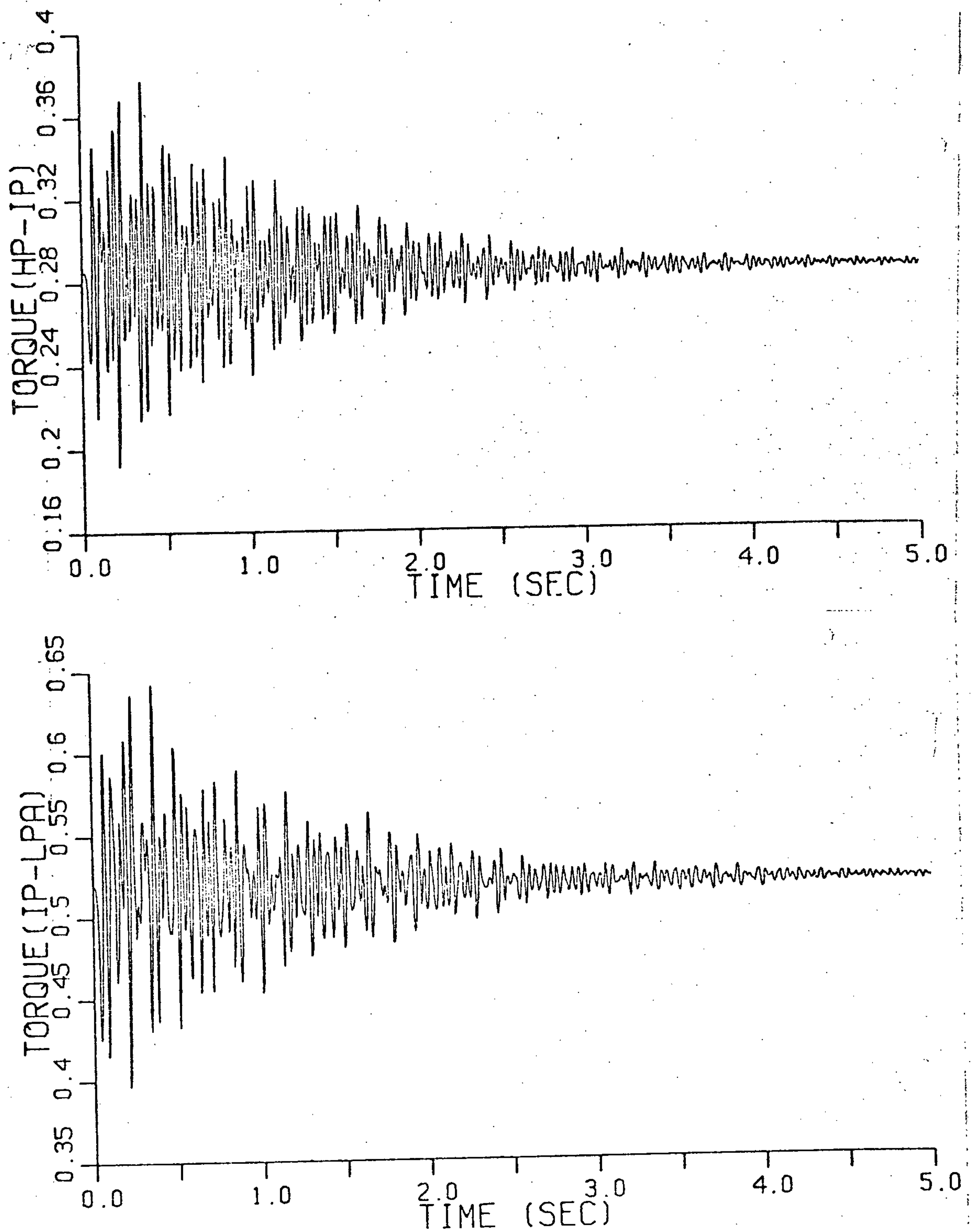

Figure 5.14 (continued)

5.7 Controller Design and Test of the Three-machine System

Since all the mechanical modes of machine 3 are stable, the controller design will be focused on machines 1 and 2. Two one-machine models for machines 1 and 2, by retaining the strongest torsional interaction path and the critical electrical frequency for each model are chosen as follows:

1) Among the three transmission lines 1, 3, and 6 connected to machine 1, only line 6 is retained because it has the largest per unit current indicating the strongest interaction path. The rest of the system can be replaced by an equivalent reactance X_{E1} of 0.07 p.u. .

2) For machine 2, only line 2 is retained and the rest of the system is replaced by an equivalent reactance X_{E2} of 0.1 p.u. .

Again, the same controller of (4.37) is used for machine 1, because the operating conditions, the machine and transmission line parameters for machine 1 are almost the same as those of the system previously studied.

The operating conditions for machine 2 are

$$P_{e2} = 0.906 \text{ p.u.}, \quad Q_{e2} = 0.341 \text{ p.u.}, \quad V_{t2} = 1.0 \text{ p.u.}$$

Using the 14th order model of (5.1) together with the techniques develpoed in Chapter 4, an 8th order excitation control for SSR is designed by choosing the same weighting matrices as shown in (5.2).

When both controllers are applied to the three-machine system, all unstable torsional modes in the system are stabilized over the entire range of the prescribed operating conditions. However, mode 0 of machine 2 remains unstable due to the inadequacy of the one-machine model by which the dynamic interaction between machines is neglected. But either one of the two controllers can be adapted also to stabilize mode 0 using the iterative scheme as shown in Figure 5.7 .

5.7.1 Sensitivity Studies and Choice of Weighting Elements in [Q]

Dynamic interaction between machines is transmitted through the electrical network by the line current. Therefore, proper choice of weighting elements in conjunction with current is important to enhance the mode 0 damping in a multi-machine system.

For the three-machine system, the controller for machine 2, originally based on a one-machine model, is adapted by studying the sensitivity of mechanical damping with respect to the weighting elements of ΔI_{kd2}, ΔI_{kq2}, ΔI_{d2}, ΔI_{q2}. ΔI_{kd2} and ΔI_{kq2} are included because they affect the self damping of machine 2 which in turn affect the dynamic interaction between machines. Keeping other weighting elements of [Q] in (5.2) constant, the effect of the weighting elements of ΔI_{kd2} and ΔI_{kq2} on the mechanical modes of machine 2 is shown in Figure 5.15 and that of ΔI_{d2} and ΔI_{q2} in Figure 5.16.

Two observations are as follows:

1) As the weighting elements Q_{Ikd2} and Q_{Ikq2} increase (more penalty on the deviation of damper winding currents are imposed), mode 0 damping of machine 2 increases and that of machine 1 decreases. Damping of machine 2's torsional modes also decrease, but at a much slower rate.

2) As the weighting elements Q_{Id2} and Q_{Iq2} decrease (penalty on the deviation of stator currents is reduced), mode 0 damping of machine 2 increases and that of machine 1 decreases. Damping of the torsional modes of machine 2 remains fairly constant.

Since the weighting elements of the damper winding currents affect the damping of machine 2's torsional modes, they must be chosen such that all mechanical modes in the three-machine system have reasonable positive damping. In this case Q_{Id2} and Q_{Iq2} of (5.2) are adapted to 50, Q_{Ikd2} and Q_{Ikq2} adapted to 100. The resulting weighting matrice are

$$
\begin{aligned}
[\,R\,] &= 1 \\
[\,Q\,] &= \mathrm{diag}\,[\,5000,50,50000,50,100,25;50,50,0 \\
&\qquad 100,100,1,1,0\,]
\end{aligned}
\tag{5.3}
$$

and the designed state feedback control after simplification from eigenvalue sensitivity analysis becomes

$$
\begin{aligned}
U_{E2} = {} & 549.26\Delta\omega_{LPB2} + 67.118\Delta\theta_{LPB2} - 80.172\Delta\delta_{Gen2} + 47.76\Delta I_{d2} \\
& +12.289\Delta I_{q2} - 48.478\Delta I_{f2} - 41.527\Delta I_{kd2} - 0.249\Delta V_{R2}
\end{aligned}
\tag{5.4}
$$

Applying (4.36), the control of (5.4) in terms of output variables becomes

$$
\begin{aligned}
U_{E2} = {} & 549.26\Delta\omega_{LPB2} + 67.118\Delta\theta_{LPB2} - 80.172\Delta\delta_{Gen2} - 14.041\Delta P_{e2} \\
& -12.196\Delta Q_{e2} - 6.95\Delta I_{f2} + 99.296\Delta I_{t2} - 0.249\Delta V_{R2}
\end{aligned}
\tag{5.5}
$$

With controller of (4.37) on machine 1 and (5.5) on machine 2 of the three-machine system, all unstable modes in the system are stabilized over the entire range of the prescribed operating conditions. Typical results are shown in Table 5.12 .

Table 5.12

Typical mechanical modes of the three-machine with control

Line compensation	Machine 1	Machine 2	Machine 3
Line 1 60% Line 2 70% Line 3-9 60% (except 7)	-0.1820±j298.18 -1.0612±j202.58 -0.3141±j160.49 -0.7058±j127.16 -0.5637±j99.549 -1.9871±j10.923	-0.1222±j276.41 -0.6101±j189.31 -0.3091±j151.04 -0.6588±j103.29 -1.3621±j5.4707	-0.1334±j353.24 -0.2016±j190.16 -0.7333±j167.73 -3.3618±j17.607
Line 1-8 50% (except 7) Line 9 30%	-0.1820±j298.18 -0.6224±j202.15 -0.2893±j160.48 -0.7071±j127.15 -0.5635±j99.507 -2.1187±j9.8608	-0.1221±j276.41 -0.4904±j189.45 -0.2752±j151.12 -0.9266±j102.71 -1.0805±j5.2511	-0.1337±j353.24 -0.2366±j190.09 -0.7334±j167.73 -3.1780±j17.277
Line 1-3 50% Line 4 30% Line 5-9 50% (except 7)	-0.1820±j298.18 -0.6799±j202.25 -0.3017±j160.31 -0.6629±j127.14 -0.5368±j99.606 -2.1820±j9.8276	-0.1221±j276.41 -0.3588±j189.41 -0.3372±j151.36 -0.9538±j102.42 -1.1479±j5.2261	-0.1335±j353.24 -0.1876±j190.05 -0.7313±j167.73 -3.2170±j17.439
Line 1,5 40% Line 9 35% Line 2-4,6,8 70%	-0.1820±j298.18 -1.5122±j202.49 -0.3139±j160.46 -0.6738±j127.17 -0.5616±j99.859 -1.9833±j11.218	-0.1221±j276.41 -0.5766±j189.39 -0.3147±j151.17 -0.2140±j102.85 -1.5807±j5.6033	-0.1336±j353.24 -0.2310±j190.14 -0.7336±j167.73 -3.2409±j17.489

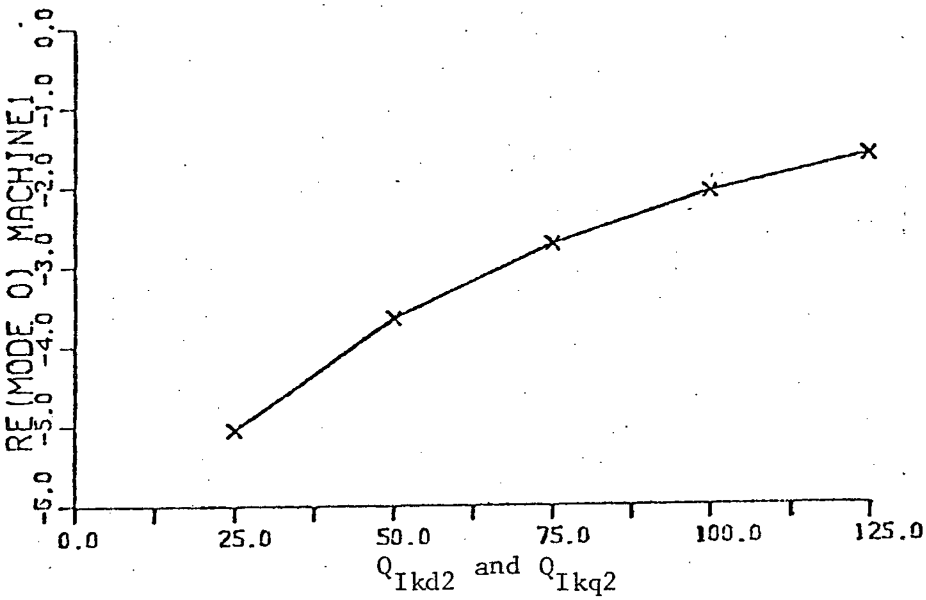

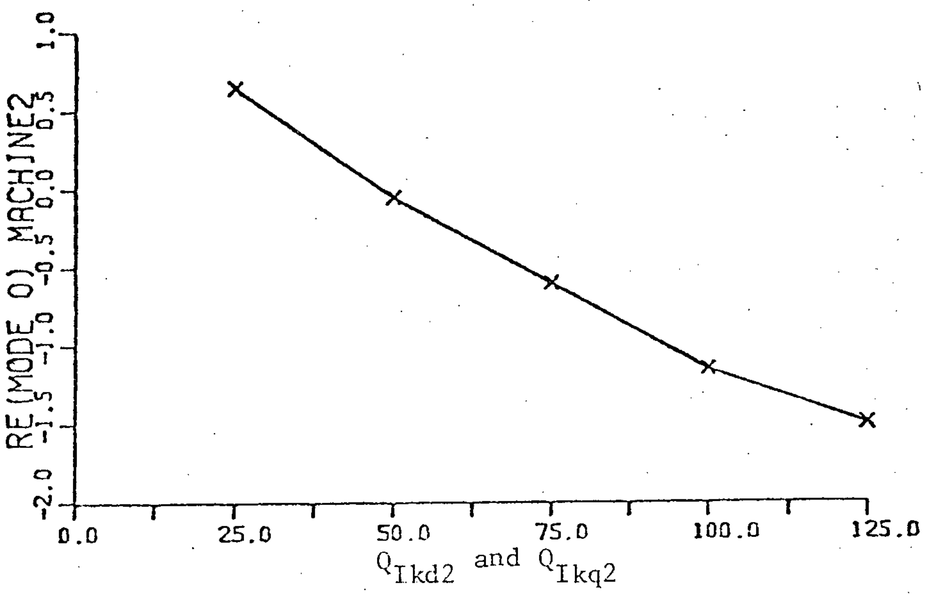

Figure 5.15 Variation of mechanical damping as weighting elements Q_{Ikd2} and Q_{Ikq2} change while Q_{Id2} and Q_{Iq2} constant at 50.

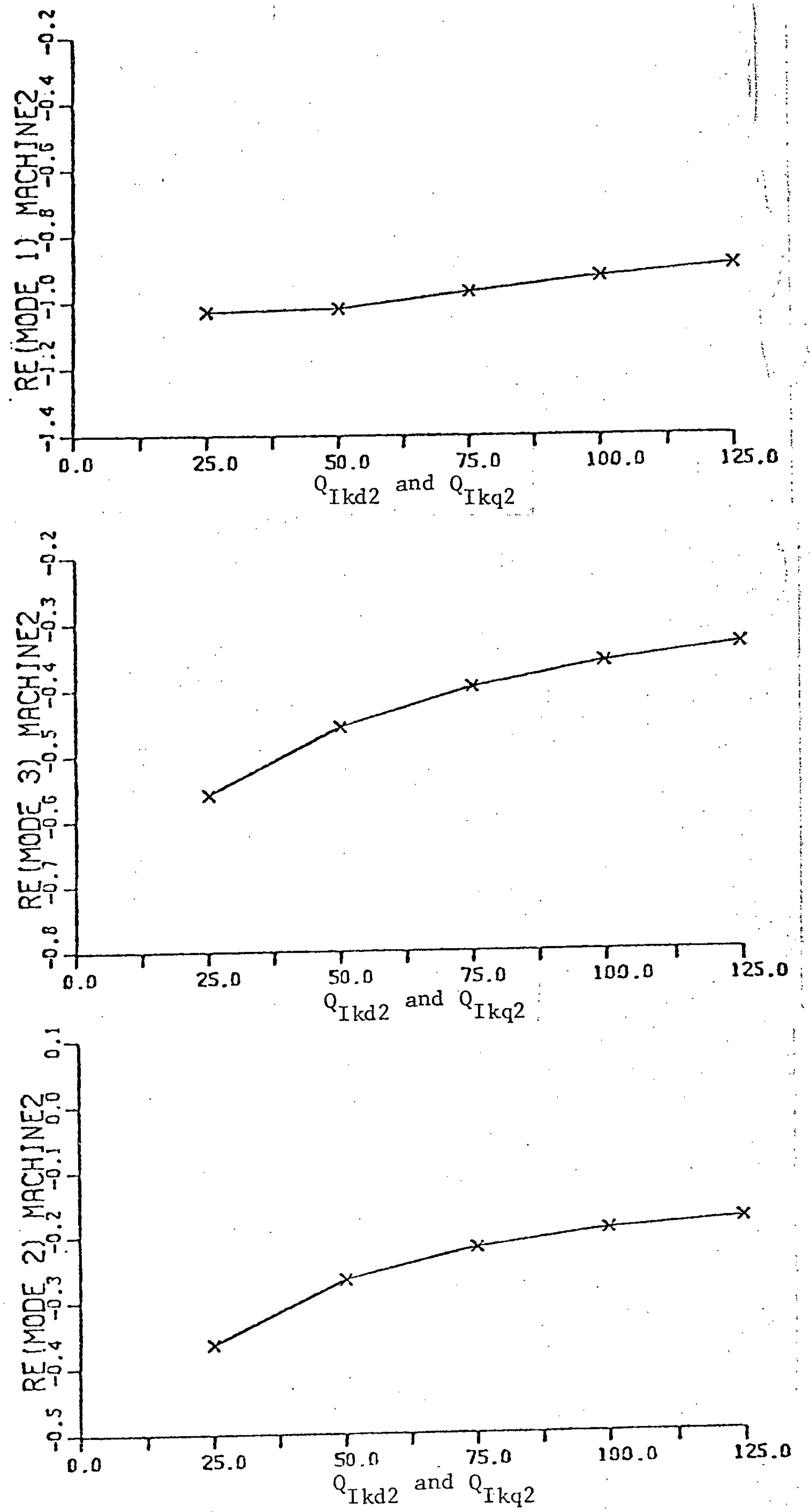

Figure 5.15 (continued)

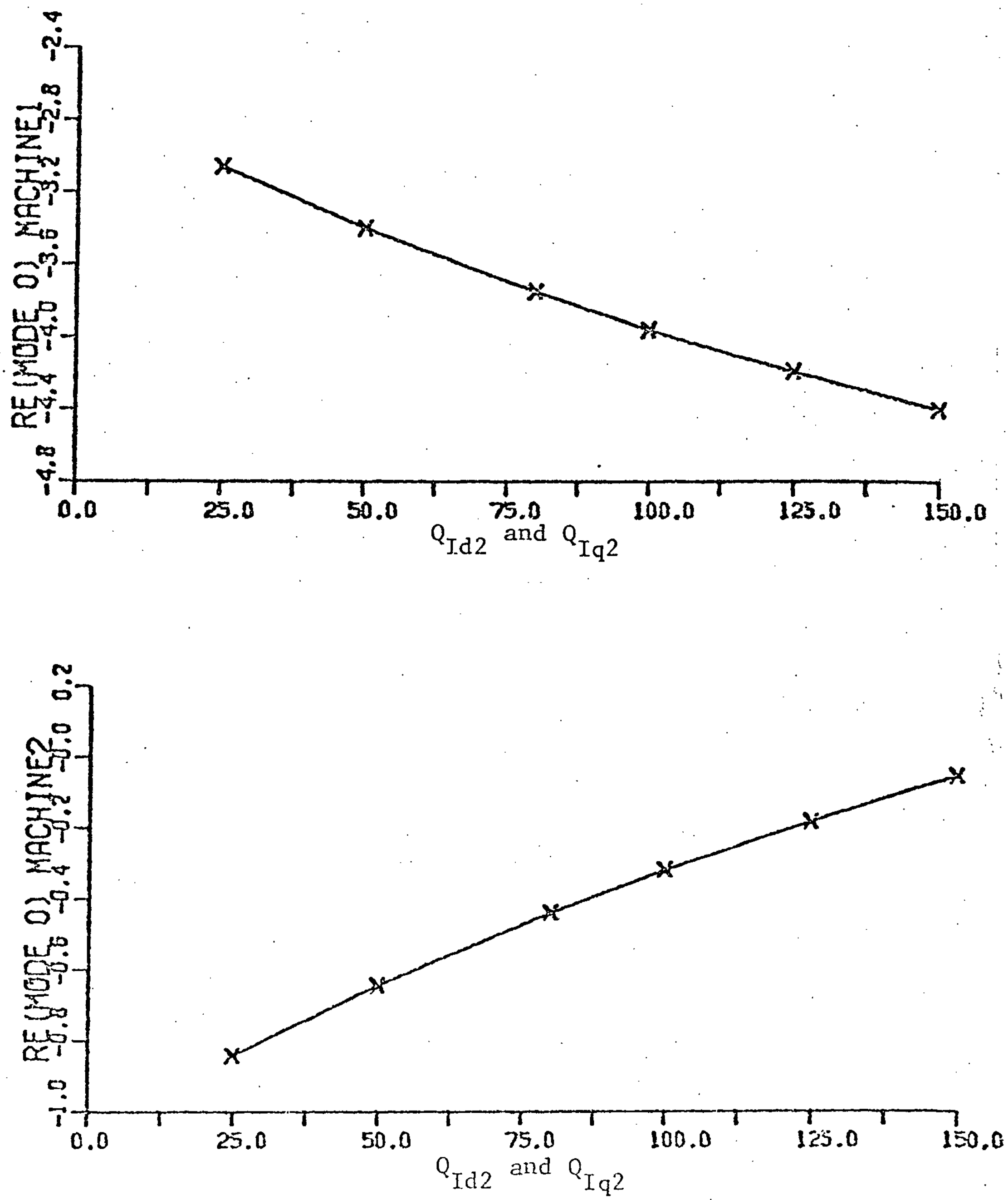

Figure 5.16 Variation of mechanical damping as weighting elements Q_{Id2} and Q_{Iq2} change while Q_{Ikd2} and Q_{Ikq2} constant at 50.

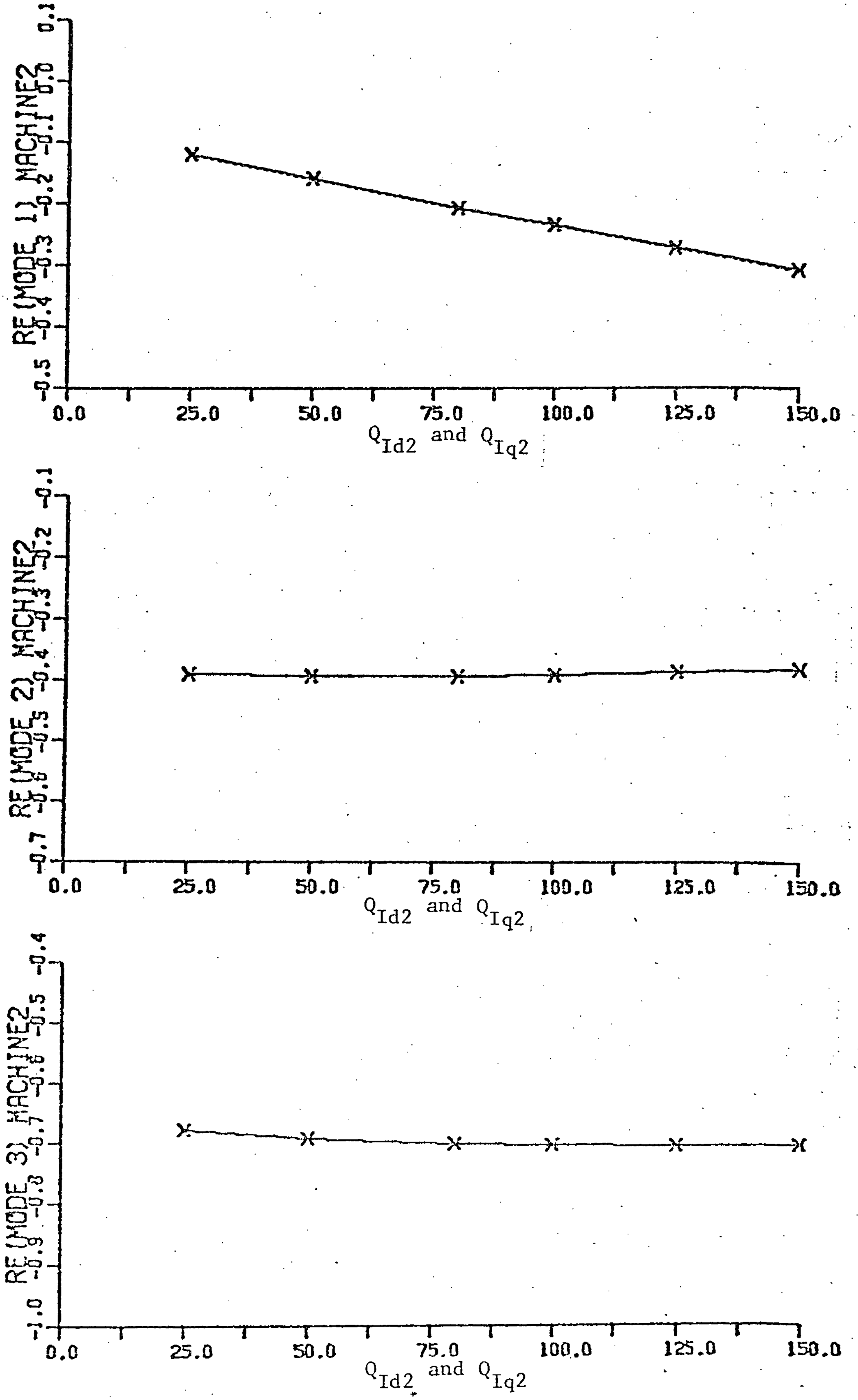

Figure 5.16 (continued)

5.7.2 Dynamic Performance Test of the Three-machine System

The dynamic performance of the three-machine system without and with excitation control is tested using the nonlinear system model. A resistive load is switched into the system at bus 8 for 0.075 second as shown in Figure 5.17 , so that the bus voltage will drop 20% . Typical responses of the system without control are shown in Figures 5.18 through 5.20, and those with control in Figures 5.21 through 5.23 respectively. The line compensation of the system is 50% for all lines, except for line 7 and line 2 which has no compensation and 70% compensation respectively.

For the system without control, some responses of machines 1, 2, and 3 are unstable, but the responses of all machines are stable for the system with the excitation control.

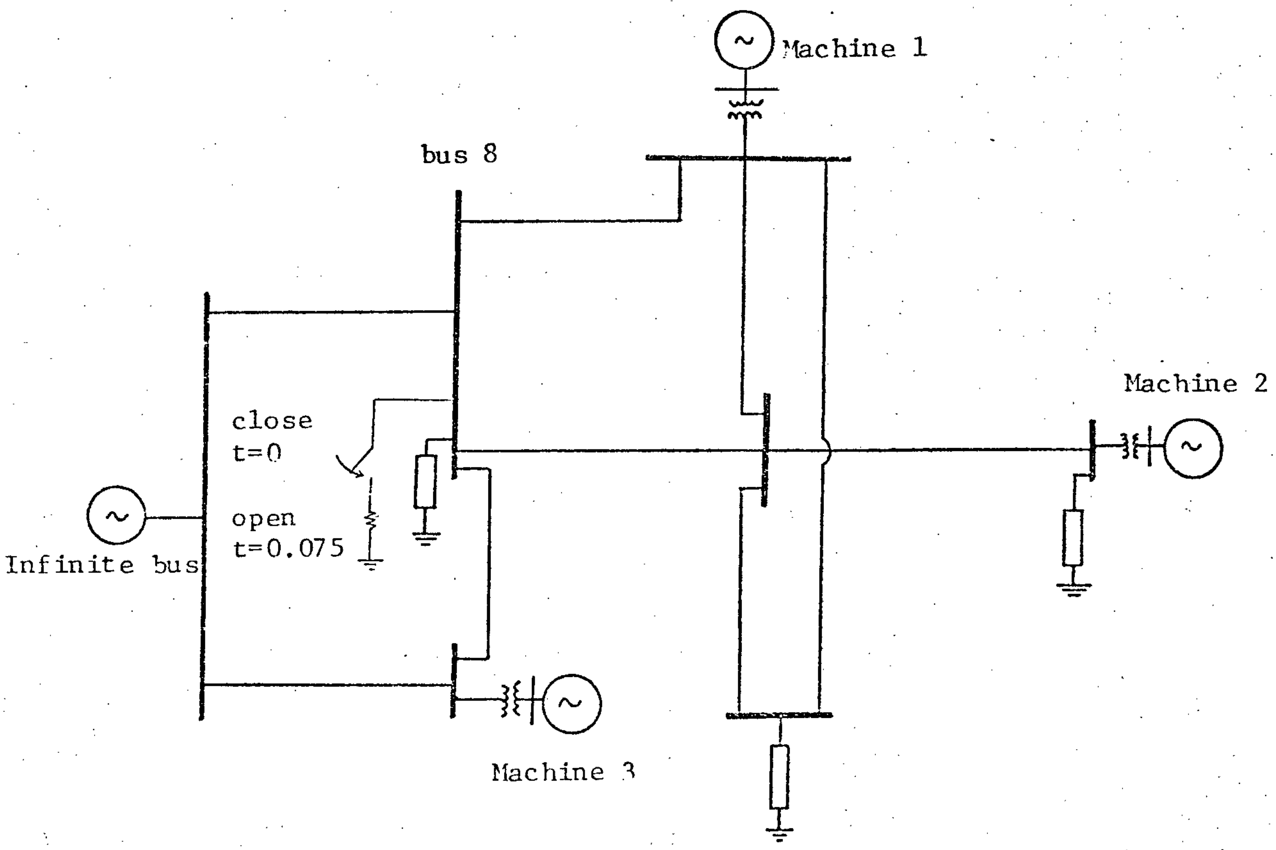

Figure 5.17 The three-machine system subjected to disturbance.

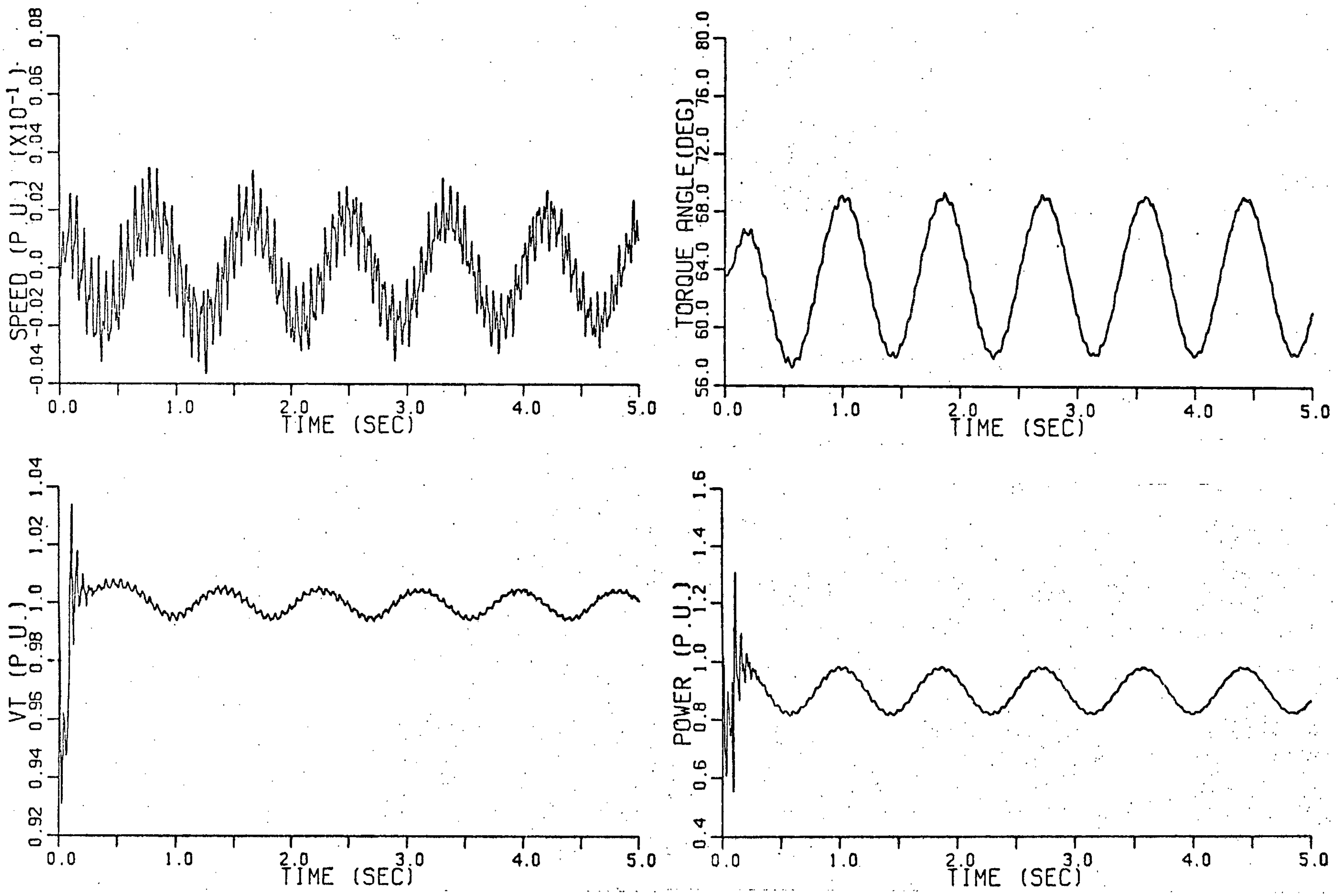

Figure 5.18 Typical responses of machine 1 in the three-machine system without control.

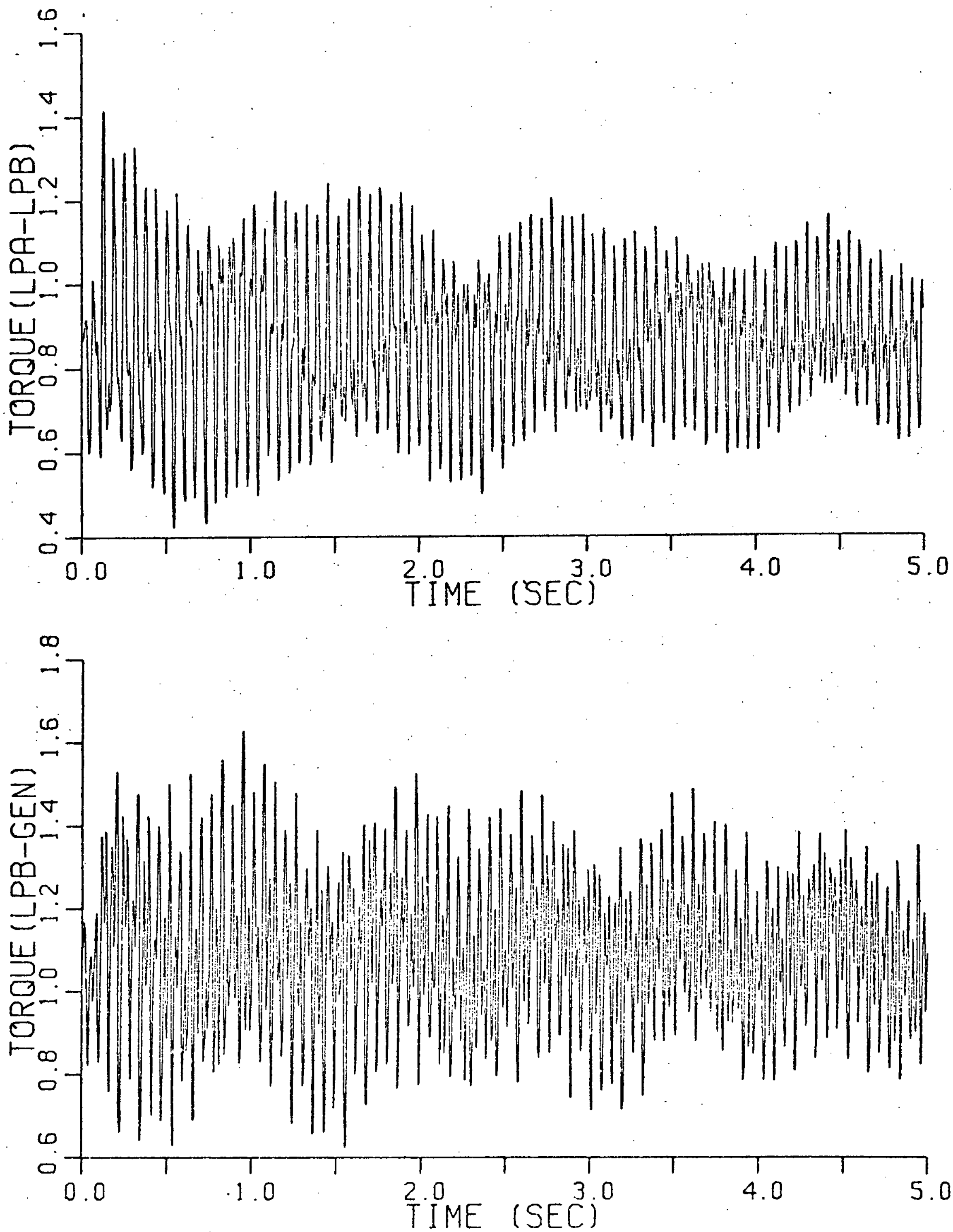

Figure 5.18 (continued)

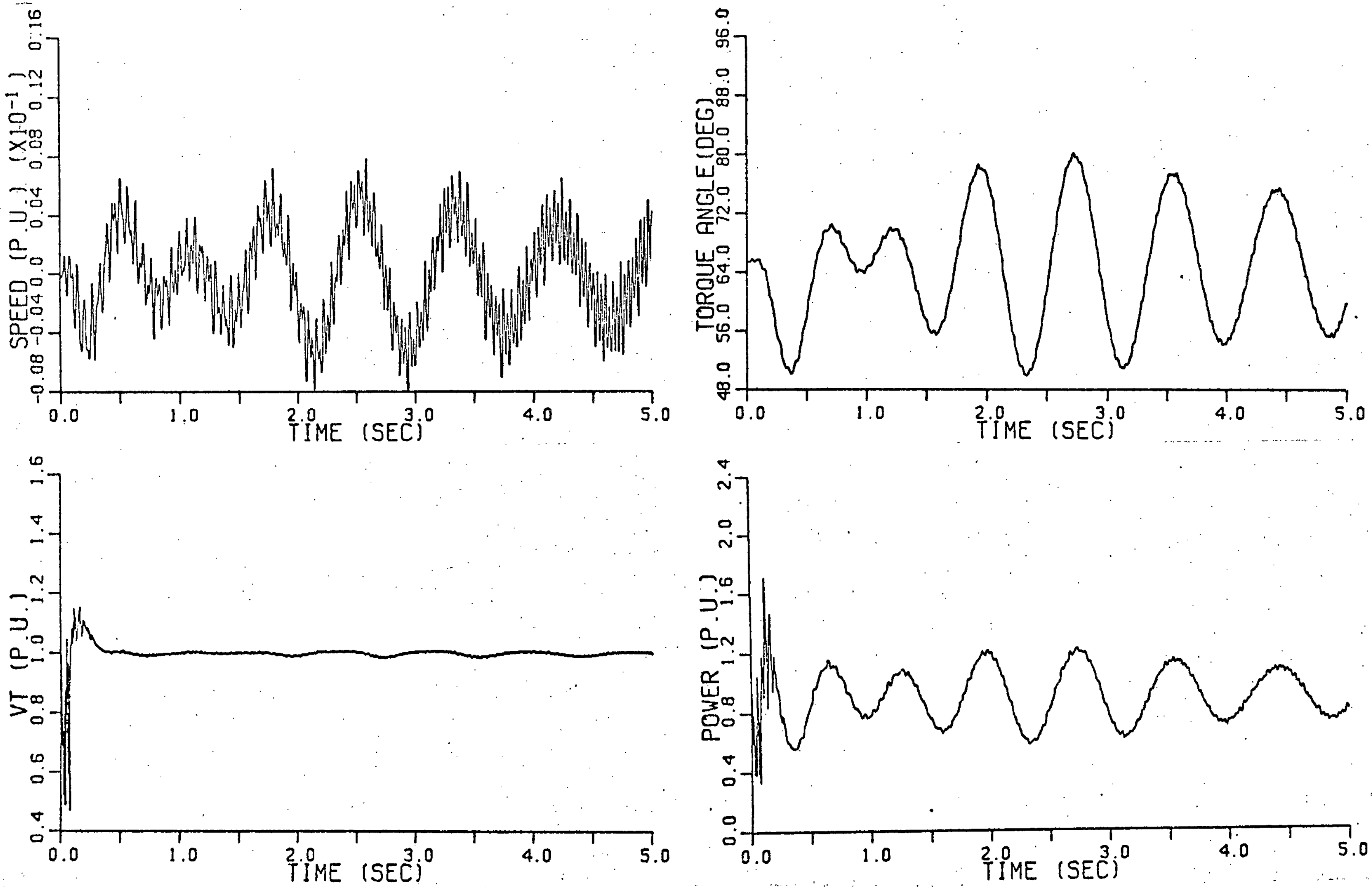

Figure 5.19 Typical responses of machine 2 in the three-machine system without control.

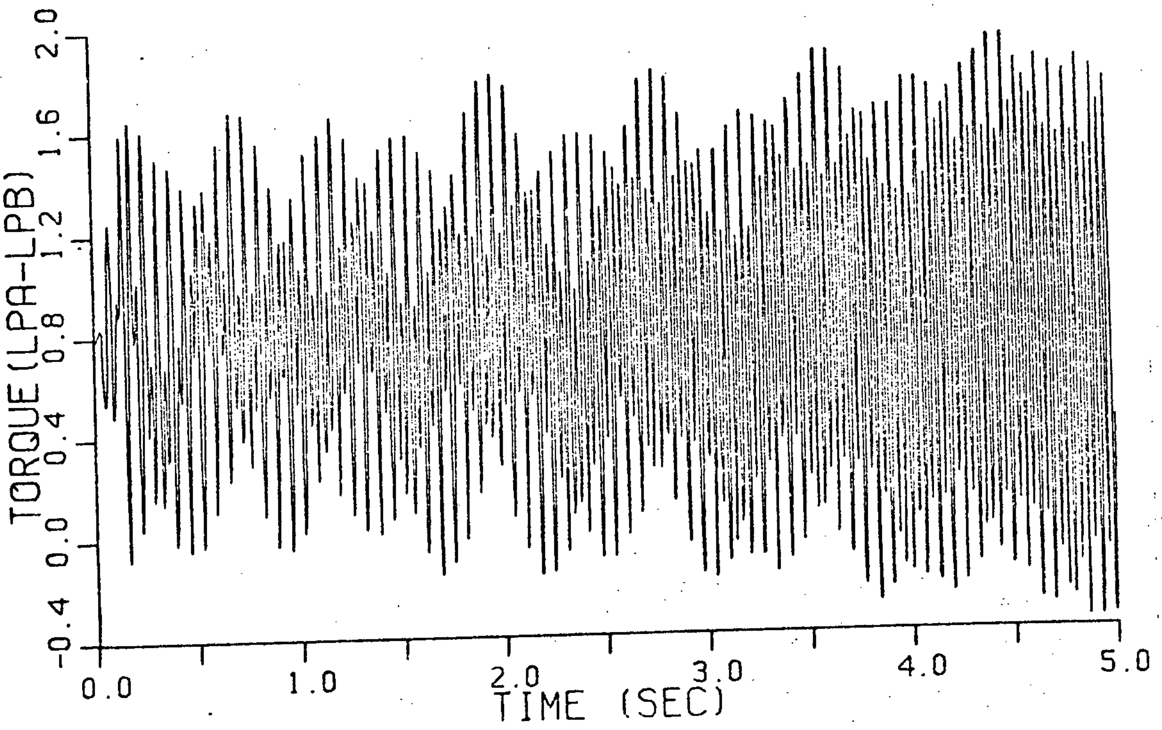

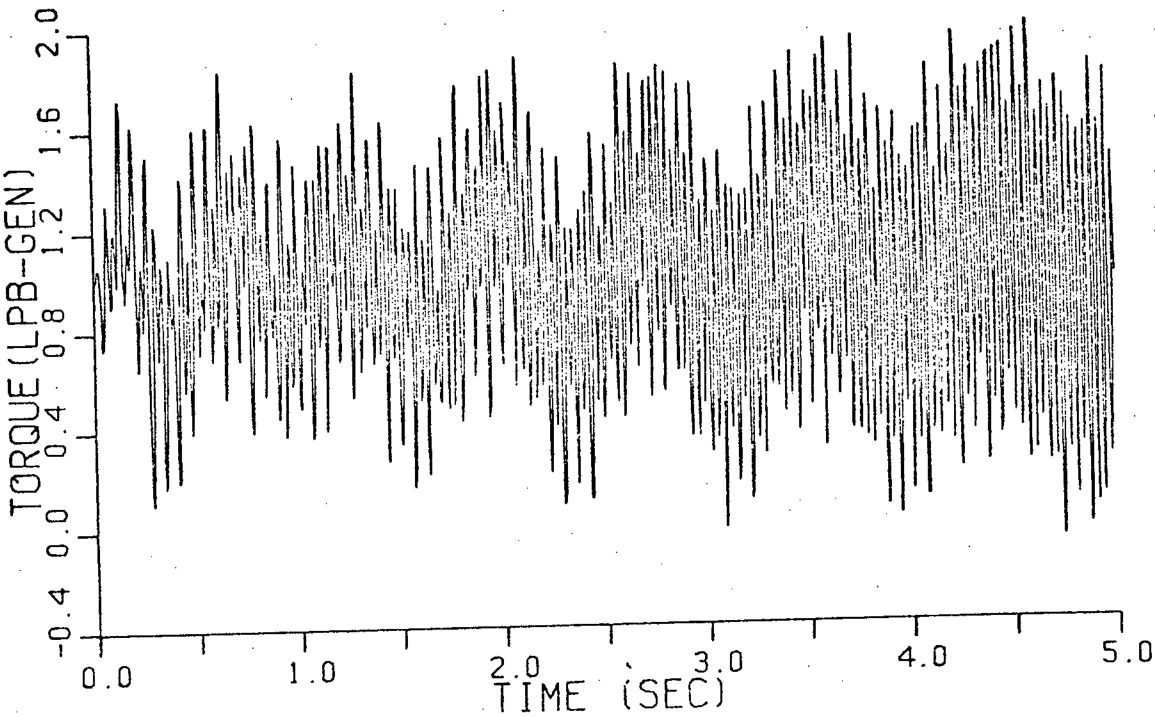

Figure 5.19 (continued)

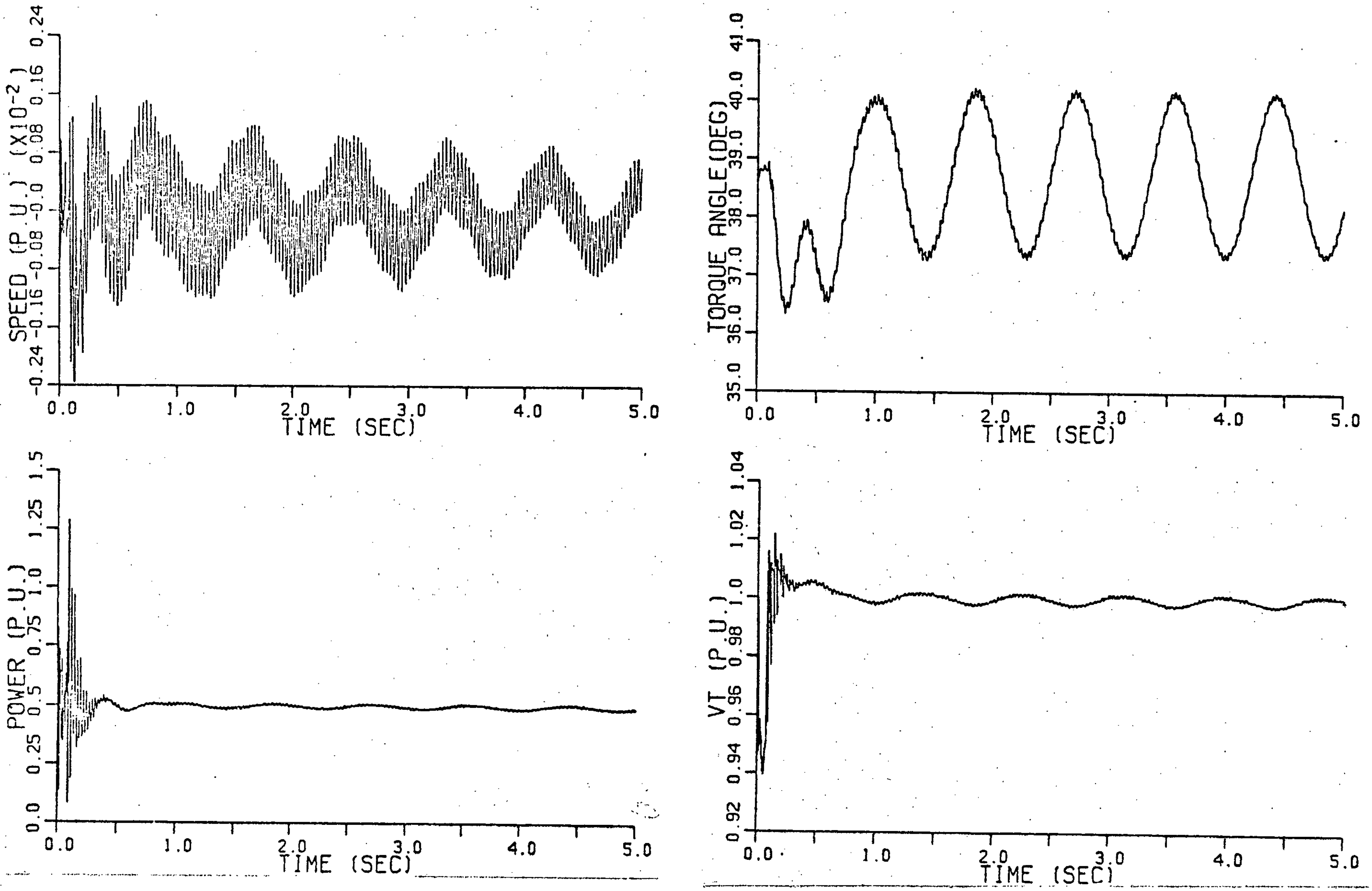

Figure 5.20 Typical responses of machine 3 in the three-machine system without control.

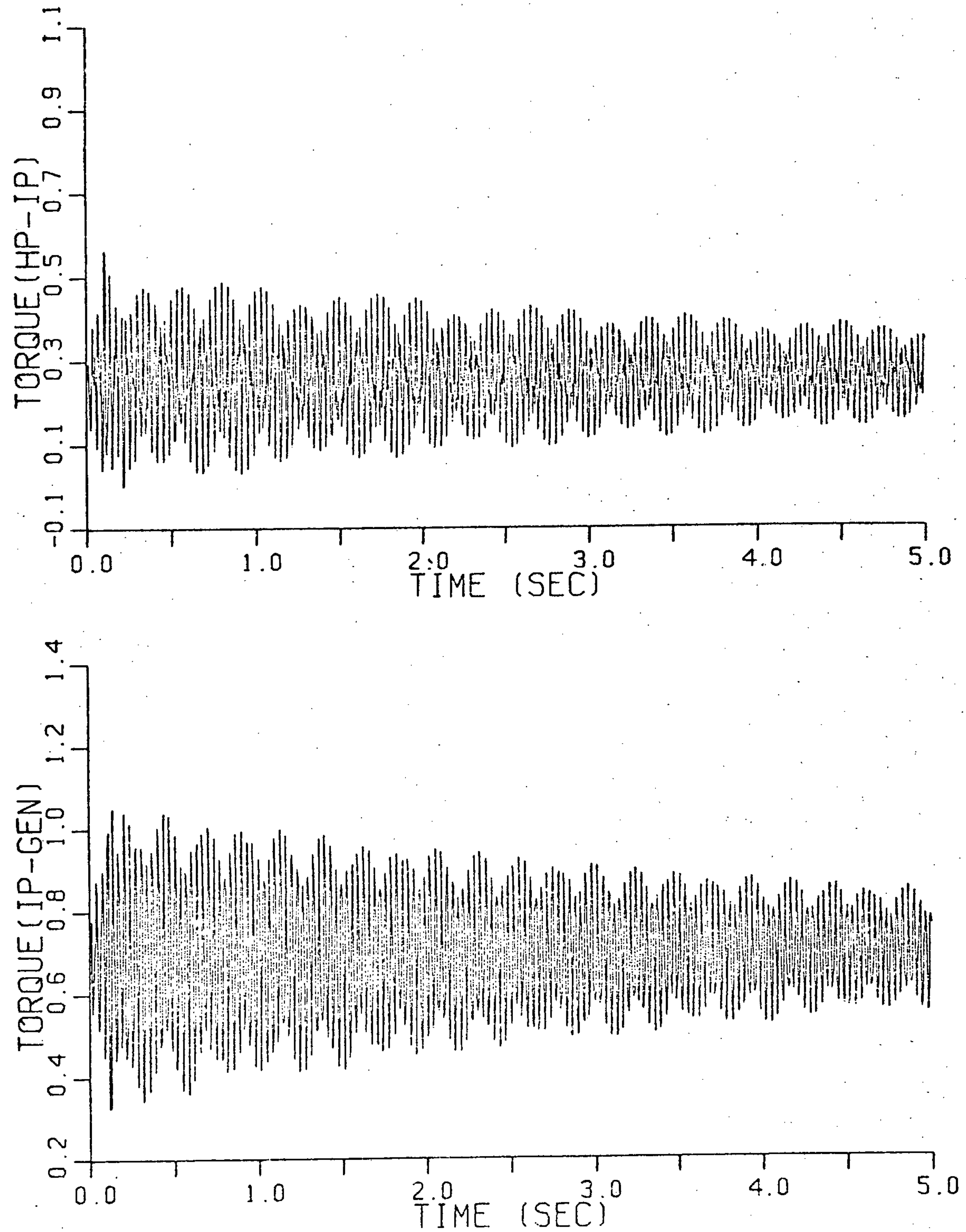

Figure 5.20 (continued)

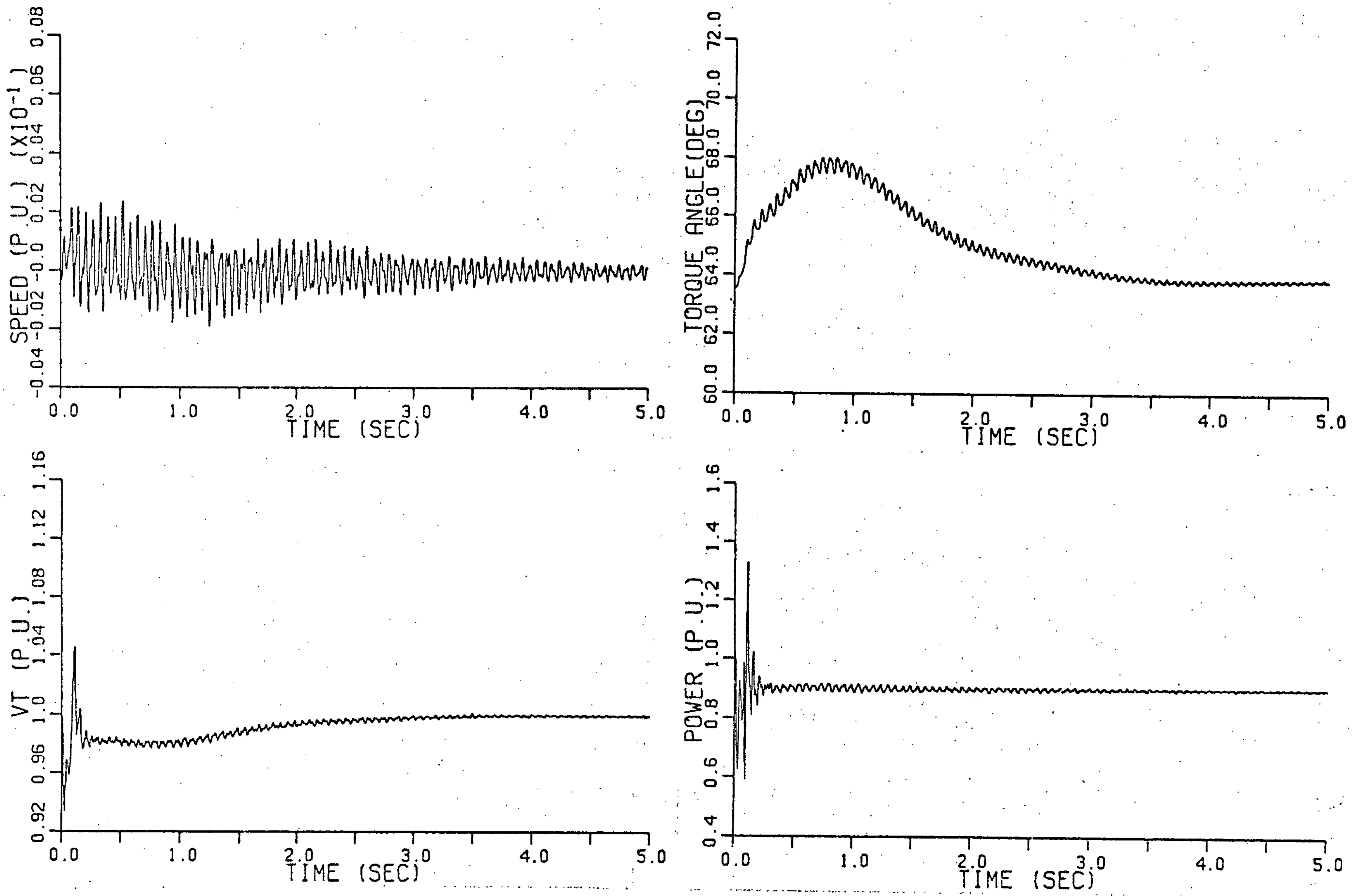

Figure 5.21 Typical responses of machine 1 in the three-machine system with control.

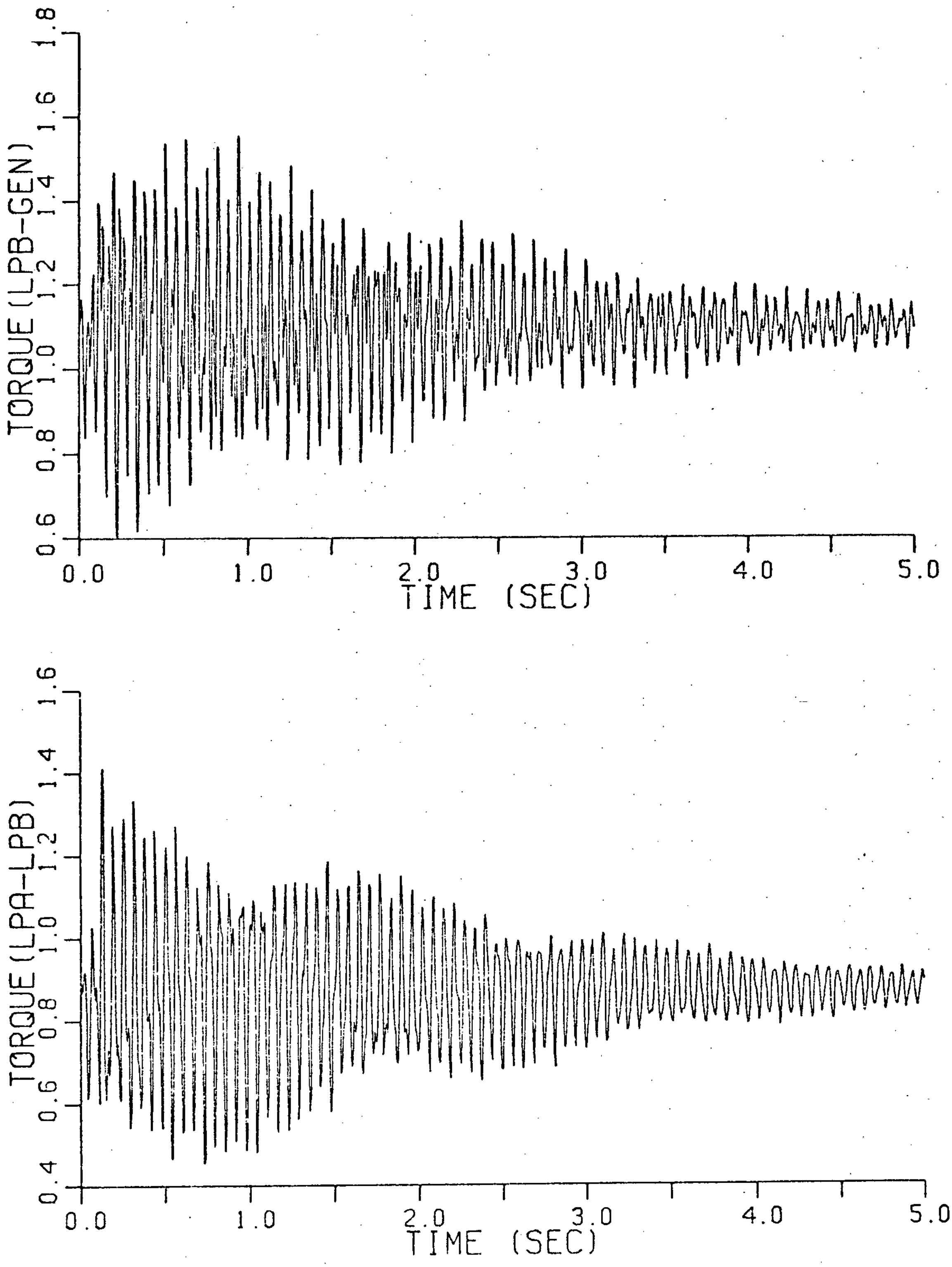

Figure 5.21 (continued)

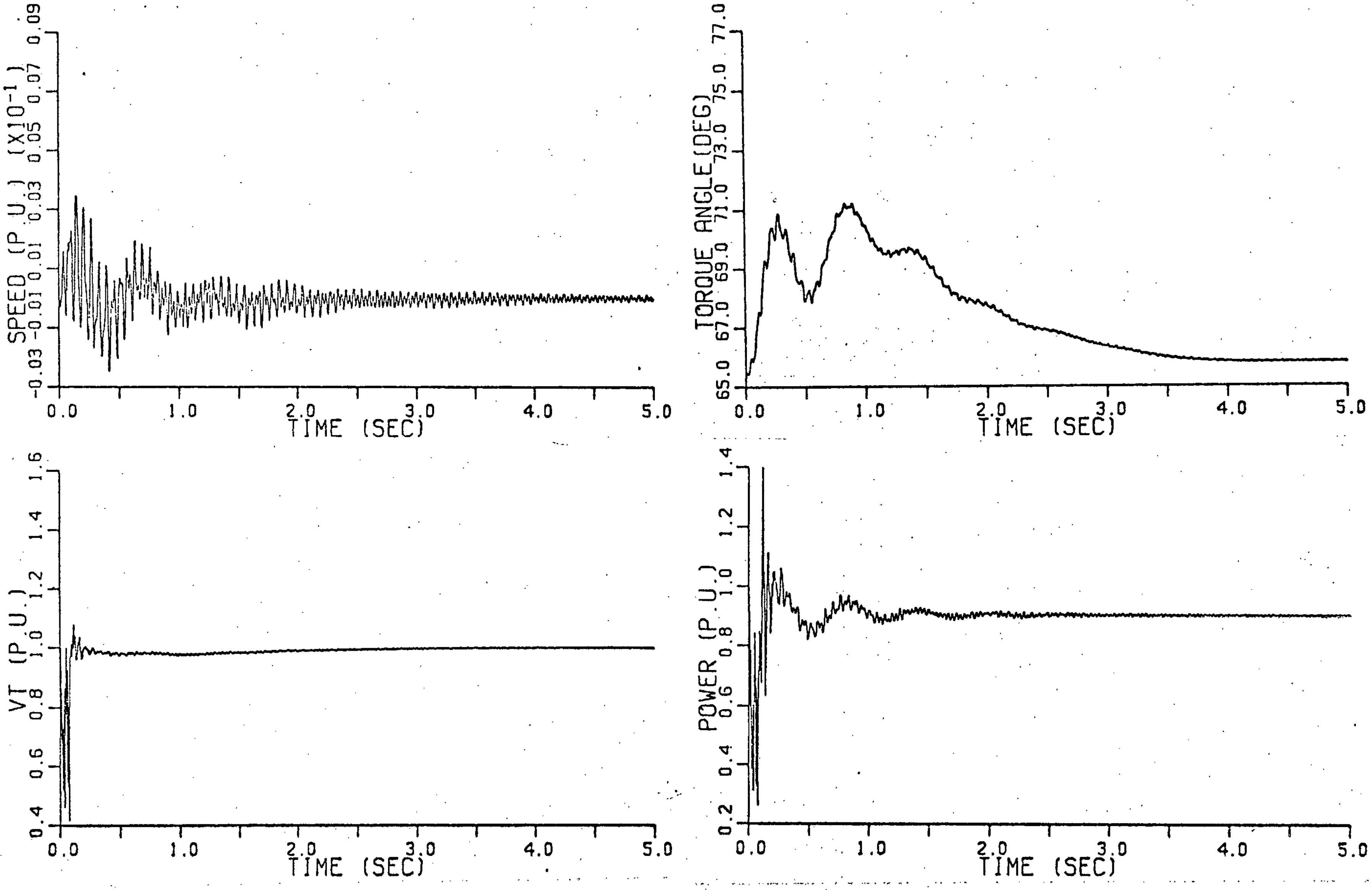

Figure 5.22 Typical responses of machine 2 in the three-machine system with control.

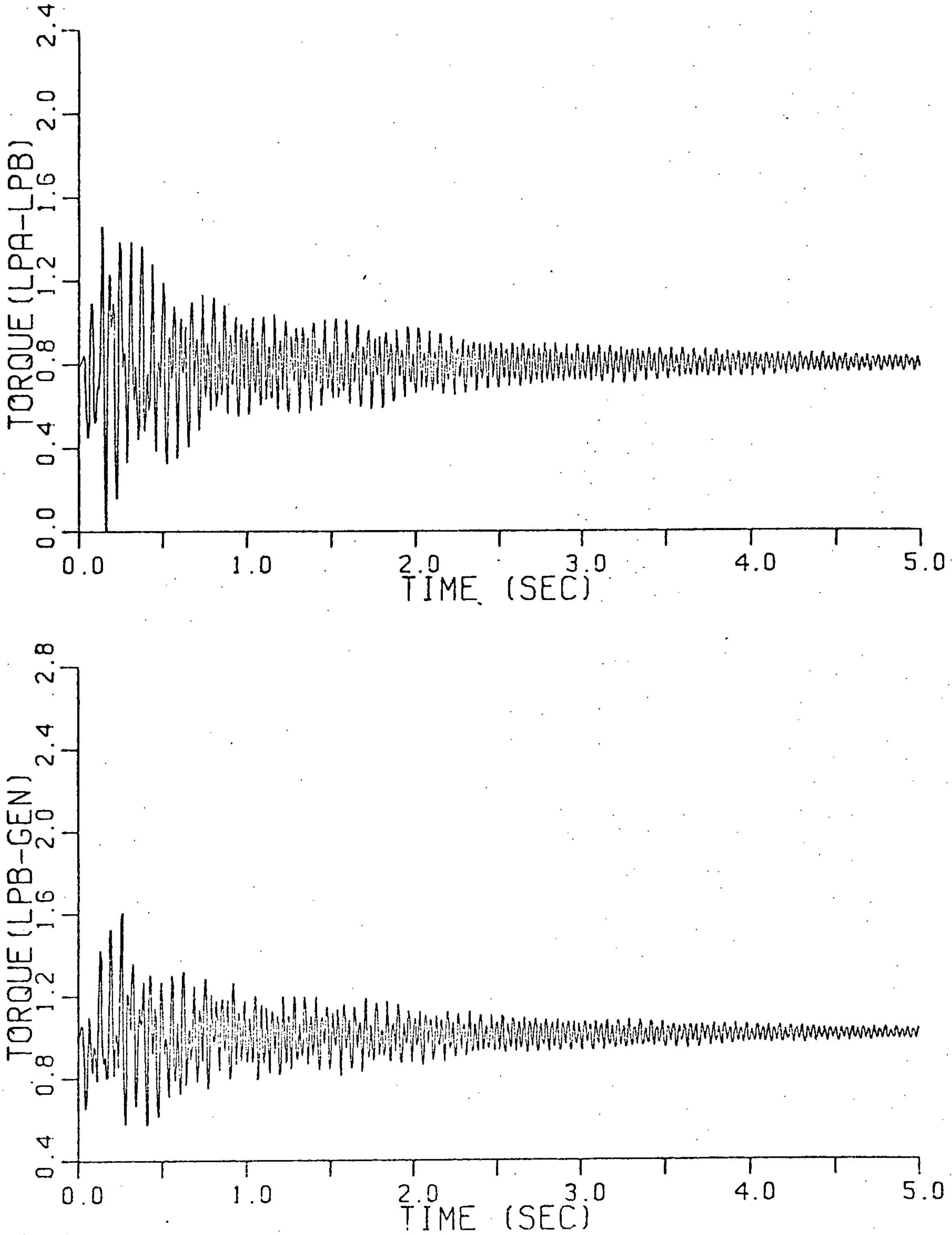

Figure 5.22 (continued)

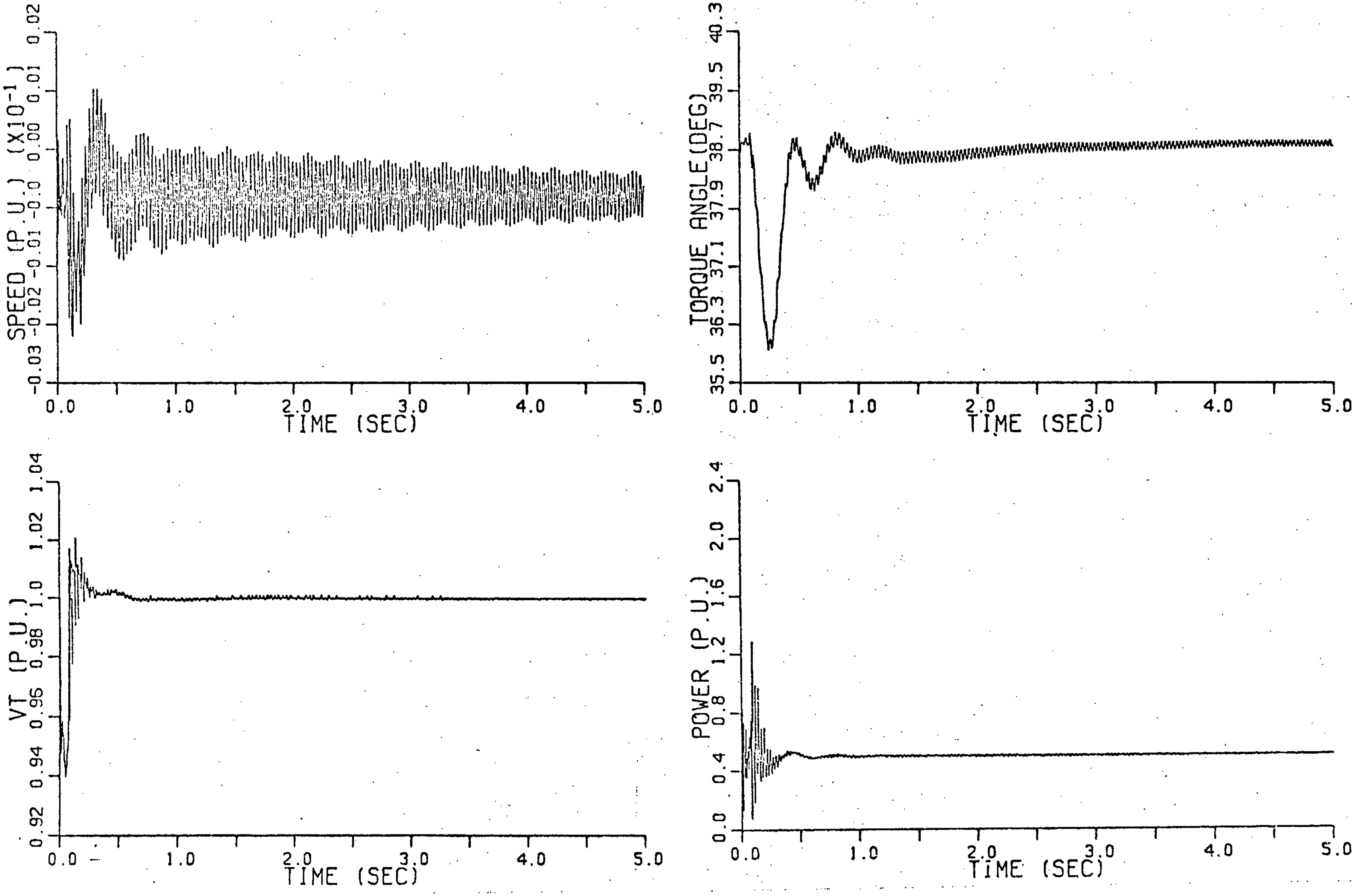

Figure 5.23 Typical responses of machine 3 in the three-machine system with control.

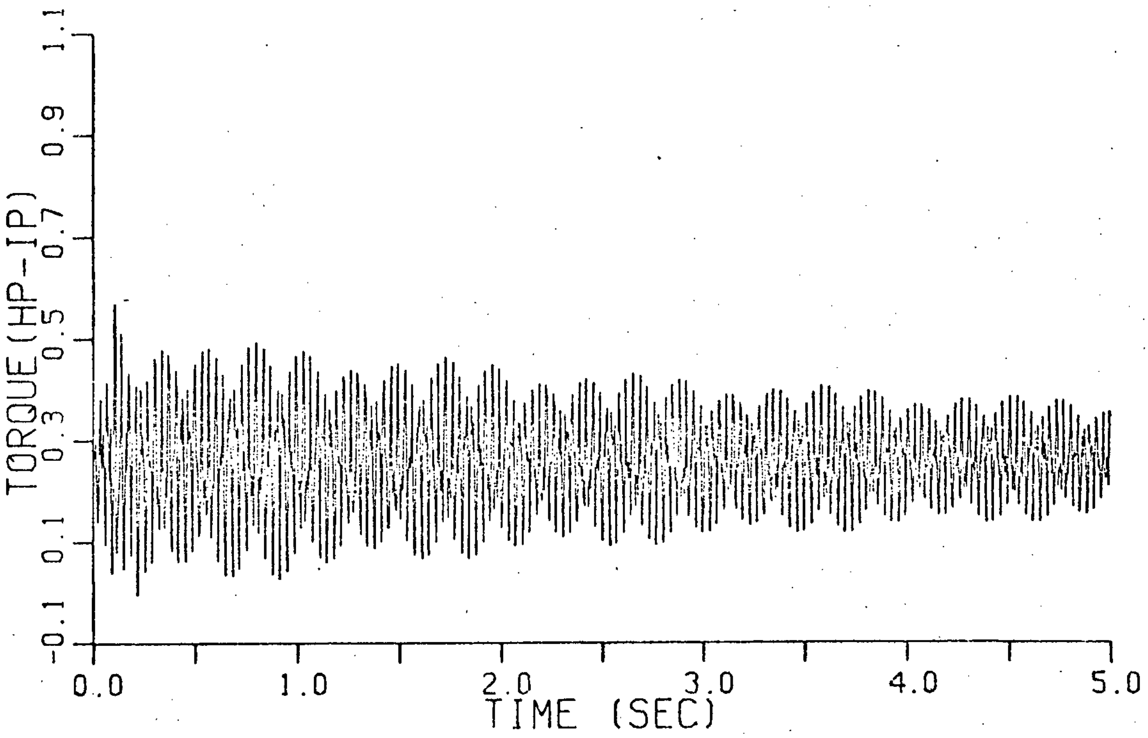

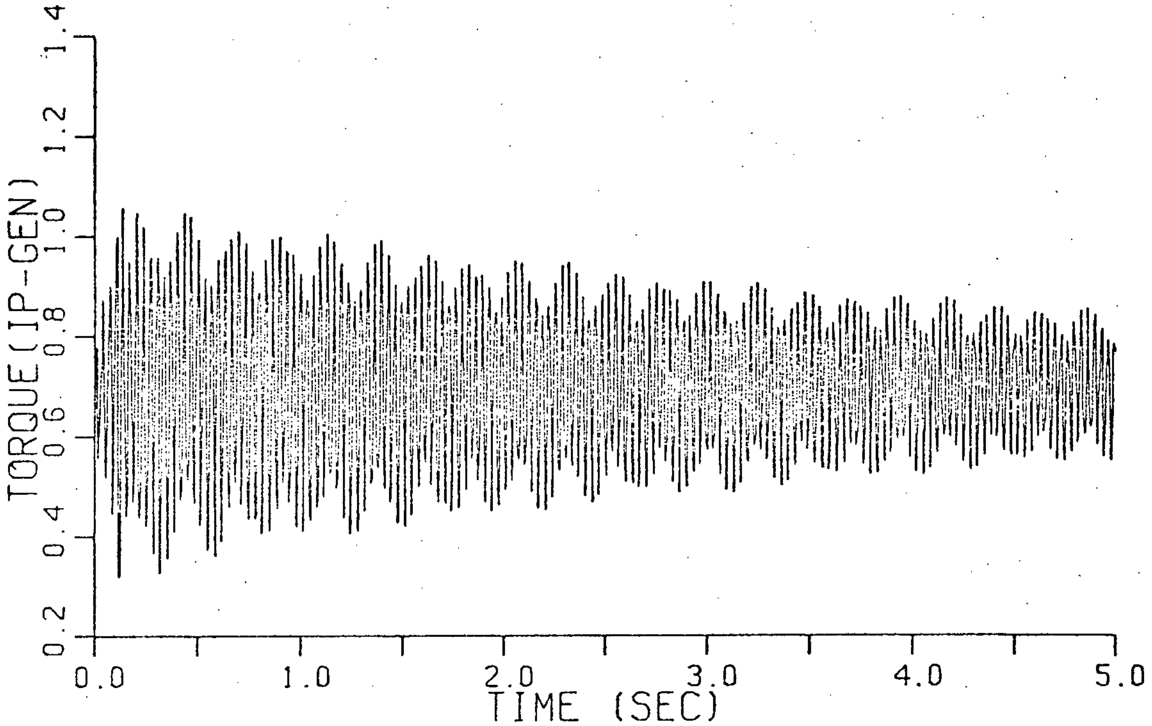

Figure 5.23 (continued)

5.8 Concluding Remarks for Multi-machine SSR Studies

From the foregoing SSR studies of the two-machine and three-machine systems, general conclusions are as follows:

1) In a multi-machine system with multiple capacitor-compensated transmission lines, there is more than one condition at which SSR may occur.
2) Interaction between torsional modes of different machines has no significant effect on SSR stability.
3) To apply the simplified output feedback excitation control design technique developed for the one-machine system to a multi-machine system, a one-machine equivalent including the strongest transmission tie and the critical electrical resonance frequency must be derived for each machine in the multi-machine system. When the controllers thus designed are applied to the multi-machine system, some adaptation may be required, which can be achieved using an iterative process.
4) Both eigenvalue analysis and dynamic performance test using nonlinear full models prove that the excitation control designed according to the procedures presented in this chapter is very effective for multi-machine multi-mode stabilization of the SSR.

6. CONCLUSION

Several useful model reduction, equivalencing, and control simplification techniques have been developed and many interesting results are found in this thesis study.

After presenting a unified electrical and mechanical model for the SSR studies in Chapter 2, it is shown in section 2.5 that, although the negative resistance concept is useful to explain the torsional interaction between the electrical and mechanical systems, the lumped mass representation of the turbine-generator is not sufficient, and the multi-mass-spring system must be used for SSR studies.

For the SSR control design, the excitable torsional modes are identified from modal analysis in Chapter 3. A mass-spring equivalencing technique is then developed for order reduction by retaining only the unstable torsional modes at certain frequencies, resulting in a lower order mass-spring system.

Based on the linear optimal control laws and with the reduced 14th and 16th order models of the original 26th order system, linear optimal excitation controllers are designed in Chapter 4. The controllers are further simplified from a sensitivity analysis by deleting some less sensitivity feedback signals, and the final controllers employ the system output signals as the feedback. Both eigenvalue analysis of the linearized full model and the computer simulated dynamic performance test using non-linear full model indicate that the linear optimal excitation control thus designed is effective in providing damping to all torsional modes of the system over a wide range of capacitor compensation and operating conditions.

The stabilization technique is further extended and applied to a two-machine and a three-machine SSR systems in Chapter 5. It is found that the SSR stabilizers still can be designed for one machine at a time but coordination may be required after all controllers are implemented. For the individual machine SSR controller design, however, it is necessary to derive a one-machine equivalent for each individual machine by retaining the strongest tie of the machine, which has the largest current, to the remaining system, an equivalent reactance is adapted so that the electrical resonance frequency which affects the vulnerable torsional mode of the machine is retained. For the coordination of the damping provided by all controllers for the entire system, an iterative process is developed. Extensive eigenvalue analysis and nonlinear computer simulation tests again indicate that linear optimal excitation controls thus designed are very effective for the SSR control.

The linear optimal excitation developed in the thesis probably provides the most effective and least expensive means to stabilize the SSR of one-machine as well as multi-machine systems.

REFERENCE

[1] M.C.Hall and D.A.Hodges,"Experience with 500Kv Subsynchronous Resonance and Resulting Turbine Generator Shaft Damage at Mohave Generating Station", IEEE Publication 76 CH1066-0-PWR, pp. 22-29, 1976.

[2] R.G.Farmer,A.L.Schwalb, and Eli Katz,"Navajo Project Report on Subsynchronous Resonance Analysis and Solution", IEEE Trans. on PAS,Vol PAS-96, No. 4 July/August 1977 pp. 1226-1232.

[3] G.A. Fischer,R.Quay,R.L.Winchester, Discussion on paper "Subsynchronous Resonance in Series Compensated Transmission Line",IEEE Trans. on PAS,Vol PAS-92,No.4,Sept/Oct.,1973 pp.1655-1657

[4] C.E.J.Bowler,D.H.Baker,N.A.Mincer,and P.R.Vandivver,"Operation and Test of Navajo SSR Protective Equipment", IEEE Trans. on PAS, Vol PAS-97, July/August 1978, pp1030-1035.

[5] L.A.Kilgore,D.G.Ramey,and W.H.South,"Dynamic Filter and other Solutions to the Subsynchronous Resonance Problems",Proceeding of American Power Conference, Vol 37,1975, pp. 923-929.

[6] O. Wasynczuk,"Damping of Subsynchronous Resonance using Reactive Power Control" IEEE Trans.on PAS, Vol PAS-100, No. 3,March 1981, pp. 1096-1103.

[7] D.G.Ramey,D.S.Kimmel,J.W.Dorney,and F.H.Kroening, "Dynamic Stabilizer Verification Tests at the San Juan Station", IEEE Publication 81 TH0086-9-PWR 1981, pp. 34-42 .

[8] R.A.Hedin,K.B.Stump,and N.G.Hingornai,"A New Scheme for Subsynchronous Resonance Damping of Torsional Oscillations and Transient Torque - Part II, Performance", IEEE Trans. on PAS,Vol. PAS-100, No. 4, April 1981, pp. 1856-1863.

[9] N.G.Hingorani,R.A.Hedin,K.B,Stump,and Bharal Bhargava,"Evalulation of NGH Damping Scheme Applied to Mohave Generator", IEEE Publication 81 TH0086-9-PWR 1981, pp. 70-80.

[10] O.Saito,H.Mukae, and K.Murotani,"Suppression of Self Excited Oscillations in Series-capacitor-compensated Transmission Lines by Excitation Control of Synchronous Machine",IEEE Trans. on PAS, Vol PAS 94, Sept/Oct. 1975, pp 1777-1788.

[11] H.M.A Hamdan and F.M.Hughes,"Excitation Controller Design for Damping of Self Excited Oscillations in Series Compensated Lines", Paper A78 565-4, IEEE PES Summer Meeting, Los Angeles, July 1978.

[12] K.Murotani and M.Asano,"Subsynchronous Resonance Oscillations of Series-Compensated Transmission System and their Suppressions" Electrical Engineering in Japan,Vol. 96,No. 6, 1976, pp. 113-121.

[13] M.M.Sartawi and B.T.Ooi, "Field Excitation Suppression of Subsynchronous Resonance by Real and Reactive Power Signal Feedback", Paper A 78 602-5, IEEE PES Summer Meeting, Los Angeles, July 1978.

[14] A.M.El-Serafi and A.A.Shaltout,"Control of Subsynchronous Resonance Oscillations by Multi-loop Excitation Controller", Paper A79 076-1, IEEE PES Winter Meeting, New York City, Feb. 1979.

[15] A.A.Fouad and K.T.Khu,"Damping of Torsional Oscillations in Power Systems with Series-compensated Lines", IEEE Trans. on PAS, Vol. PAS 97, No. 3, May/June 1978, pp. 774-751.

[16] F.M.Hughes and H.M.A.Hamdan,"Damping of Subsynchronous Resonance in Series-compensated Systems by Excitation Control", INT. J. Control, Vol 31, No. 1, 1980, pp.63-77.

[17] Yao-nan Yu,M.D.Wvong,and K.K.Tse, "Multi-Mode Wide-range Subsynchronous Resonance Stabilization", Paper A78 554-8, IEEE PES Summer Meeting, Los Angeles, July 1978.

[18] A.Yan,M.D.Wvong,and Yao-nan Yu,"Excitation Control of Torsional Oscillations", Paper A79 505-9, IEEE PES Summer Meeting, Vancouver, B.C. , July 1979.

[19] Yao-nan Yu,K.Vongsuriya,and L.N.Wedman,"Application of an Optimal Control Theory to a Power System", IEEE Trans. on PAS, Vol. PAS 89, No. 1, Jan/Feb. 1970, pp. 55-62.

[20] H.A.M.Moussa and Yao-nan Yu, "Optimal Power System Stabilization through excitation and/or Governor Control", IEEE Trans. on PAS, Vol. PAS 91, No. 3, May/June 1972, pp. 1166-1174.

[21] Habibullah and Yao-nan Yu, "Physical Realizable Wide Power Range Optimal Controllers for Power Systems", IEEE Trans. on PAS, Vol. PAS 93, No. 5, Sept/Oct. 1974, pp. 1498-1506.

[22] H.A.M. Moussa and Y.N.Yu, "Dynamic interaction of Multi-Machine Power System and Excitation Control", IEEE Trans. on PAS, Vol. PAS-94, August, 1975,pp. 1150-1158.

[23] J.M.Undrill and T.E.Kostyniak,"Subsynchronous Oscillations Part I-Comprehensive System Stability Analysis", IEEE Trans. on PAS, Vol. PAS-95, No. 4, July/August 1976, pp. 1446-1454.

[24] A.Yan and Yao-nan Yu,"Multi-Mode Stabilization of Torsional Oscillations Using Output Feedback Excitation Control", Paper 81 SM 383-9, IEEE PES Summer Meeting, Portland, July 1981. To be published in IEEE Trans. on Power Apparatus and Systems.

[25] IEEE Committee Report,"Dynamic Models for Steam and Hydro Turbines in Power System Studies", IEEE Trans. on PAS, Vol. PAS-92, Nov/Dec. 1973, pp. 1904-1915.

[26] IEEE Committee Report, "Computer Representation of Excitation Systems", IEEE Trans. on PAS, Vol PAS-87, June/July 1968, pp. 1460-1470.

[27] B.L.Agrawal and R.G.Farmer," Use of Frequency Scanning Techniques for Subsynchronous Resonance Analysis ",IEEE Trans. on PAS, Vol. PAS-98 ,No. 2, March/April 1979, pp. 341-349.

[28] J.M.Undrill and F.P.DeMello, "Subsynchronous Oscillations Part 2- Shaft-System Dynamic Interactions", IEEE Trans. on PAS, Vol. PAS-95, No. 4, July/August 1976, pp. 1150-1158.

[29] W.S.Levine and M. Athans," On the Determination of the Optimal Constant Output Feedback Gains for Linear Multivariables Systems", IEEE Trans. on Automatic Control, Vol. AC-15, No.1, Feb. 1970, pp. 44-48.

[30] N.Munro and A.Vardulakis," Pole-shifting using Output Feedback ", Int. J. Control, Vol. 18, No. 6, 1973, pp. 1267-1273.

[31] J.E.Van Ness,J.M.Boyle, and F.P.Imad," Sensitivities of Large, Multiple Loop Control System", IEEE Trans. on Autumatic Control, March 1965, pp.308-315.

[32] L.N.Wedman and Yao-nan Yu," Computation Techniques for the Stabilization and Optimization of High Order Power Systems ", The Sixth PICA Conference Proceedings, May 1969, pp. 324-343.

[33] Jan Stein and Horst Fick," The Torsional Stress Analyzer for Continously Monitoring Turbine-Generators ", IEEE Trans. on PAS, Vol. PAS-99, No. 2, March/April 1980, pp. 703-710.

[34] D.M.Triezenber ,"Characteristic Frequencies and Mode Shapes For Turbogenerator Shaft Torsional Vibrations", Paper A 78 809-6, IEEE/ASME/ASCE Joint Power Generation Conference, Dallas, TX, Sept. 10-13, 1978.

[35] IEEE Committee Report, "First Benchmark Model for Computer Simulation of Subsynchronous Resonance", IEEE Transactions on PAS, PAS-96, Sept./Oct. , pp. 1565-1572.

[36] D.N.Walker,A.L.Schwalb,"Results of Subsynchronous Resonance Test at Navajo", IEEE Publication 76 CH1066-0-PWR, pp.37-45, 1976.

[37] Charles Concordia,"Synchronous Machines - Theory and Performance", John Wiley and Son, Inc., New York, 1951.

[38] Gerald Manchur, David C. Lee, M.E. Coultes,J.D.A Griffin, and Wilfred Watson,"Generator Models Established by Frequency Response Tests on A 555 MVA Machine" IEEE Trans. on PAS, Sept./Oct.., 1972,pp. 2077-2083.

APPENDIX I

SYSTEM DATA FOR THE ONE MACHINE SYSTEM

All the data are in per unit based on 500KV and 900 MVA except the time constant which is in second.

Synchronous Machine Parameters

$X_d = 1.79$	$X_f = 1.6999$	$R_f = 0.00105$
$X_{md} = 1.66$	$X_{kd} = 1.6657$	$R_{kd} = 0.00371$
$X_q = 1.71$	$X_{kq} = 1.6531$	$R_{kq} = 0.00491$
$X_{mq} = 1.58$	$R_a = 0.0015$	

Mass-spring System

$M_{HP} = 0.185794$	$K_{12} = 19.303$	
$M_{IP} = 0.311178$	$K_{23} = 34.929$	
$M_{LPA} = 1.717340$	$K_{34} = 52.038$	$D_{ii} = 0.1$
$M_{LPB} = 1.768430$	$K_{45} = 70.858$	$i=1,2,\ldots,6$
$M_{Gen} = 1.736990$	$K_{56} = 2.8220$	
$M_{Ex} = 0.068433$		

Turbine and Governing System

$K_g = 25$	$T_1 = 0.2$	$T_2 = 0.0$
$T_3 = 0.3$	$T_{CH} = 0.3$	$T_{RH} = 7.0$
$T_{CO} = 0.2$	$F_{HP} = 0.3$	$F_{IP} = 0.26$
$F_{LPA} = 0.22$	$F_{LPB} = 0.22$	$\dot{P}_{GV} = \pm 0.1$

Exciter and Voltage Regulator

$K_A = 50$	$T_A = 0.01$	$T_E = 0.002$

Exciter voltage ceiling limits = ±7.0

Transmission line Parameters

$X_t = 0.14$	$R_t = 0.01$	$X_L = 0.56$
$R_L = 0.02$	X_c varied from 0.056 - 0.448(10% - 80%)	

APPENDIX II

SYSTEM DATA FOR THE TWO MACHINE SYSTEM

A2.1 Machine 1

Synchronous Machine Parameters

Similiar to that of the machine in Appendix I

Mass-spring System

Similiar to that of the machine in Appendix I

Turbine Torque Distribution

$F_{HP1} = 0.3$ $\quad F_{IP1} = 0.26$ $\quad F_{LPA1} = 0.22$

$F_{LPB1} = 0.22$

Exciter and Voltage Regulator

$K_{A1} = 50$ $\quad T_{A1} = 0.01$ $\quad T_{E1} = 0.002$

Exciter voltage ceiling limits = ±7.0

A2.2 Machine 2

Synchronous Machine Parameters

$X_{d2} = 1.82$	$X_{f2} = 1.92$	$R_{f2} = 0.0067$
$X_{md2} = 1.65$	$X_{kd2} = 1.76$	$R_{kd2} = 0.0043$
$X_{q2} = 1.73$	$X_{kq2} = 2.05$	$R_{kq2} = 0.0089$
$X_{mq2} = 1.59$	$R_{a2} = 0.0015$	

Mass-spring System

$M_{HP2} = 0.248$	$K_{12} = 21.8$	$D_{ii} = 0.1$
$M_{IP2} = 0.464$	$K_{23} = 48.4$	$i=1,2,..,5$
$M_{LPA2} = 2.31$	$K_{34} = 74.6$	
$M_{LPB2} = 2.38$	$K_{45} = 62.3$	
$M_{Gen2} = 1.71$		

Turbine Torque Distribution

$F_{HP2} = 0.3$ $F_{IP2} = 0.26$ $F_{LPA2} = 0.22$

$F_{LPB2} = 0.22$

Exciter and Voltage Regulator

$K_{A2} = 50$ $T_{A2} = 0.01$ $T_{E2} = 0.005$

Exciter voltage ceiling limits = ± 7.0

A2.3 Transmission System

Transformer

$X_{t1} = 0.14$ $R_{t1} = 0.01$

$X_{t2} = 0.1$ $R_{t2} = 0.01$

Transmission Line

Line 1 $X_{L1} = 0.42$ $R_{L1} = 0.02$

X_{c1} varied from 0.042 to 0.336 (10% - 80%)

Line 2 $X_{L2} = 0.4$ $R_{L2} = 0.01$

X_{c2} varied from 0.04 to 0.32 (10% - 80%)

Line 3 $X_{L3} = 0.2$ $R_{L3} = 0.01$

Line 4 $X_{L4} = 0.28$ $R_{L4} = 0.05$

Load $R_{load} = 0.9$

APPENDIX III

SYSTEM DATA FOR THE THREE MACHINE SYSTEM

A3.1 Machine 1

All parameters are similiar to those given in A2.1 of Appendix II.

A3.2 Machine 2

All parameters are similiar to those given in A2.2 of Appendix II .

A3.3 Machine 3

Synchronous Machine Parameters

$X_{d3} = 1.78$	$X_{f3} = 1.7781$	$R_{f3} = 0.00109$
$X_{md3} = 1.6845$	$X_{kd3} = 1.7368$	$R_{kd3} = 0.0117$
$X_{q3} = 1.7067$	$X_{kq3} = 1.6409$	$R_{kq3} = 0.0151$
$X_{mq3} = 1.6063$	$R_{a3} = 0.00357$	

Mass-spring System

$M_{HP3} = 0.262$	$K_{12} = 47.48$	$D_{ii} = 0.1$
$M_{IP3} = 0.525$	$K_{23} = 61.85$	$i=1,2..,4$
$M_{Gen3} = 1.85$	$K_{34} = 4.51$	
$M_{Ex3} = 0.0595$		

Turbine Torque Distribution

$F_{HP3} = 0.4$ $\qquad F_{IP3} = 0.6$

Exciter and Voltage Regulator

$K_{A3} = 50$ $\qquad T_{A3} = 0.02$ $\qquad T_{E3} = 0.002$

Exciter voltage ceiling limits = ±7.0

A3.4 Transmission System

Transformer

X_{t1}	= 0.14	R_{t1}	= 0.01
X_{t2}	= 0.14	R_{t2}	= 0.01
X_{t3}	= 0.14	R_{t3}	= 0.01

Transmission Line

Line 1 $X_{L1} = 0.47$ $R_{L1} = 0.035$

X_{c1} varied from 30% to 70% compensation

Line 2 $X_{L2} = 0.4$ $R_{L2} = 0.02$

X_{c2} varied from 30% to 70% compensation

Line 3 $X_{L3} = 0.14$ $R_{L3} = 0.01$

X_{c3} varied from 30% to 70% compensation

Line 4 $X_{L4} = 0.39$ $R_{L4} = 0.03$

X_{c4} varied from 30% to 70% compensation

Line 5 $X_{L5} = 0.34$ $R_{L5} = 0.025$

X_{c5} varied from 30% to 70% compensation

Line 6 $X_{L6} = 0.51$ $R_{L6} = 0.04$

X_{c6} varied from 30% to 70% compensation

Line 7 $X_{L7} = 0.11$ $R_{L7} = 0.01$

No capacitor compensation

Line 8 $X_{L8} = 0.3$ $R_{L8} = 0.02$

X_{c8} varied from 30% to 70% compensation

Line 9 $X_{L9} = 0.32$ $R_{L9} = 0.024$